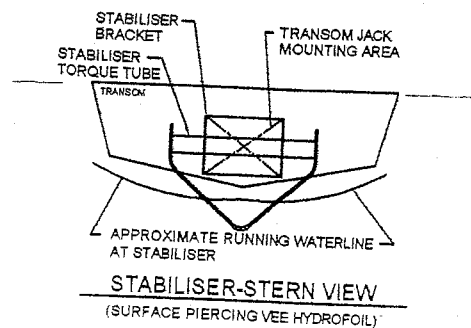
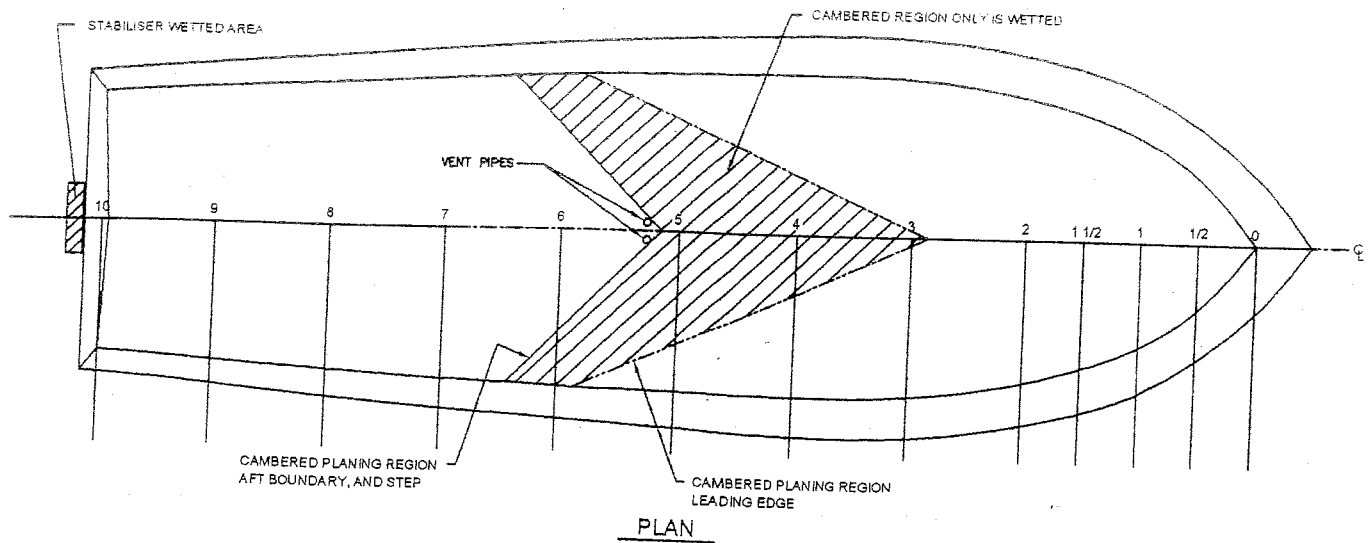


# How to Design an Efficient Stepped Planing Boat (Dynaplane Boat)

Eugene P. Clement



How to Design an Efficient Stepped Planing  
Boat  
(Dynaplane Boat)

Eugene P. Clement

Copyright © 2006 by Eugene P. Clement  
All rights reserved  
Published by the author  
104 Woodward Ave.  
Asheville, NC 28804, USA  
E-mail: [Eclement5@aol.com](mailto:Eclement5@aol.com)

## Contents

Nomenclature .....	i
Introduction .....	1
Chapter 1	
A Comparison of the Dynaplane with Other Types of Planing Motorboats .....	1
Chapter 2	
Details of and Design Procedure for a Dynaplane-Type Stepped Planing Boat ..	13
Chapter 3	
Shortcomings of Previous Stepped Boats, and the SweptBack Step .....	25
..	
Chapter 4	
Design Procedure for a Planing Surface Having Camber .....	29
Chapter 5	
Design of the Step and Afterbody, and Drag at the Hump .....	48
Chapter 6	
A Surface-Piercing Vee Hydrofoil as the Trim-Control Device for a Stepped Planing Boat .....	52
Appendix A	
Results of Tests of a Planing Surface Model with the Johnson 3-Term Camber .....	58
References .....	65

## Nomenclature

A or AR	aspect ratio, $b^2/S$
b	breadth of planing surface, ft
$C_D$	drag coefficient normalized on area, $D/\frac{1}{2}\rho v^2 S$
$C_{Lb}$	drag coefficient normalized on beam, $D/\frac{1}{2}\rho v^2 b^2$
$C_L$	lift coefficient normalized on area, $L/\frac{1}{2}\rho v^2 S$
$C_{Lb}$	lift coefficient normalized on beam, $L/\frac{1}{2}\rho v^2 b^2$
$C_{Lb0}$	lift coefficient, zero deadrise
$C_{Lb_s}$	lift coefficient, deadrise surface
$C_L$	lift coefficient normalized on area, $L/\frac{1}{2}\rho v^2 S$
$C_{L,d}$	two-dimensional design lift coefficient for a cambered planing surface
$C_f$	skin friction coefficient
c	chord length of camber curve
D	drag, lb
F	Froude number based on volume of water displaced at rest, $v/\sqrt{g\nabla^{1/3}}$
g	acceleration due to gravity, 32.16 ft/sec
L	lift, lb
L	projected chine length
$l_{cp}$	distance of center of pressure forward of trailing edge of planing surface, ft
$l_r$	root-chord wetted length (i.e., keel wetted length)
$l_t$	tip-chord wetted length (i.e., chine wetted length)
$l_m$	mean wetted length
R	resistance, lb
Re	Reynolds number
S	projected wetted area bounded by spray-root lines, chines and step, measured on a plane normal to the centerline and containing the keel, $(b\bar{x}_m)$ sq ft
V	horizontal velocity, mph, or knots, as indicated
v	horizontal velocity, fps
W	weight of boat, lb
$\alpha$	angle of attack, deg
$\beta$	deadrise angle, deg
$\phi$	sweepback angle of 50% chord line, projected on a plane containing the keel, deg
$\gamma$	angle between a spray-root line and the centerline, projected on a plane containing the keel, deg
$\theta$	sweepback angle of the step, projected on a plane containing the keel, deg
$\rho$	mass density of water, slugs per cu ft
$\tau$	trim angle, angle between straight portion of forebody keel and horizontal, deg.
$\nabla$	volume of water displaced at rest, cu ft

# **How to Design an Efficient Stepped Planing Boat (Dynaplane Boat) By Eugene P. Clement**

## **Introduction**

This booklet is a revised version of a previous publication about the Dynaplane-type of stepped planing boat. The previous booklet, Reference 1, included material on how to design several different types of main planing surfaces for stepped boats. Planing surfaces both with camber and without camber were treated. It is now apparent that to achieve optimum performance camber should be incorporated for most design cases, and only that type of planing surface is considered in this booklet. This version of the booklet also includes the particulars about a model of a Dynaplane design with an adjustable Vee hydrofoil at the stern as the stabilizing device. Drawings of the model and the results from towing tank tests are given.

## **Chapter 1 A Comparison of the Dynaplane with Other Types of Planing Motorboats**

### **Contemporary deep-vee motorboats with spray rails are inefficient**

The type of planing motorboat that is present in the largest numbers throughout the world is the unstepped deep-vee type, with longitudinal spray rails. This type has proven to be very suitable for offshore operation, or wherever sizeable waves will be encountered. It is much less suitable, however, for operation on the sheltered waters of rivers and lakes, because the type has high drag. Accordingly, it requires large amounts of installed power and is wasteful in regard to fuel consumption. (Comparative numerical values are given below.) The design continues to be popular, however, because it has the marketing appeal of being patterned after the design of high-speed offshore racers. Also, the high-horsepower engines required are readily available, and relatively inexpensive, and for the time being the same factors obtain for the fuel. With the emphasis now on reducing motorboat fuel consumption rates and pollution effects, the stepped type of hull, although more complex to design and to build, deserves, because of its very low drag, to find a number of applications

### **Dynaplane design is the most efficient stepped type**

The stepped type that has particularly efficient performance is the one termed the "Dynaplane" design. This design has a swept-back step of very small depth, a cambered planing surface, and an adjustable stabilizer at the stern. An example is shown in Figure 1-1. Figure 1-2 illustrates a basic reason for the superiority of this design over a conventional planing boat. That figure compares the wetted areas at planing speed, for a Dynaplane boat, and a conventional planing boat. Each plan-view drawing represents a

boat 32 ft. long, weighing 10,000 lbs., and traveling at 45 mph. The deadrise angle for both cases is 12.5 deg. Wetted area for the Dynaplane design (including both upper and lower surfaces of the stabilizer) is 38 ft.<sup>2</sup> and for the conventional design it is 136 ft.<sup>2</sup>. That is, running wetted area for the conventional design is 3½ times as much as it is for the Dynaplane design. Accordingly, when running at the same speed and the same weight, the conventional design will have 3½ times as much frictional resistance as the Dynaplane design. The camber curvature contributes to the small size of the lifting area that is needed and also results in a low value of pressure drag on the planing area. The feature of having an adjustable stabilizer enables the pilot to maintain the optimum trim angle for different speeds and different loading conditions and also provides enhanced boating fun for both pilot and passengers.

### **Planing boat performances compared on a graph of volume Froude number**

Figure 1-3 shows a comparison of the relative performances of the major types of planing boats. In this figure values of resistance/weight ratio (from model tests) are plotted against the appropriate speed coefficient,  $F_{\nabla}$ . Data are given for a variety of hull types - including the unstepped deep-vee and the Dynaplane type of hull. (The speed coefficient used,  $F_{\nabla}$ , or volume Froude number, is particularly appropriate for comparing the performances of different types of boats. It realistically uses gross weight, rather than length, as the significant index of size, and compares different boats on the basis of equal weight and equal speed. The nomograph in Figure 1-4 shows the relationship of  $F_{\nabla}$ , to craft speed and craft gross weight. This nomograph is for salt water, but the values for fresh water are only slightly different.)

### **Model test results for contemporary designs compared with model test results for stepped Swedish designs**

Contemporary planing boats generally correspond to either the one or the other of the two unstepped types for which performance data are given in **Figure 1-3**. Davidson Lab Model No. 2879 was a model of a Ray Hunt deep-vee hull design. DTMB Model No. 4667-1 was the parent hull form for the DTMB unstepped planing boat Series 62. The particulars about that series are given in Reference 2. The Swedish tank-test data for a stepped hull are taken from Reference 3. That reference reported the results from model tests of twenty-seven different single-step hull configurations. The features varied were deadrise, depth of the step, angle between the fore- and after-body keel lines, and length of the afterbody. The data points from the Swedish tank-tests that are given in Figure 1-3 are for the model that had the least drag and that also ran stably. (Seventeen of the twenty-seven stepped configurations tested porpoised when they were run relatively fast).

### **Dynaplane designs have one half as much drag as contemporary designs**

Results from the tests of two models of the Dynaplane type (DTMB Models 5115 and 5115A) are included in Figure 1-3. Both had the basic Dynaplane features of a sweptback step (of small depth), a cambered planing surface, and an adjustable stabilizer

at the stern . Model 5115 utilized a Plum-type planing stabilizer, and Model 5115A had a Vee-hydrofoil stabilizer. Particulars of Model 5115 were given in Reference 1, and drawings of Model 5115A are shown in Figures 1-5 - 1-7. The comparison in Figure 1-3 of the performance of the unstepped Model 4667-1 with that of the stepped Dynaplane models (5115 and 5115A) shows that the Dynaplane designs have slightly more drag in the lower part of the speed range, but much less drag at high speed. At speeds above about 40 mph, and a boat weight of 10,000 lb, a Dynaplane design would have only one-half as much drag as the best of the conventional (unstepped) planing boat designs. The graph also shows that if the speed coefficient of a projected new design is about 3.5 or higher, an appropriately designed Dynaplane boat will have appreciably lower drag than the other available planing boat types.

### **Favorable load carrying characteristics of the Dynaplane design**

The extensive testing at DTMB of stepped models with trim-control devices showed that the Dynaplane type has particularly favorable load-carrying characteristics. First, its very low drag at planing speeds is achieved with a mean LCG location close to the mid-length point of the hull. Accordingly the full length of the hull can be used for carrying useful items of payload. This is in contrast to the case for a conventional unstepped planing boat for which the CG is usually located an appreciable distance aft of mid-length in order to counteract to some extent its inherently inefficient performance. If the CG of the conventional type is moved forward to a point near mid-length the resistance will be substantially increased. Furthermore, the testing of the Dynaplane-type models at DTMB included tests to determine what the effect on resistance would be of changes in the CG location. The result consistently found was that the moving the CG either forward or aft of the mean (design) had no effect at all on the resistance at planing speeds and only a relatively small effect on the resistance at low speeds. The relationship between LCG location and floating angle at rest is of interest and importance. This relationship is shown for Dynaplane Model No. 5115A (and also for the conventional unstepped Model No. 4667-1) in Figure 1-8. It was found from the testing of the various Dynaplane-type models that the best performance was achieved when the floating angle at rest was in the range between  $\frac{1}{2}$  degree by the bow and  $1\frac{1}{2}$  degrees by the stern. It can be seen from the figure that this corresponds to an LCG range from  $43\%L_P$  to  $52\%L_P$  . The figure also indicates that mean or design condition values to aim for are a floating angle at rest of about  $\frac{1}{2}$  degree by the stern and an LCG location at  $48\%L_P$  . It is interesting to note from Figure 1-8 that Model 5115A floated at even keel when the LCG was at exactly midlength. Notice should also be taken of the fact that the mean step position for the model was at  $45\%L_P$  .

### **Dynaplane designs require less than one half as much horsepower as other contemporary designs**

The desired top speed for a planing boat will usually correspond to a value of the speed coefficient  $F_{\nabla}$  of about 4.5 (or higher). As mentioned previously, Figure 1-3 shows that at a speed coefficient of 4.5, hull drag (at equal weight) for the better of the two types



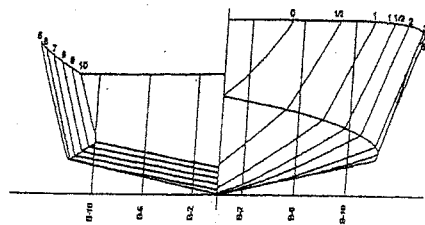
of stepped hulls would be only one-half as much as the hull drag of the better of the two types of unstepped hulls. This comparison of the two types on the basis of equal weight indicates that horsepower required and fuel consumption rate would be approximately half as much for a Dynaplane boat as for a comparable unstepped boat. However, if the comparison is more realistically made, between two boats which are designed for the same mission or purpose, the Dynaplane boat will be considerably lighter in weight (because of its smaller engines and lighter fuel load), and this will lead to further reductions in its drag, horsepower required, and fuel consumption rate. The significant final results are that fuel consumption rate, fuel cost, and the pollution produced, will be less than half as much for a Dynaplane design as for a comparable conventional planing boat.

### **Dynaplane hull drag does not increase with increase in speed**

The Dynaplane design is suitable for a wide range of sizes (a length range from about 20 ft. to about 100 ft.) Furthermore, a striking fact about the performance of the type is that as the design speed increases the hydrodynamic hull drag remains practically the same (and in some cases actually decreases). For example, a Dynaplane-type boat designed for, and running at, a speed of 45 mph will usually have lower hydrodynamic hull drag than a corresponding Dynaplane boat (of equal weight) designed for, and running at, a speed of only 35 mph. Appendage drag and air drag will, however, be greater for the faster boat. A number of models and full-scale boats were built and tested during the evolution of the design, and these have contributed to, and verified, its superior performance

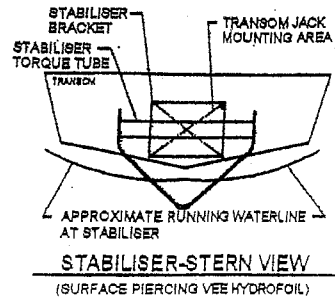
### **Dynaplane design is suitable for deadrise angles up to 15°**

A limitation on the range of the applicability of the Dynaplane design needs to be pointed out. The extensive design studies that have been made show that the Dynaplane's goal of low drag at high speed can be attained for a deadrise-angle range up to a maximum of about 15°. The L/D value attainable for a Dynaplane design decreases significantly if the deadrise angle is higher than 15°. It would not be suitable, for example, as a design for an offshore racing boat. With relatively low deadrise, however, very high efficiency can be attained by a Dynaplane type of hull. The design would be particularly suitable as a recreational motorboat and as a passenger-carrying boat for operation on rivers and lakes.

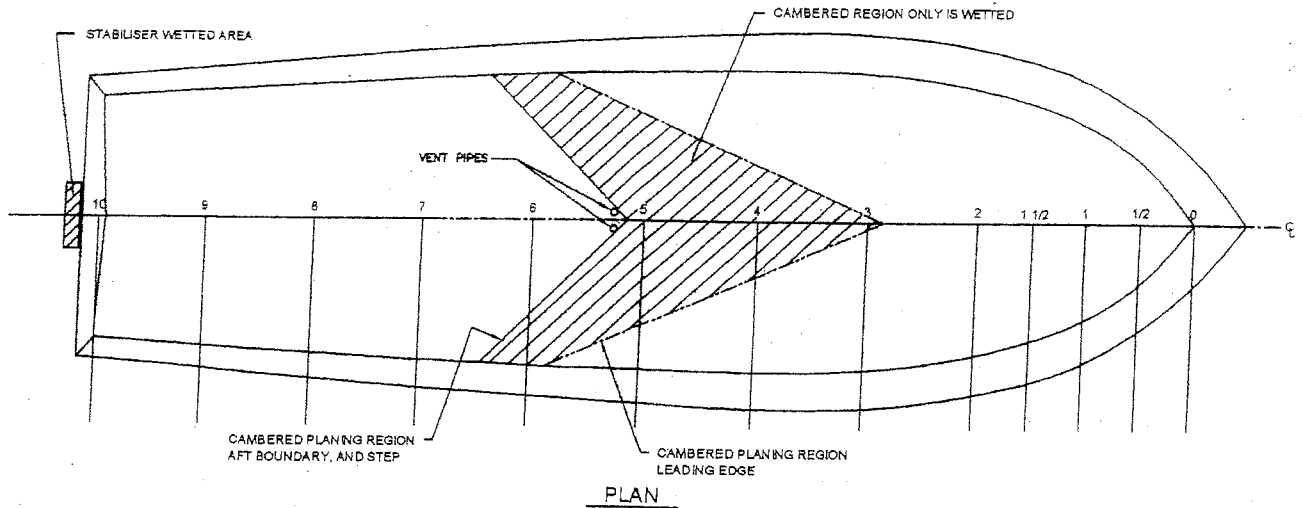


**BODY PLAN**

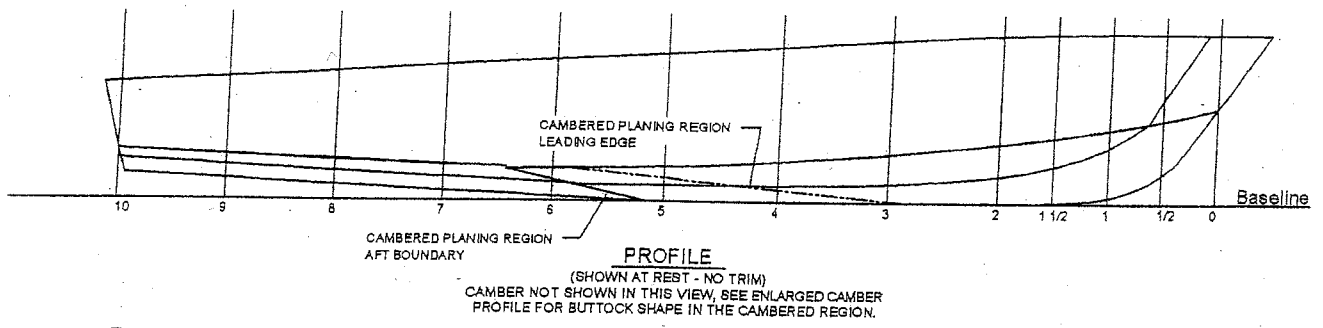
CAMBER NOT SHOWN IN THIS VIEW



**STABILISER-STERN VIEW**  
(SURFACE PIERCING VEE HYDROFOIL)

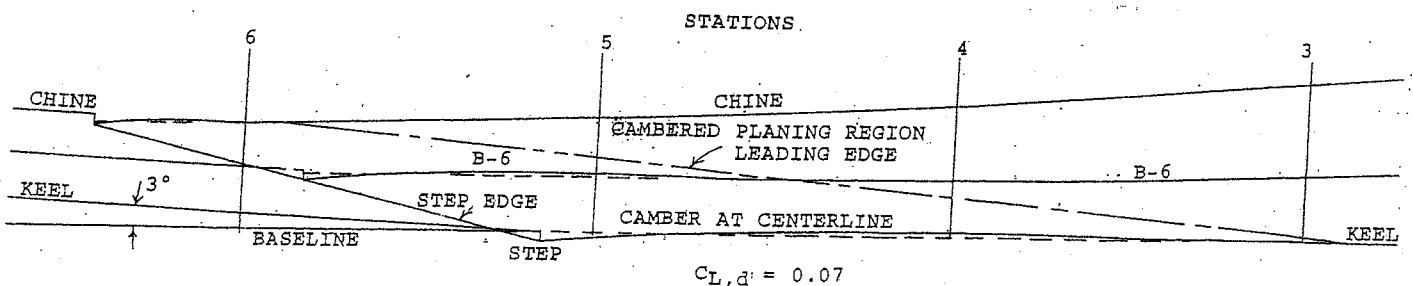


**PLAN**



**PROFILE**

(SHOWN AT REST - NO TRIM)  
CAMBER NOT SHOWN IN THIS VIEW, SEE ENLARGED CAMBER PROFILE FOR BUTTOCK SHAPE IN THE CAMBERED REGION.



**CAMBER PROFILE**

Length (Sta. 0 to Sta. 10) = 20 ft; Maximum Chine Beam = 5.7 ft;  
Deadrise = 12.5 deg; Depth of Step = 0.65 in.

Figure 1-1 - Example of a Design for a Dynaplane Boat.

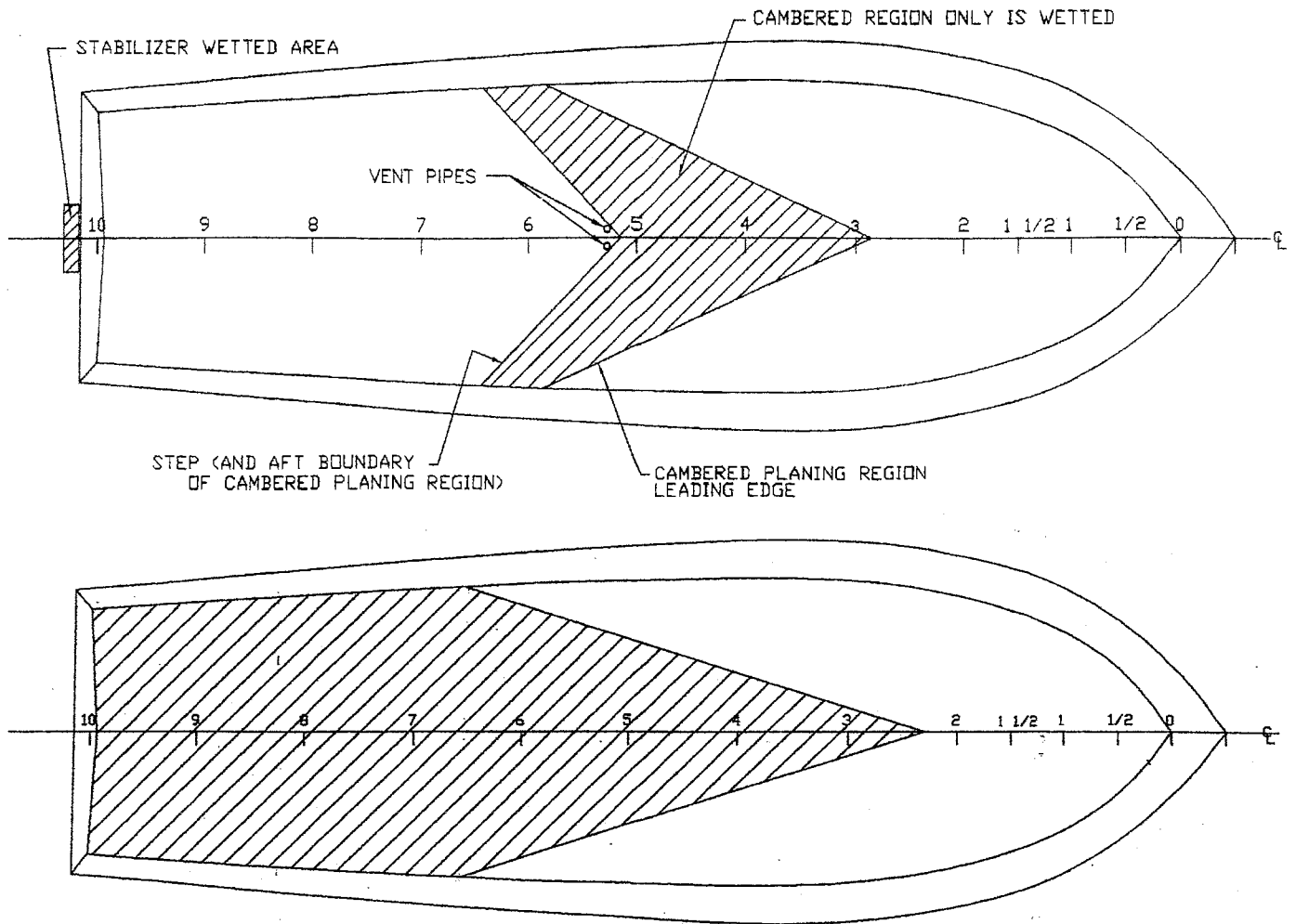


Figure 1-2 - Comparison of Wetted Areas at Planing Speed for a Dynaplane Boat and a Conventional Planing Boat. For Both Boats Length is 32 ft., Weight is 10,000 lb., Deadrise is 12 1/2 deg., and Speed is 45 mph.

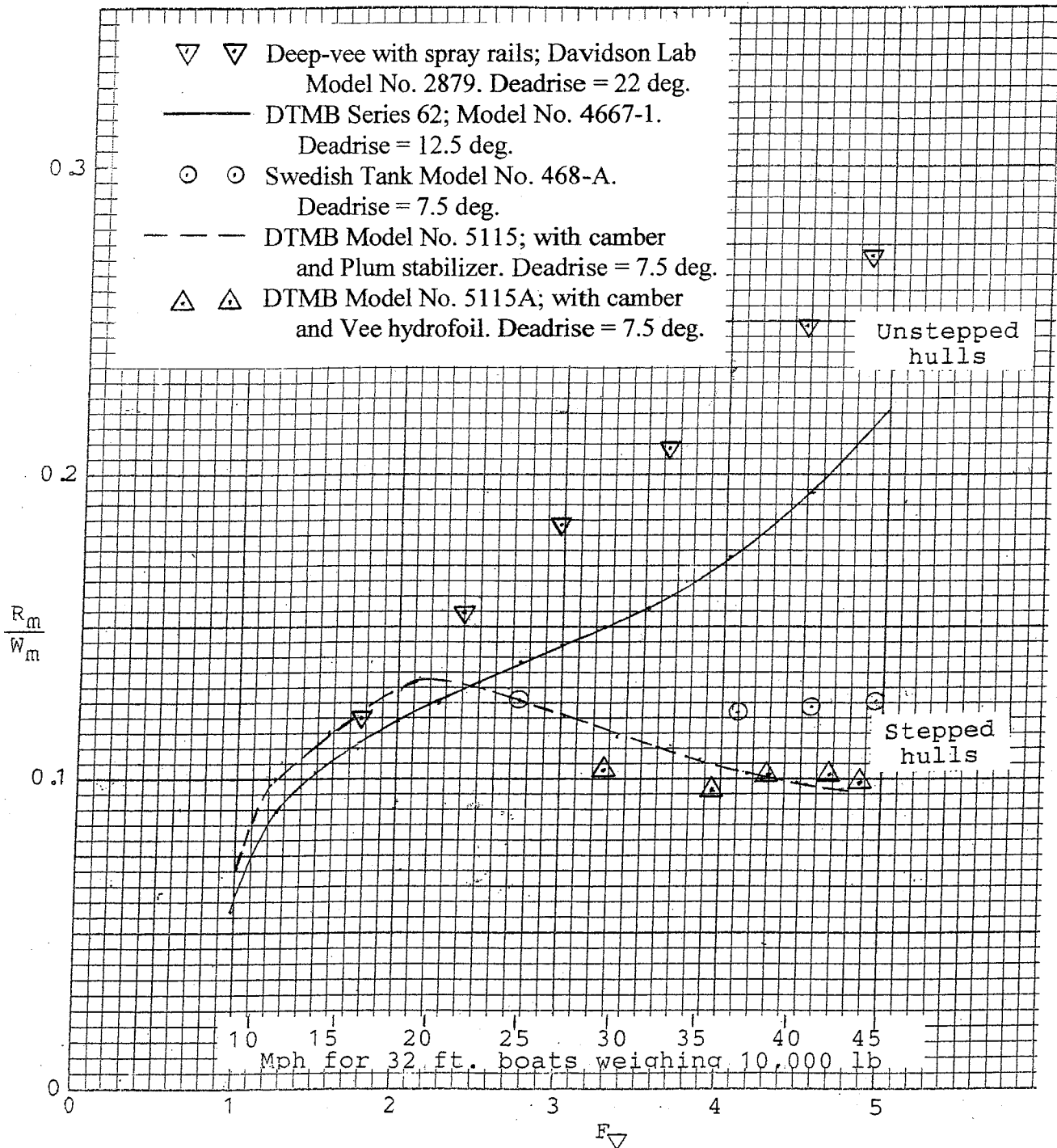
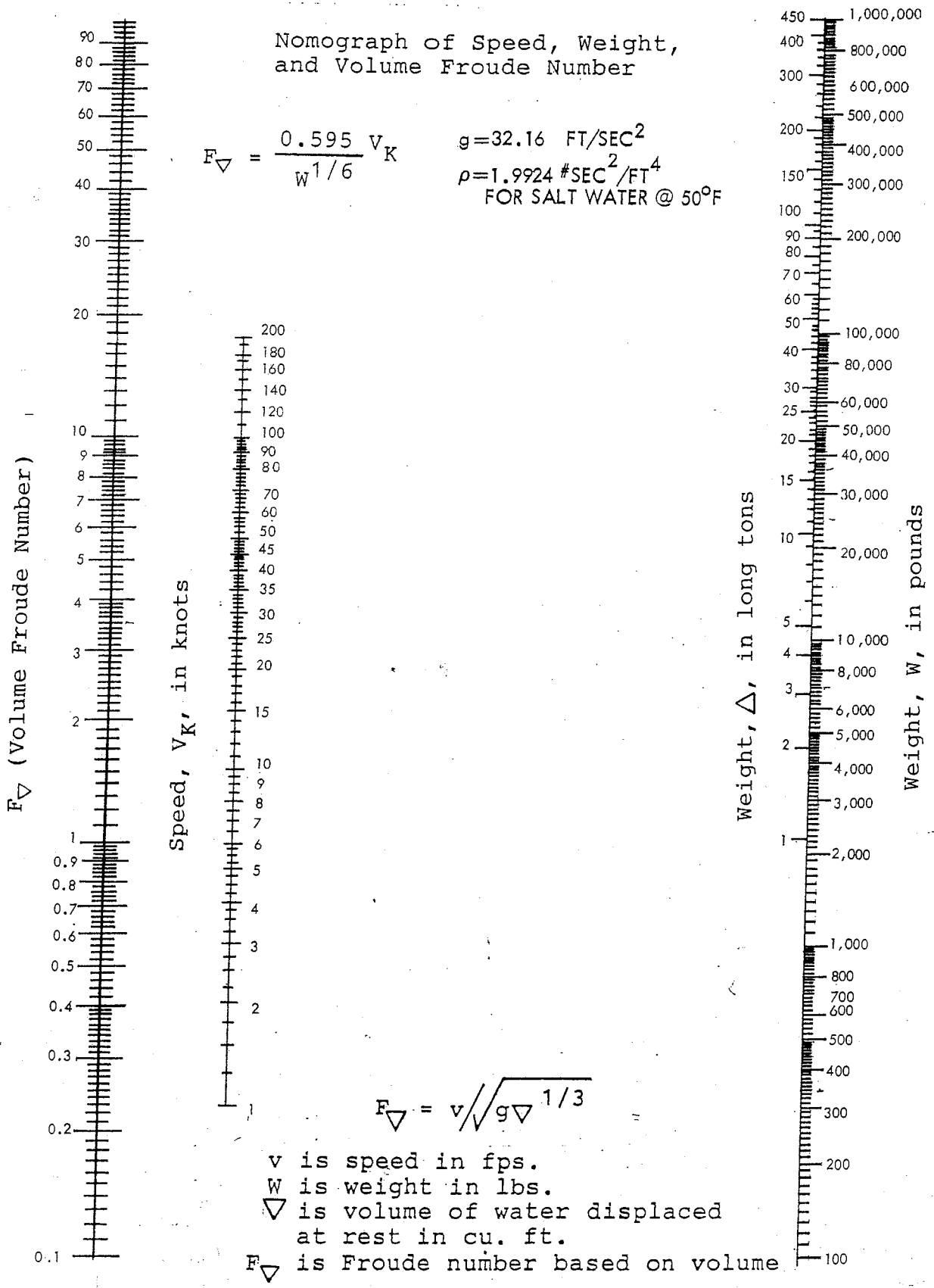


Figure 1-3 - Values of Model Resistance/Weight Ratio, Versus Speed Coefficient, for Different Types of Planing Hulls.

# Nomograph of Speed, Weight, and Volume Froude Number



$v$  is speed in fps.  
 $W$  is weight in lbs.  
 $\nabla$  is volume of water displaced at rest in cu. ft.

$F_{\nabla}$  is Froude number based on volume.

Figure 1-4 -- Nomograph of Speed, Weight, and Volume Froude Number.

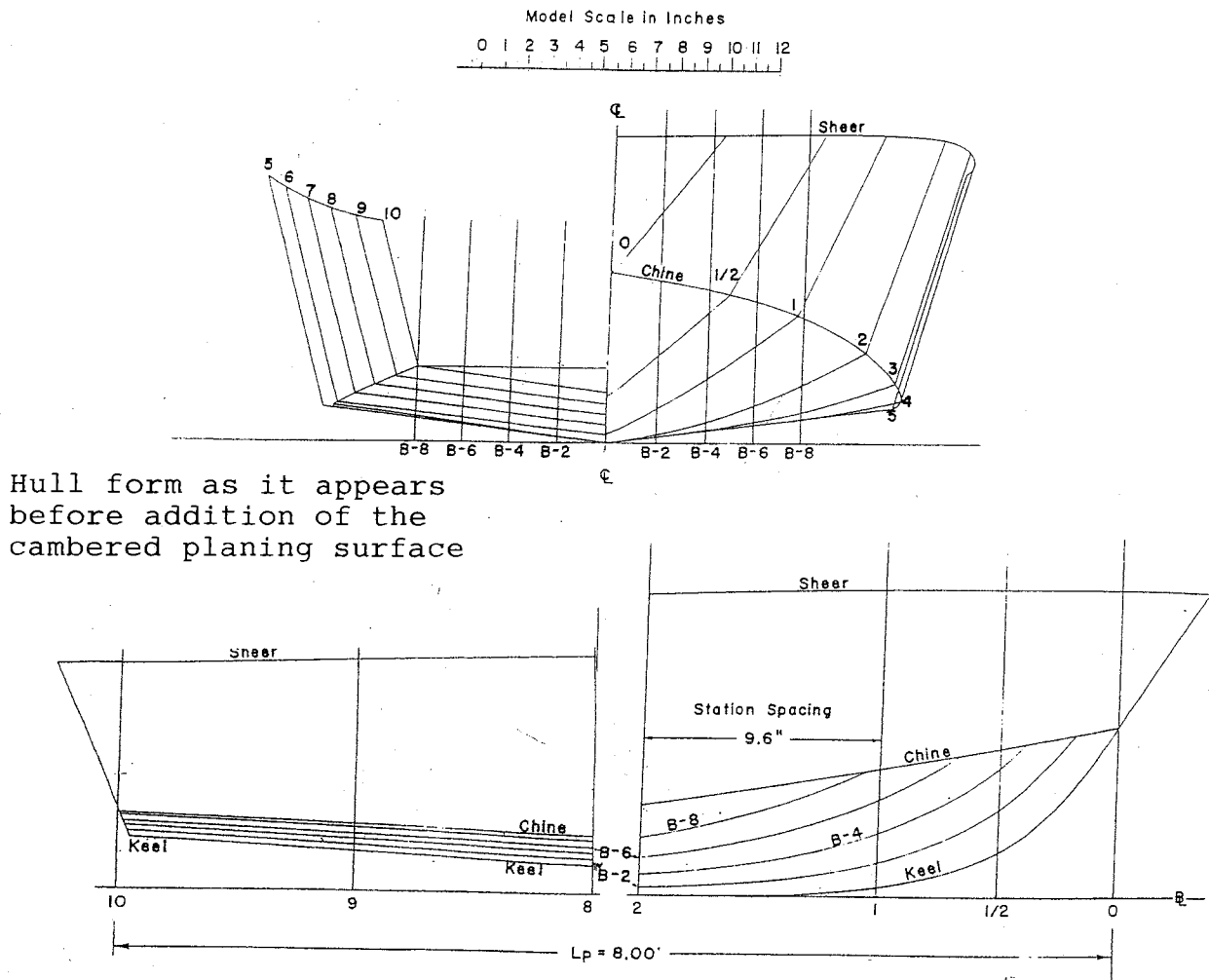


Figure 1-5 - Plan of the Hull of Model 5115A.

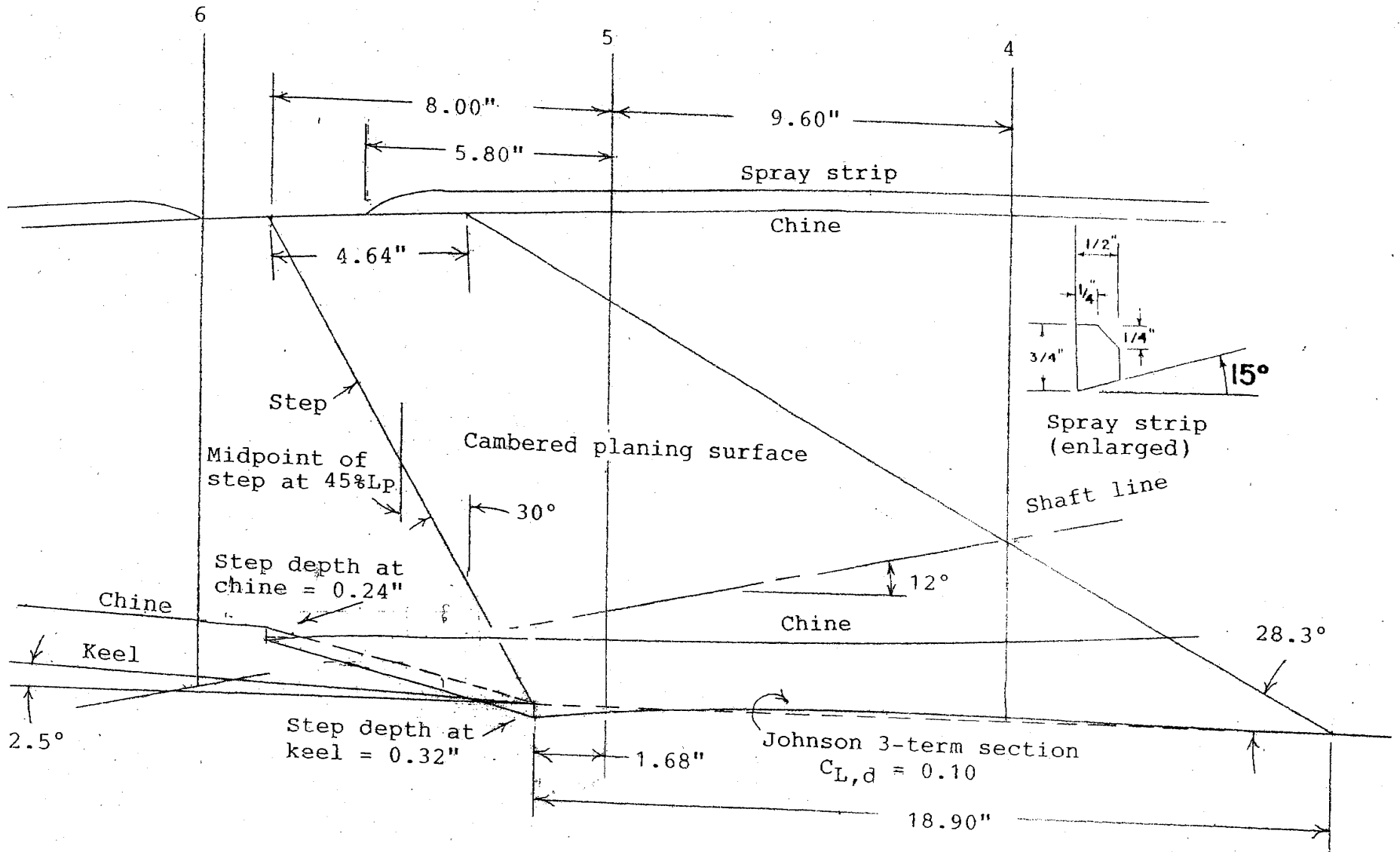


Figure 1-6 - Cambered Planing Region of Model 5115A.

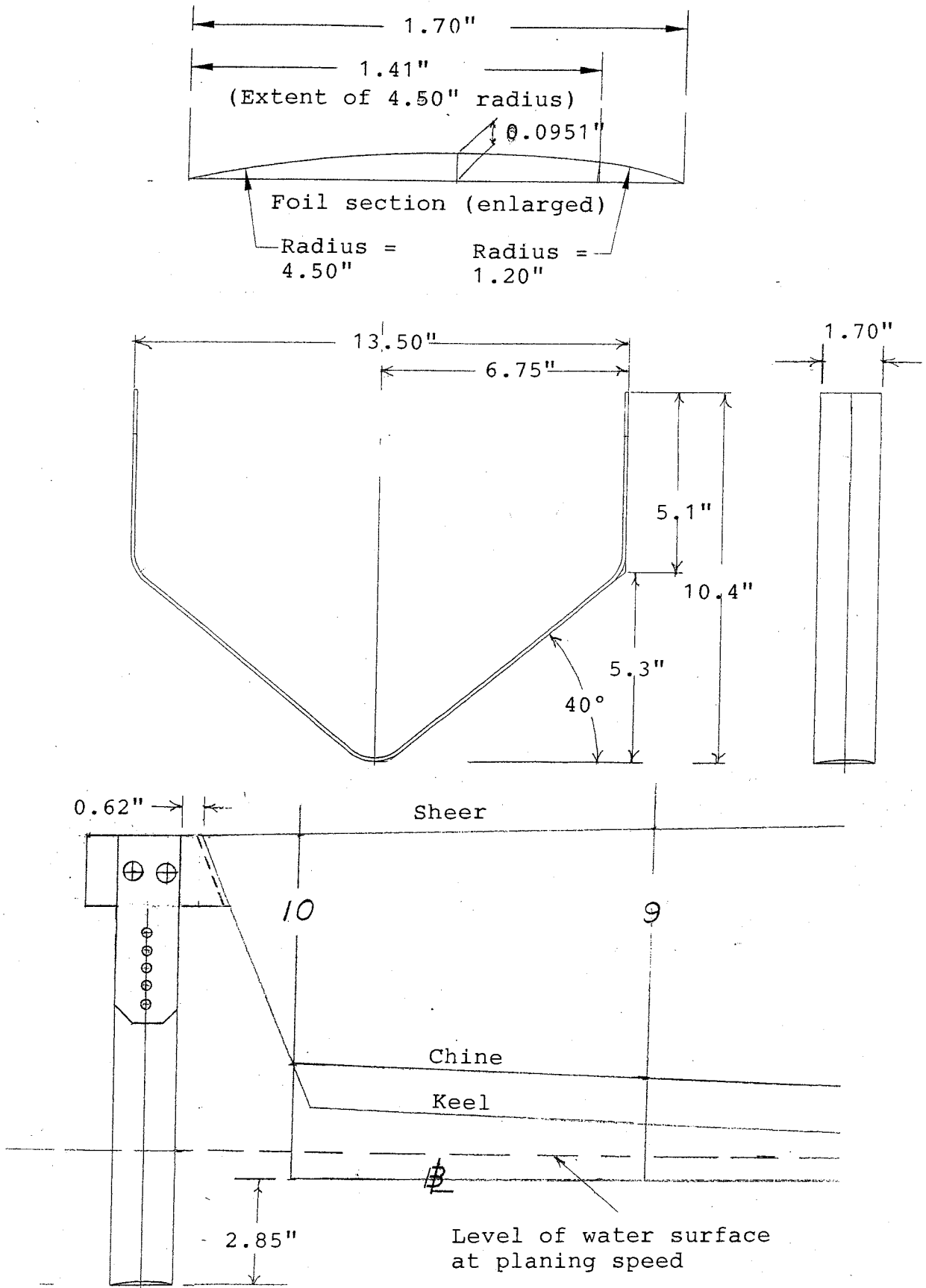


Figure 1-77--The Stern Hydrofoil of Model 5115A



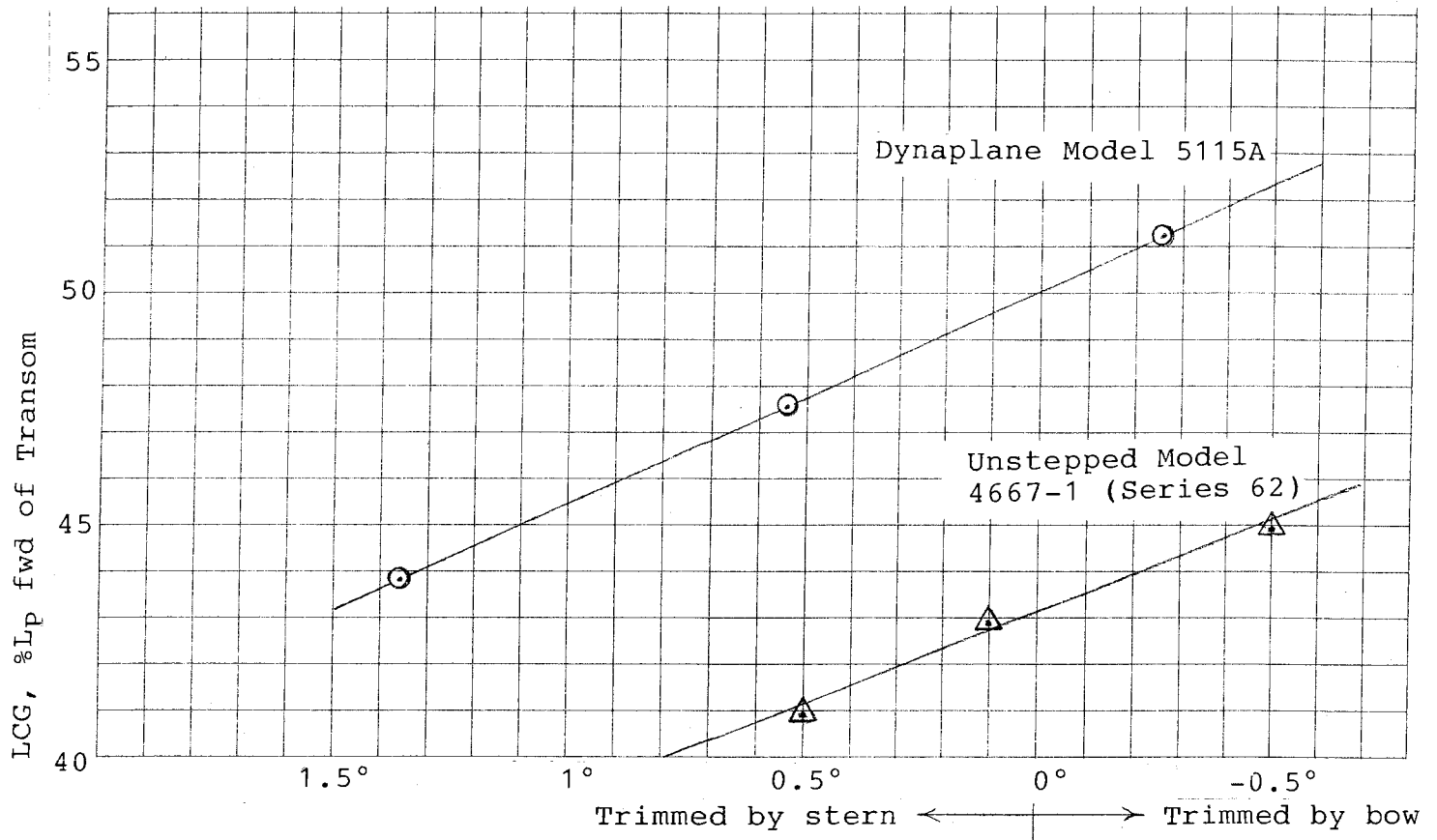


Figure 1-8 - LCG Location vs Floating Angle  $\alpha_0$  for a Dynaplane Model and a Conventional Unstepped Model.

## **Chapter 2**

### **Details of and Design Procedure for a Dynaplane-Type Stepped Planing Boat**

#### **Trim-control feature enables designing for optimum high-speed performance**

An important reason for the superiority of the Dynaplane design is that (because it has the feature of trim-control) it is possible to make calculations that will define, precisely, a configuration that will result in optimum high-speed performance. For the case of the usual single-step boat (without trim-control), however, the designer does not know what the running trim angle of the boat will be at different speeds, weights, and LCG locations. Accordingly any calculations that can be made are very limited in their usefulness and applicability.

#### **Model testing was required in order to develop a hull-form that would have satisfactory performance at the lower speeds**

The calculation procedure that is available for optimizing the high-speed performance of the Dynaplane design provides a method for designing those regions of the boat that are wetted at the high-speed design point, i.e., the cambered region of the forebody, and the stabilizer. However, in addition to attaining efficient high-speed performance, it is essential for the case of a satisfactory stepped boat that its resistance in the lower part of the speed range, and particularly at the hump, be suitably low. A calculation procedure for developing a design that will give satisfactory performance in that part of the speed range is not available. Development of a Dynaplane-type hull form that will give efficient performance at speeds below the high-speed design point was achieved, therefore, with the aid of an extensive program of model testing.

#### **A succession of stepped-hull models with stabilizers was tested**

A succession of models of stepped hulls with adjustable stern stabilizers was built and tested at the David Taylor Model Basin in order to achieve the foregoing goal. The models ranged in length from 8 ft. to 9 1/2 feet, and each one was tested at a number of speeds, weights, and LCG locations. The large DTMB towing carriages made it possible for the test engineer to ride alongside the models and thereby observe the patterns of the water-flow in such critical regions as the step and the afterbody. In addition underwater photographs were taken in order to reveal the details of the flow under the bottoms of the hulls. The observations that were made, and the data that were recorded and analyzed, made it possible to make progressive improvements in the successive models, and ultimately to achieve a very satisfactory hull form..

#### **The suitability of a step of very small depth was investigated**

The first model that was designed and tested had a straight transverse step (and no camber in the forebody planing region). It incorporated a Plum-type planing stabilizer for

trim-control. It was evident from the beginning of the project that it would be desirable, if possible, to utilize steps of small depth. This would be advantageous from the points of view of boat-construction weight and cost. The weight and cost of incorporating a step of very small depth into the bottom of a boat would be minimal. Accordingly the initial test of the first model was made with a step only 1/16 inch deep. The step was formed by fitting a metal strip into the bottom of the model, 2 in. wide, and forming a 1/16 inch-deep step at its trailing edge. This step configuration is shown in Figure 2-1. It was gratifying that the small step performed its intended function in an entirely satisfactory manner. Therefore the next two models that were tested were also designed with steps only 1/16 inch deep and formed in a similar fashion.

### **Single-step boats of the past have had steps that were several inches deep**

The single-step boats of the past have, on the other hand, typically had steps that were several inches deep. Now, incorporating a step several inches deep in the bottom of a motorboat involves considerable amounts of both weight and cost. An important contributing factor is the problem of providing adequate continuity of longitudinal strength of the hull. (Small step depth also contributes to low drag at slow speeds.) Now, the intended high-speed running condition of the stepped boats of the past was to have the after end of the afterbody plane on the surface of the water - and thereby provide stability and the needed aft-end lift. A step several inches deep was necessary in order to give a suitable average clearance of the bottom of the afterbody above the water surface.

### **Clearance of the Dynaplane afterbody above the water surface at high speed**

The foregoing state of affairs is beneficially altered in the case of the Dynaplane design. Since this design incorporates a stern stabilizer which, at high speed, lifts the afterbody clear of the water, a suitable average clearance of the afterbody can be attained with a step of very small depth. The relationship between the afterbody and the level of the water-surface, for the case of a Dynaplane-type boat, when it is running at high speed, is depicted in Figures 1-1, 1-7, and 2-2.

### **Additional details of the first three models that were tested**

The first three models all incorporated a Plum-type planing stabilizer for trim-control. Deadrise angle for each of these was 16°. The forebodies were of simple Vee form with straight buttock lines in the planing regions. Afterbody keel angle in each case was approximately 4.5°. The afterbodies were tapered, in plan view, in the region of the step. (Some details of one of the three models are shown in Figure 2-1.) The testing of these models confirmed that for good performance in the lower part of the speed range a stepped hull should have the following features:

1. A step near mid-length that is of very small depth.
2. An afterbody that is tapered in plan view.

3. An angle between the forebody and after body keels
4. A hull form consisting of developable surfaces. (This also gives the desirable convex bow sections, and facilitates economy of construction.)

### **The satisfactory performance of a step of very small depth was substantiated**

The satisfactory behavior of a step of very small depth was substantiated by the successful performance of the first three models. Close observation also revealed the way in which the tapered afterbody contributes to the successful operation of a small step. When a Dynaplane-type model is at rest, or running at low speed, the level of the water surface is an appreciable distance above the step and there is no pathway for air to ventilate the step. However, the tapered afterbody causes the flow to separate from the chines, in the region of the step, at a relatively low speed. The hull sides in this region then become dry and thereby allow a pathway for air to reach the small step.

### **Selecting a suitable value for the angle of the afterbody keel**

A critical factor in designing a satisfactory Dynaplane-type boat is selecting a suitable angle for the afterbody keel relative to the angle of the forebody keel. One consideration relating to the selection of this important angle is that it should be large enough so that the afterbody will run clear and dry above the water surface at high speed. (This consideration suggests the adoption of a relatively high value for the afterbody keel angle.) A conflicting consideration, however, is that in the speed range at which a hump in the curve of resistance occurs, the afterbody should be sufficiently immersed so as to provide a substantial amount of planing lift. This lift contribution from the afterbody tends to prevent a high trim angle and a high value of hump resistance. The testing of the first three models involved revising and retesting in order to try a number of afterbody keel angles. The testing showed that a suitable angle for the afterbody keel relative to the forebody keel was approximately  $4.5^\circ$ . (One of the models, having an afterbody keel angle of  $4.7^\circ$ , was shown in Figure 2-1.) Since the models incorporated an adjustable stabilizer for trim-control it was possible at each test speed to trim the model to the optimum angle (i.e., the angle giving the lowest resistance). The testing showed that the optimum angle of attack of the forebody, at high speeds, for all three of the models was  $4.5^\circ$ . Accordingly the test results showed that, consistently, at high-speed the best result was attained when the afterbody was running very nearly parallel to the level of the undisturbed water surface. In each case the afterbody ran clear and dry above the wake behind the forebody. This result occurred because in each case the flow came off the step at a downwash angle of approximately  $2^\circ$ . The desired result was accordingly achieved that the wetted area of the hull afterbody was eliminated. It was concluded from the foregoing test results that an important design guide for a Dynaplane-type boat is that the afterbody keel angle should be selected so that the afterbody will be running very nearly parallel to the undisturbed water surface at the high-speed design point.

### **Models 5115 & 5115A (both with camber) substantiated the suitability of the design guide for the afterbody keel angle**

The next two models that were tested (DTMB Nos. 5115 & 5115A) incorporated camber curvature in their forebody planing surfaces. In order to achieve very low resistance those hulls were given a low value of forebody deadrise angle ( $7.5^\circ$ ). The hulls of the two models were basically the same. Drawings of Model 5115A were previously shown in Figures 1-5 - 1-7. Model 5115 was tested with an adjustable Plum-type planing stabilizer for trim control and Model 5115A was tested with an adjustable Vee hydrofoil stabilizer. The cambered regions of the two models were of different sizes. The cambered region of Model 5115 extended a distance of 10.8 in. along the keel and the cambered region of Model 5115A extended the greater distance of 18.9 in. It was explained that for the earlier models, having  $16^\circ$  deadrise and no camber, optimum running trim angle at planing speeds was  $4.5^\circ$ . Optimum running trim angle for a forebody planing surface with camber (the case for Models 5115 & 5115A) is lower than for one without camber. This factor, together with the lower deadrise, resulted in the calculation that for Models 5115 and 511A optimum running trim angle would be approximately  $2.5^\circ$ . Accordingly the afterbody keel angle was given that value in order to adhere to the design guide explained previously that the afterbody keel should run approximately parallel to the undisturbed water surface in the high-speed planing condition. The measured values obtained during the testing showed that at high speed the optimum running trim angle for Model 5115 was slightly above  $3^\circ$  and for Model 5115A, having a different (and larger) cambered region, it was  $2^\circ$ . It was interesting that the afterbody of Model 5115 ran clear and dry above the water surface at planing speeds even though the afterbody then extended aft of the step at a slight ( $\frac{1}{2}$  deg.) "downhill" angle.

### **The testing of Models 5115 and 5115A substantiated the suitability of a step of small depth**

Step depth for Model 5115 was 0.17 in. and average step depth for Model 5115A was 0.28 in. Again, however, the data obtained and the underwater photographs taken of those models substantiated the fact that steps of small depth will perform in an entirely satisfactory fashion. As before, at a relatively slow speed, water separated from the chines of the hulls in the region of the step. The dry chine sides in that region then permitted air to flow onto the faces of the small steps and from there over a portion of the bottoms of the afterbodies. Initially a small region of each afterbody, immediately behind the step, ran clear and dry above the water surface. The dry region of the afterbody that began at the step then progressively increased as the speed of the model increased. That is, the forward boundary of the region of the afterbody bottom that remained wetted moved progressively aft. At planing speeds the entire bottom of each afterbody ran clear and dry above the surface of the water and all frictional resistance from this region of the bottom of the hull was accordingly eliminated.

### **Designing for the high-speed régime**

The design problem for the high speed régime involves developing procedures for

designing an efficient cambered planing surface and an efficient and practical adjustable stern stabilizer. The cambered planing surface should be located near the LCG of the boat and should be designed to carry approximately 90% of the weight of the boat. The overall efficiency of the design in the high-speed régime will accordingly depend chiefly on the performance of this planing surface. In the high-speed planing mode only the planing surface and the small stern stabilizer are in contact with the water. Therefore the remainder of the hull plays no part in determining the performance (apart from contributing a component of air drag). A procedure for designing the efficient planing surface that is wanted was developed with the aid of extensive computer calculations together with the testing of a number of planing surfaces that had deadrise, camber, and sweptback trailing edges. The procedure for designing the cambered planing surface is given in Chapter 4.

### **Example of a complete Dynaplane design**

An example of a complete Dynaplane design is shown in Figure 2-2. The figure illustrates the essential Dynaplane features - a sweptback step of small depth, a cambered planing surface forward of the step, and an adjustable Vee-hydrofoil stabilizer at the stern. The step (and the center of gravity also) are near mid-length. The reason for the sweep-back of the step will be explained subsequently. Vent pipes are provided just behind the step, adjacent to the centerline. With the aid of a flow of air through the vent pipes, the water separates from the bottom of the afterbody at a relatively low speed, beginning at the step. At high speed the entire afterbody bottom runs clear and dry above the surface of the water, and the needed lift aft is provided by the adjustable stabilizer. The high-speed running condition was previously shown in Figures 1-1, 1-7, and 2-2. The water surface levels shown in those figures are based on measurements of the contours of the wake behind models of cambered planing surfaces.

### **A practical procedure for drawing the plan of a Dynaplane boat**

A practical and convenient procedure for developing a plan for a Dynaplane boat is to initially draw the Body Plan and Profile views as they appear without inclusion of the feature of camber. The lines drawings as they appear in Figure 1-1 are shown in this mode. It has also been found to be helpful, during the design procedure, to draw the buttock lines of the forebody, forward of the step, and for some distance forward of it, initially straight, and parallel to the baseline. Then, when the design for the cambered region has been developed, it can be conveniently incorporated into flat regions forward of the step. (The cambered region that was incorporated into the hull form of Figure 1-1 is shown, in enlarged scale, at the bottom of the figure.) The afterbody bottom should be a simple vee shape (with straight and parallel buttock lines) so that it will perform its needed function of providing a significant proportion of the lift at intermediate speeds and at the hump. The entire hull form that has been developed, including the cambered regions, consists of developable surfaces. A result of the developable surface hull form is that the bow sections have the convex shape which is desirable for good rough-water performance. Also, the skins of the corresponding full-scale boats can be economically

made from large sheets of either aluminum or plywood.

### **Suitable forebody and afterbody deadrise angles**

It was mentioned previously that the Dynaplane design is appropriate for deadrise angles up to a maximum of about 15 degrees. (For the case shown in Figure 1-1 the forebody deadrise angle is 12 1/2 deg.) The afterbody deadrise is ordinarily made less than that of the forebody in order to give an approximately constant depth of the step across its span. The afterbody is, of course, tilted up with respect to the forebody so that it will run clear and dry above the water surface at planing speeds. The square transom, with relatively low deadrise, plays an important role at intermediate speeds and at the hump. At these lower speeds the stern hydrofoil will provide only a relatively small amount of lift. Therefore the afterbody has an essential role to play in providing lift and in constraining the hull to run at a trim angle that will give suitably low resistance at the hump. The tapered stern tends to give low drag in the lower part of the speed range, and the wide forebody provides good transverse stability in the high-speed planing condition. The model testing program included trying a variety of spray strip arrangements. The spray strip design that gave the best result is shown in Figure 1-6. The forebody spray strips extended to the bow and the afterbody spray strips extended to the stern. The bottom edges of the spray strips were horizontal when installed on the hull model.

### **Selecting the chief dimensions**

The dimensions and the deadrise angle (15 deg max.) of a design for a Dynaplane-type of boat can be selected in the same manner as for the case of designing a conventional (unstepped) planing motorboat. Accordingly, with the boat's purpose and desired speed specified, determinations of the length, the beam, the deadrise angle, and the weight can be made in the usual way. Examples of previous successful stepped and unstepped designs can be referred to for guidance in selecting suitable values for a projected new design. The center of gravity of a stepped planing boat that is intended to be of maximum utility should be located close to the mid-length point of the hull. This will result in a suitable floating trim angle (angle of the straight portion of the forebody keel with the horizontal) of between zero and one degree by the stern. Because of the very high density of the fluid medium the amidships lifting area needed to support the major portion of the weight of a stepped boat (about 90%) is extremely small. The initiate to the art of designing a Dynaplane-type of boat is likely to be very surprised to find how small an appropriately designed main lifting area will be. A hull bottom width of the usual size will accordingly provide the needed span dimension, and a relatively short wetted length will provide the needed fore-and-aft dimension. (The possibility of developing a planing boat design analogous to a "tailless" airplane obviously suggests itself. However, experience has shown that a short planing surface running by itself will not operate stably. It has further been found that if approximately 90% of the weight of a stepped planing boat is carried by a short planing area located near amidships, and the remainder of the weight is carried by a small lifting area at the stern, this will result in a configuration which will run stably.)

## **A table of offsets**

Table 1 presents a table of offsets for a 35 in. long (model) version of the Dynaplane hull-form that is shown in Figure 1-1. These offsets can be utilized to derive full-scale offsets for Dynaplane hull-forms of a wide range of lengths, beams, and deadrise angles. When the dimensions and the forebody deadrise angle of a projected new design have been selected, appropriate constants can be applied to the offsets in Table 1, to produce suitable and accurate offsets for the new design. The new design will retain the virtue of consisting of developable surfaces, even though the length/beam ratio and/or the deadrise angle, have been changed. The foregoing procedure is chiefly applicable for defining the bow portion of the new hull (i.e., the region forward of the step). The afterbody (i.e., the region aft of the step) consists chiefly of flat surfaces. The procedure for designing that portion of the hull, which includes selecting the afterbody keel angle and the depth of the step, are explained in Chapter 5.

## **Benefits of having an adjustable stabilizer**

The adjustable stern stabilizer of a Dynaplane-type boat introduces a complication, but this makes it possible to maintain the trim of the boat to the angle for minimum drag, and also makes it possible to avoid two types of misbehavior to which a stepped boat with a fixed rear lifting surface is susceptible - porpoising, and nosediving in a following sea. The possibility of the nosediving should be of particular concern since that type of misbehavior has occurred in the case of a number of stepped boats of the past (which had fixed sterns). This event can occur when the forward planing surface of a stepped boat encounters the downward-moving water particles in the back of a wave, and therefore loses lift, while at the same instant the rear planing surface is developing a relatively high lift. The combined effect is that the boat may be trimmed down to such a dangerously low angle that the bow buries itself in the back of a wave. This likelihood can be avoided with an adjustable rear lifting surface, which can be used to trim the boat to a suitably high and safe angle when running in a following sea. An adjustable rear surface can also be utilized to prevent porpoising.

## **A Vee hydrofoil as the adjustable stern stabilizer**

The type of stern device (for trim-control and stabilization ) that is obviously eminently suitable to use for a Dynaplane boat is a surface-piercing Vee hydrofoil. A foil of this type was shown in Figure 1-7. This foil will typically carry about 10% of the weight of the boat at the design speed. It will provide inherent stabilization in heave and trim when fixed in position. However, provision should be made for vertical adjustment of the foil in order to provide the wanted control over the running trim angle of the boat. (It is proposed that the vertical adjustment be provided by mounting the hydrofoil on a power-actuated transom jack of the type used for adjusting the heights of outboard motors.) Results from the tank testing of Vee hydrofoils, at different depths of submersion, and up to high speeds, were given in Reference 4. Results from that



reference which are of interest for the present case are given in Chapter 6. That chapter also includes guidelines to foil design that have been learned from the experiences of enterprising entrepreneurs who have designed, built, and tested hydrofoil-supported motorboats. It should be noted that the type of foil shown in Chapter 6 is suitable for speeds up to a maximum of approximately 50 mph. At higher speeds cavitation or ventilation is likely to occur, with significantly adverse effects on the performance of the hydrofoil. Adopting a speed limit of 50 mph makes it possible to calculate appropriate limits on installed hp for ranges of values of weight and deadrise angle. The recommended limits on installed power are shown in Figure 2-3.

### **Boating satisfaction from the trim-control feature**

There is a significant point to be made about the trim-control feature in relation to the highly important factor of marketing. Particular enjoyment and satisfaction are derived from the operation of a fast runabout when the pilot is able to adjust the angle of attack of his craft. The experience of skimming over the water on an efficient cambered planing area, and, with the throttles fixed, adjusting the position of the stern hydrofoil up or down to find the optimum running angle of attack (as shown by the speed gauge and the tachometer) is outstanding fun! This is in marked contrast to the case for a conventional (unstepped) boat with adjustable stern trim flaps. Such flaps are only useful at low speeds for getting over the hump. At planing speeds such a craft runs at a low, and inefficient, trim angle, and activation of the stern flaps will lower the running trim angle further and make the craft even more inefficient. Therefore, at planing speeds such flaps are usually retracted clear of the water.

### **Contents of the remaining chapters**

Chapter 3 of this booklet gives details of the shortcoming of stepped boats of the past, and Chapter 4 explains how to design the highly important (cambered) main planing surface. Chapter 5 gives pointers about designing a step and an afterbody, and also explains how to predict the drag at the "hump." Finally, Chapter 6 provides particulars about the surface-piercing the hydrofoil that is recommended as the stern trim control device. It should be noted that this booklet is not a complete text on how to design a Dynaplane-type of stepped motorboat. Its intention, instead, is to supply the additional information that will enable an experienced motorboat designer to design a successful boat of that type. A design produced on the basis of the information given here, by someone other than an experienced motorboat designer, should be thoroughly checked by a suitably-qualified person, before construction of a boat.

Table 1

Offsets in Inches for a Model of a Dynaplane Hull, Before Inclusion of the Forebody Camber

Chine length (Sta. 0 to Sta. 10) = 35 inches

Station spacing = 3.50 inches

Forebody deadrise equals 12.5 deg; afterbody deadrise equals 10.7 deg; afterbody keel angle equals 3 deg.

	Heights												
Stations	0	½	1	1.5	2	3	4	5	6	7	8	9	10
Sheer	5.58	5.58	5.58	5.54	5.48	5.31	5.10	4.88	4.68	4.48	4.25	4.04	3.85
Chine	3.13	2.75	2.42	2.15	1.93	1.59	1.33	1.14	1.06	1.20	1.36	1.49	1.64
Keel	3.13	0.94	0.20	0.03	0	0	0	0	0.16	0.33	0.52	0.70	
0.82in. Btk	4.00	1.68	0.69	0.36	0.26	0.20	0.20	0.18		0.48	0.67	0.85	
2.45in. Btk		3.52	1.86	1.22	0.89	0.65	0.58	0.55		0.79	0.97	1.16	
4.09in. Btk			4.40	2.59	1.76	1.24	1.03	0.94		1.10	1.29	1.45	
	Half-Breadths												
Sheer	2.01	3.59	4.63	5.31	5.74	6.18	6.22	6.03	5.85	5.58	5.29	4.98	4.64
Chine	0	1.99	3.17	3.90	4.37	4.90	5.01	4.87	4.80	4.63	4.44	4.23	4.00
3.27in. WL			3.58	4.39	4.91	5.47							
4.91in. WL	1.55	3.23	4.32	5.06	5.54								

The afterbody sections in the body plan view consist of straight lines.  
The afterbody buttocks are all straight lines.

Before inclusion of the camber:

The keel is straight from the step forward to Station 1.7.

Btk 2	"	"	"	"	"	"	"	"	"	"	"	"	3
Btk 6	"	"	"	"	"	"	"	"	"	"	"	"	4
Btk 10	"	"	"	"	"	"	"	"	"	"	"	"	5

This hull form consists entirely of developable surfaces. Alternative hull forms, having different length/beam ratios, or different deadrise angles, can be derived, by changing the station spacing, or by multiplying all of the height dimensions or all of the half-breadth dimensions by a constant. The resulting hull forms will consist of developable surfaces.

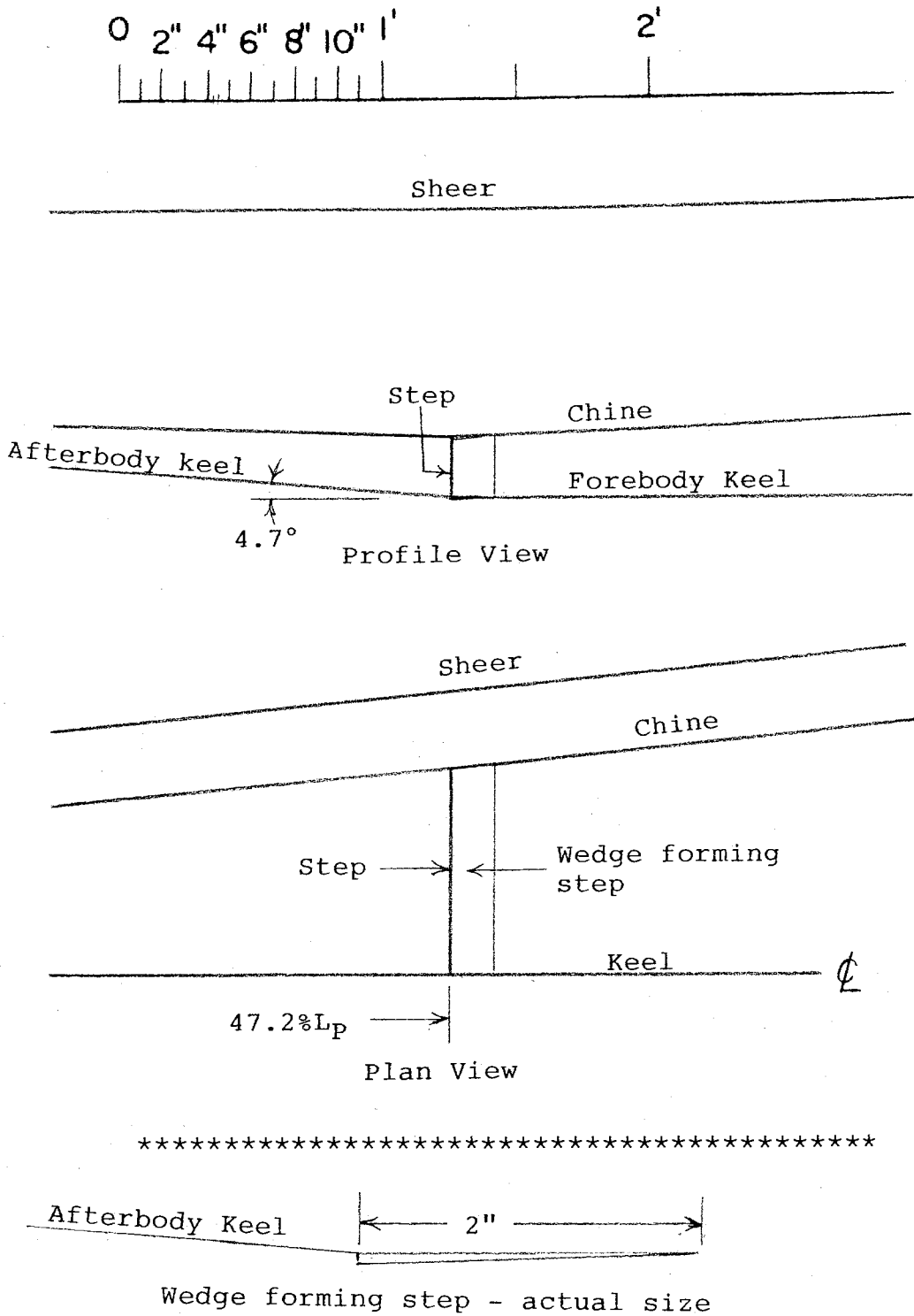


Figure 2-1 - Midbody Region of One of the Models of Stepped Hulls that was Tested at DTMB. Depth of the Step is 1/16 Inch.

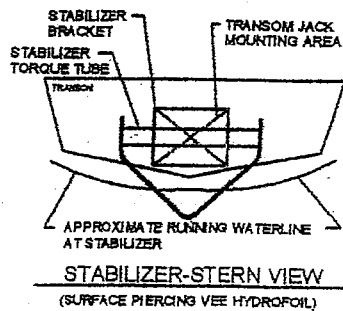
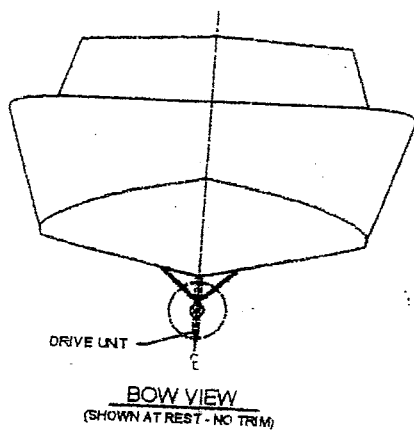
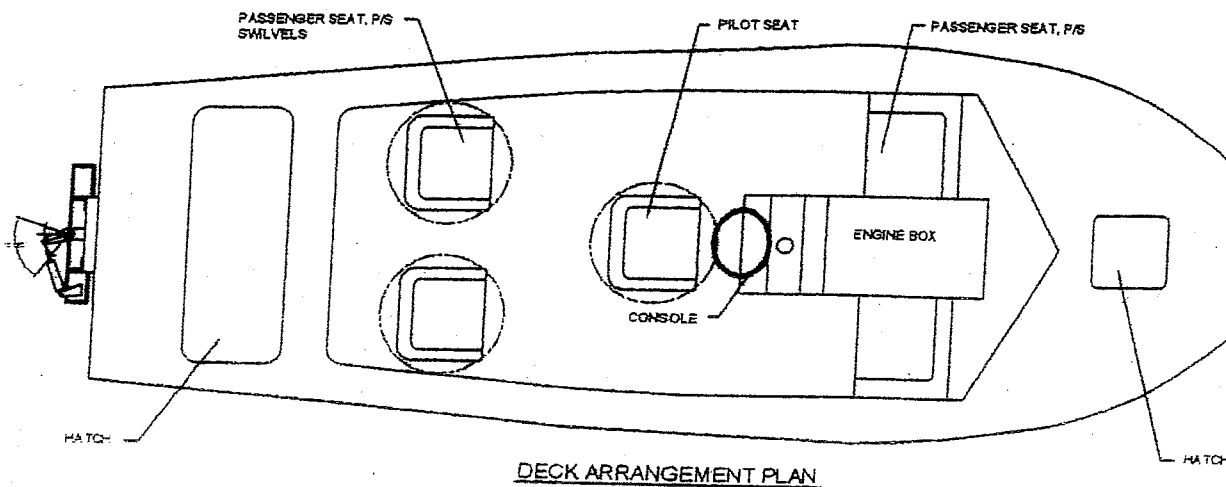
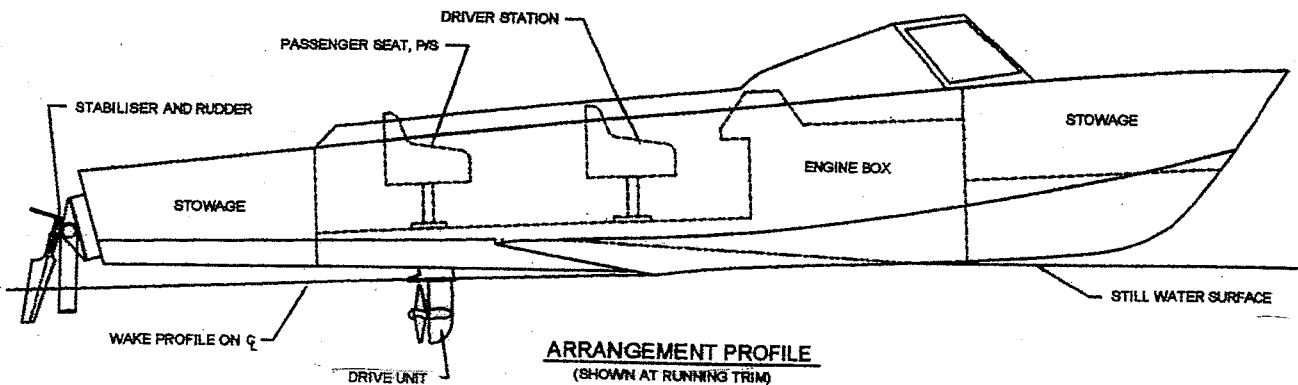


Figure 2-2 - A Dynaplane-Type Recreational Motorboat

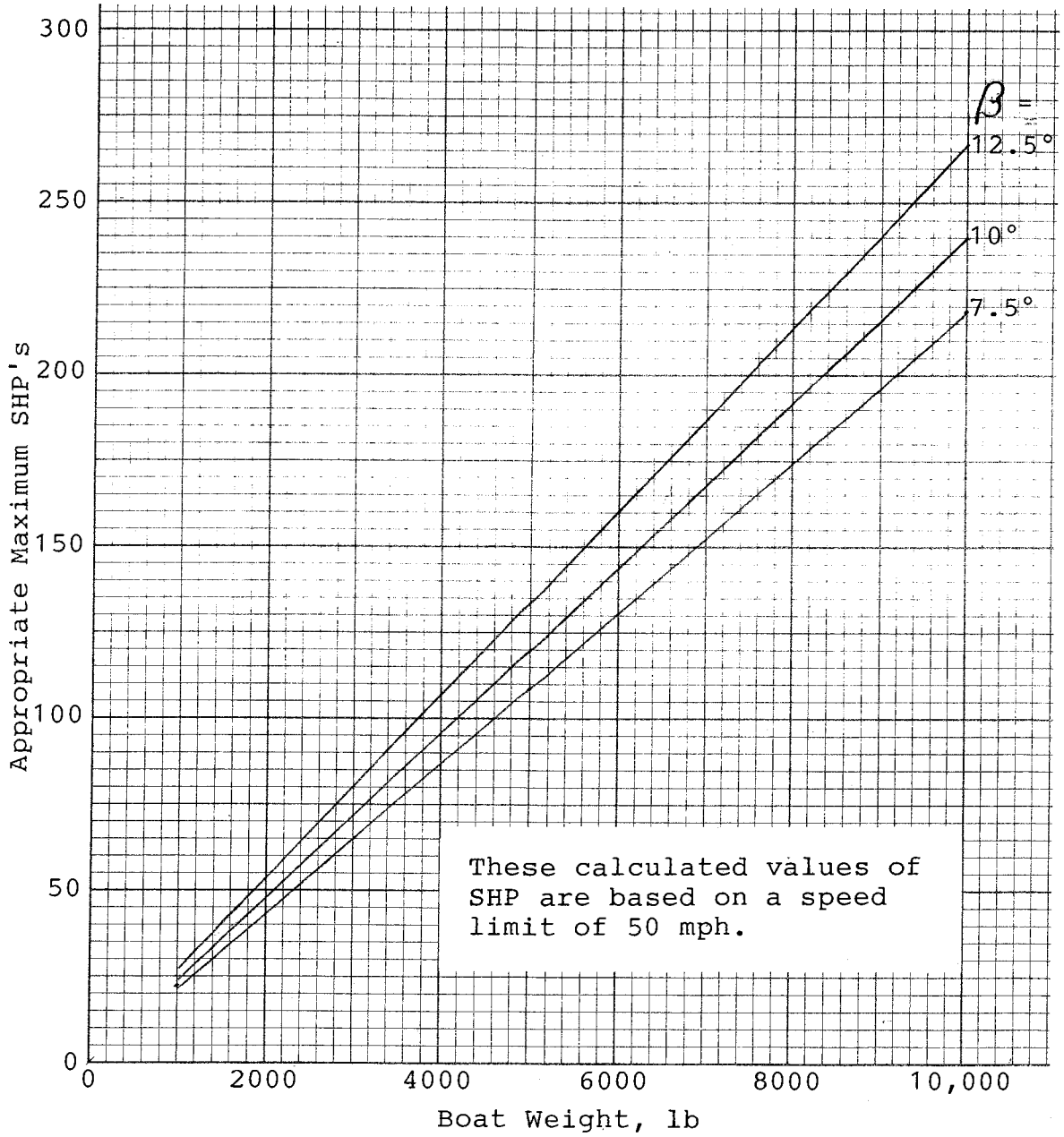


Figure 2-3 - Appropriate Maximum Values of Installed Horsepower for Dynaplane-Type Boats of a Range of Values of Weight and Deadrise Angle.

## **Chapter 3**

### **Shortcomings of Previous Stepped Boats, and the Sweptback Step**

#### **The typical stepped boat of the past**

A great many stepped motorboats were built during the past century. In most cases those boats incorporated a single, relatively deep, transverse step at approximately mid-length. Figure 3-1 is a plan view showing the chine lines and the step of a typical configuration. This figure also indicates the regions of forebody and afterbody that are wetted at high speed if the boat runs stably and in the intended manner. Unfortunately, however, as explained in Reference 5, stepped boats of the past have tended to exhibit a variety of types of misbehavior. Those included porpoising, bow steering, barrel rolling, end-for-end broaching, and running right through waves. Chapter 1 referred to a series of 27 models of stepped planing hulls which were tested in Sweden. Those models were representative in form of many of the stepped boats built during the past century. The susceptibility of the type to porpoising is indicated by the fact that the majority of the models of the series tested in Sweden porpoised when running relatively fast. The model from the Swedish series which is represented in Figure 1-3 ran stably at a particular condition of weight and CG location, but would be liable to porpoise at other conditions. Furthermore, Figure 1-3 indicates that the resistance of the type at high speed is more than 25 percent higher than the resistance of the proposed Dynaplane type of stepped planing boat.

#### **A step can reduce the resistance**

For those cases where the stepped type of the past has run without porpoising, and at a condition approaching the hoped-for condition shown in Figure 3-1, it has had lower resistance than a corresponding unstepped boat. If the step is suitably sharp it will result, at a relatively low speed, in the flow separating from the bottom of the hull immediately behind the step; then, as the speed increases, the extent of the region of the afterbody bottom from which the flow is separated also increases, and at high speed only the aft-most portion of the bottom of the afterbody remains in contact with the water. This condition is displayed in Figure 3-1. The extent of the afterbody bottom that now remains wetted, and therefore also the amount of the frictional resistance of the afterbody, are therefore substantially reduced. (The region of the forebody bottom that is wetted at planing speed is also less than when the boat is at rest, whether a planing hull is stepped or unstepped.)

#### **Trim-control needed to maintain optimum running trim**

When running at high speed most of the weight of a single-step boat (typically about 90% ) will be carried by the main (forward) planing surface. This will be the result in the typical case where both the step and the LCG are near the mid-length of the boat. The small wetted region of the hull bottom near the stern will therefore be carrying about 10% of the weight. The significant index of the performance of the design (i.e., the

lift/drag ratio), will accordingly be close to the value of the lift/drag ratio of the main (forward) planing surface. A design goal for such a craft will, of course, be to maximize its high-speed lift/drag ratio. Achievement of this will require that the important forward planing surface consistently operate, at the different speed and loading conditions of the boat, at its optimum angle of attack. Now, the angle of attack at which the forebody runs is chiefly determined by the relative positions of the forebody and the aft end of the afterbody. Now, the requirement that the forebody consistently run at its optimum angle of attack cannot be achieved by the usual type of stepped boat, having a fixed afterbody, since the position of the afterbody (relative to the forebody) that will give this result changes with the changes in the speed, weight, and CG location of the boat. If an adjustable rear lifting surface is used instead, however (a feature of the Dynaplane design), optimum angle of attack of the forward planing surface can be maintained at different speeds, weights, and CG locations, and therefore minimum resistance can be achieved for a wide range of conditions of operation.

### **The problem of spray wetting the afterbody**

The stepped boats of the past have been further limited in their performance by a particular type of spray from the forebody wetting the afterbody and causing a large increase in drag. Examples from model tests of the occurrence of this drag rise were presented in Reference 6. The phenomenon can be explained by reference to Figure 3-1. When a typical stepped hull is planing on the surface of the water the forebody bottom (i.e., the region ahead of the step) is wetted by two different types of flow. There is a region beginning at the step and extending some distance forward of it which is wetted by solid water. This is a region of relatively high pressure which supports most of the weight of the boat. The forward boundary of this region is the "spray-root" line. When planing most of the afterbody bottom should be clear of the water in order to reduce the frictional component of the hull drag. Forward of the region of the forebody which is wetted by solid water there is a region which is wetted by a thin sheet of "whisker spray." A second type of spray is also produced by the forebody - a pair of "main spray blisters." Details of the origin and shape of this spray formation have been explained in Reference 7. It is this latter spray formation which can produce an objectionable large drag rise. As indicated in the figure the main spray blisters ordinarily originate at the intersection of the spray root lines with the chines of the boat. The main spray blisters are jets of water which shoot upward and outward from their points of origin, forming approximately the shapes of cones. The spray root lines on the bottom of the forebody are lines of high pressure, so it is readily understandable that strong jets of water will occur at the chines, where the high pressures are released. Now, the spray root lines are near the bow at the lower planing speeds, and move progressively aft as the speed increases. This shift occurs because the lift per unit of area on the bottom of the forebody is proportional to the square of the speed, so that as the speed increases, less and less bottom area is required for it to provide its needed proportion of lift. In other words, the forward boundary of the wetted region moves aft in such a way as to maintain a balance between the downward weight and the planing lift. Eventually, when a relatively high speed is reached, the chine ends of the spray root lines come close to the step. This condition is shown in Figure 3-2. Then, with

further increase in speed, the spray root lines will intersect the step rather than the chines. The points of origin of the main spray blisters will now be under the bottom of the afterbody. Accordingly, each upward-shooting cone of water will now wet a portion of the afterbody, and will thereby produce a substantial increase in drag. Since in this condition the width of the hydrodynamic pressure area supporting the weight of the boat is diminished, the transverse stability will also deteriorate. A further highly undesirable effect of the afterbody-wetting phenomenon is that it tends to cut off the flow of ventilating air to the step and the afterbody. In some instances a subsequent result of this effect is that a reduced pressure is produced on the bottom of the afterbody. The hull will then be sucked down, and the entire afterbody bottom will become wetted. The drag rise in this condition will, of course, be very great indeed. It will readily be appreciated, too, that when a stepped boat is running in even small waves the spray-root lines on the bottom of the forebody will be continuously moving back and forth. If those spray-root lines cross the step, then, intermittently, large increases in drag will occur. Accordingly, it will be apparent that in order to avoid the problem, it is necessary that the spray-root lines consistently intersect the chines an adequate distance forward of the step. Or, in other words, it is necessary that, at the intended operating conditions, there is an adequate value of tip-chord wetted length.

#### **Spray on afterbody can be avoided with a sweptback step**

The problem for a stepped hull of spray wetting the bottom of the afterbody, and causing a large drag rise, can be overcome by adopting sweep-back of the step, as was proposed in Reference 8. By sweeping the step back, good planing efficiency can be maintained up to very high speeds. The method of designing planing surfaces having camber and trailing edge sweepback is given in Chapter 4. Some of the alternative plan-form configurations that can be adopted for a swept-back step are shown in Figure 3-3. If the step is given an appropriate sweepback angle, then boat speed can be increased to a high value (when the wetted bottom area of the forebody will decrease to a low value) without producing wetting of the afterbody by the main spray blisters produced by the forebody. Accordingly, high speeds can be attained, and, also, waves can be negotiated, without encountering the drag-rise produced by impingement of spray on the bottom of the afterbody. If the step is swept back so that it is parallel to the spray-root line, then as the speed increases the supporting wetted area can decrease almost to zero without producing wetting of the afterbody by the main spray blisters (step a in Figure 3-3). However, a configuration similar to b is generally preferable, because a highly swept-back step causes some reduction in lift/drag ratio, and also may be difficult to ventilate adequately. Alternatively, the step can be curved in plan view, like c.

#### **High values of aspect ratio can be attained with a sweptback step**

It is significant that with a transverse step the aspect ratio will increase, with increase in speed, only up to the point where the forward boundary of the region wetted by solid water intersects the step. With further increase in speed the aspect ratio remains constant. With a sweptback step, on the other hand, the aspect ratio will continue to increase as the speed increases. High values of planing aspect ratio can therefore be attained, and the planing efficiency is improved as a result. This explains the point made in Chapter 1 that, as the design speed of a Dynaplane boat increases, the main component of the hydrodynamic hull drag ordinarily decreases.



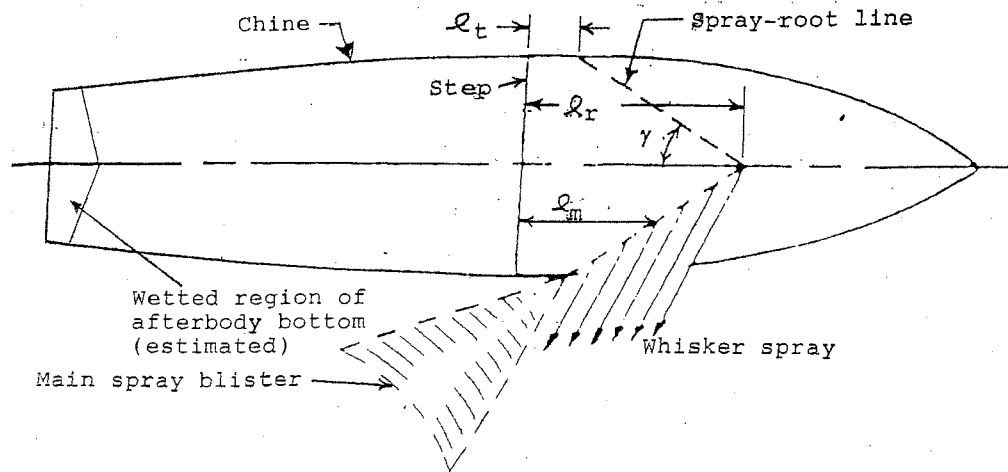


Figure 3-1 - Typical Planing Configuration for the Case of a Stepped Boat With a Main Planing Surface Having a Square Trailing Edge, When Running at High Speed.

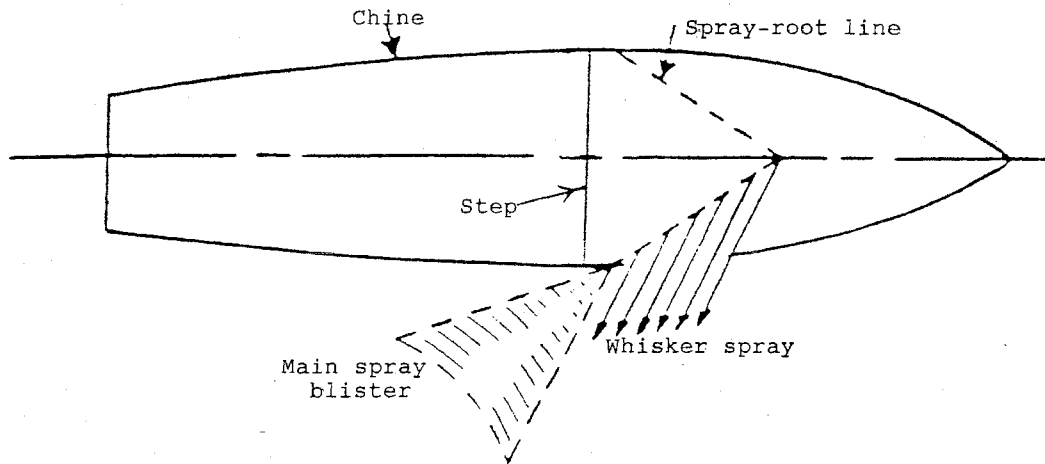


Figure 3-2 - Planing Configuration with the Chine Ends of the Spray-Root Lines Close to the Step.

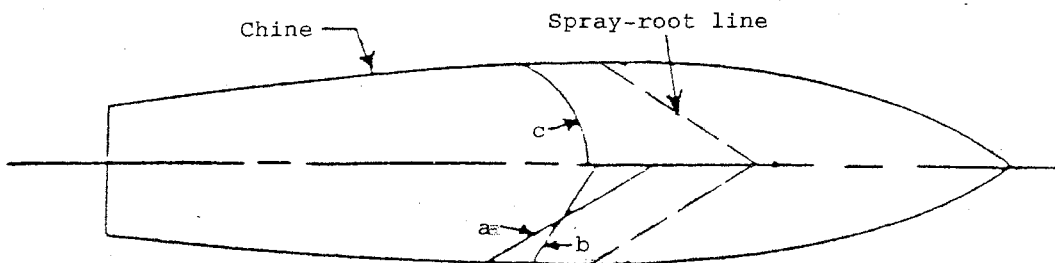


Figure 3-3 - Several Alternative Configurations for a Sweptback Step.

## **Chapter 4**

### **Design Procedure for a Planing Surface Having Camber**

#### **The Virgil Johnson camber shapes**

Appropriate camber curvature is essential for the attainment of optimum performance (i.e., maximum lift/drag ratios) from the planing surfaces of stepped motorboats. The subject of suitable camber shapes for stepped boats has not received anything approaching the attention devoted to camber shapes for airplane wings. However, one outstanding research publication is available that can be utilized for designing camber shapes for stepped planing boats. This is Reference 9, by Virgil Johnson. The goal of Johnson's work was to develop equations defining optimum hydrodynamic camber shapes (and their performance characteristics) for the lower surfaces of supercavitating hydrofoils when operating near the free water surface. Johnson succeeded in his objective, and he reported in Reference 9 that the results of his theoretical and experimental investigation showed that substantial improvements in lift/drag ratios could be achieved over the values for flat plates. Johnson's equations are limited, however, to the case of rectangular planform and zero deadrise. At DTMB Johnson's equations were solved for the condition of zero depth of the leading edge of the camber section (this is the planing case), and the results were used to prepare graphs that could be used for boat-design purposes. The graphs are based on Johnson's "3-term" camber shape which appeared to be the camber-type that would be most suitable to use for stepped planing boats. Comprehensive sets of the graphs for the 3-term camber are given in References 10 and 11. By means of those graphs it is possible to determine values of lift/drag ratio and center of pressure for planing surfaces (having rectangular planform and zero deadrise), for wide ranges of values of aspect ratio, trim angle, and amount of camber curvature.

#### **High L/D's attainable with the Virgil Johnson camber**

The substantial increases in attainable values of lift/drag ratios promised by Johnson's theory are shown by Figure 4-1. This figure compares calculated values of lift/drag ratio for a flat plate, with the values calculated for a surface having the Johnson 3-term camber. The aspect ratio is 2 for both cases. It can be seen that the maximum calculated value of lift/drag ratio for the flat plate was 11.5, whereas for the cambered surface it was 17.5. The extent of the anticipated improvement in lift/drag ratio is accordingly more than 50%. The validity of the very high values of L/D predicted by Johnson's theory were verified by testing a planing surface model which incorporated Johnson's 3-term camber. The model had a rectangular planform, zero deadrise, and an aspect ratio of 2.0. (Further particulars of the model that was tested, and also the data obtained from the testing, are given in Appendix A.) The gratifying result was obtained that the experimental values of lift/drag ratio were even higher than those predicted by the theory. This can be seen from Figure 4-1, which includes a comparison of predicted with experimental values of lift/drag ratio for a surface having the 3-term camber. The testing of the planing surface model also yielded the interesting result that the experimental

values of lift coefficient corresponded very closely to the calculated values derived using Johnson's equations. Accordingly the graphs of References 10 and 11 can be relied upon to give dependable guidance for the selection of suitable values of size, aspect ratio, trim angle, and amount of camber, for the planing surfaces of stepped boats.

### **Correction factors needed for deadrise and sweepback**

The graphs in References 10 and 11 are for the case of rectangular planform and zero deadrise. In any practical design case the main planing surface of a stepped boat will have deadrise, and the planform shape will usually be swept back like the wing of a high-speed airplane. Both of these factors tend to decrease the lift and to increase the drag. Accordingly, when utilizing the graphs based on Johnson's equations, for a practical design case, it is necessary to apply suitable correction factors to account for the effects of deadrise and planform sweepback. Several planing surface models having deadrise and sweepback, as well as camber, have been tested, and the needed correction factors have been derived from the results of those tests. The factors are included in the design procedure which is provided in this chapter. The procedure for designing an efficient (cambered) main planing surface for a Dynaplane-type stepped boat (and for determining the drag), is given by the numbered steps of the design procedure provided at the end of this chapter. The graphs needed to facilitate the procedure are included as well as an example of the procedure.

### **Design procedure for cambered planing surface**

The first step of the design procedure is to select a suitable value for the deadrise angle of the main (forebody) planing surface. That value will depend on whether the boat is intended for operation in smooth and protected waters, or in relatively rough water. For the case of a stepped boat having camber the deadrise angle will ordinarily be in the range between about 5 degrees and 15 degrees. The design angle of attack can then be determined from Figure 4-2. The shape and dimensions of the chine line in plan view will have been determined by the method explained in Chapter 2. The width of the forebody cambered planing surface can then be taken to be equal to the chine width at 45% of the bottom length from the stern. The values for the forebody deadrise and the chine width, together with the specified maximum speed and the estimated gross weight of the boat, provide the input values needed for designing the cambered main planing surface. This surface should be designed to carry 90% of the weight of the boat, with the remaining 10% carried by an adjustable hydrofoil stabilizer at the stern. Figures 4-3 through 4-7 are included as needed components of the design procedure. Figure 4-8 shows a plan view of the planing surface, and also a "balance diagram," for the design example. Figures 4-9 through 4-11 are graphs (taken from Reference 11) that are required for the particular design example. That is, the graphs are applicable for an aspect ratio of 2.0, and a trim angle of 2.5 deg. The offsets for the Johnson three-term camber curve are needed for the design procedure. These are given (in dimensionless form) in Figure 4-12.

### **Determining locations of center of pressure and of step**

The distance of the center of pressure on a cambered planing surface forward of the trailing edge, as a proportion of the mean wetted length, is determined at step 15 of the design procedure. The significant mean wetted length (or mean hydrodynamic chord), for the case of a planing surface with taper and sweepback, is analogous to the "Mean Aerodynamic Chord" (M.A.C.) of an airplane wing. The M.A.C. (or, in this case, the M.H.C.) can be determined by the graphical process indicated in Figure 4-8a. Then, with the position of the center of pressure located on the plan view of the cambered planing surface, the fore-and-aft location of this planing surface, and therefore of the step, can be determined by means of a balance diagram like that shown in Figure 4-8b. That diagram is for the case of a hydrofoil-type stabilizer at the stern, like the design shown in Figure 1-1 of Chapter 1.

Design procedure for a cambered planing surface after the speed, weight, and planing surface beam have been determined.

1. Calculate the lift coefficient,  $C_{Lb\beta} = \frac{0.9W}{\frac{1}{2} \rho v^2 b^2}$
2. Select type of camber curve - Johnson 3-term.
3. Select value of deadrise angle,  $\beta$ .
4. Select ratios of tip chord to beam,  $l_t/b$  (typically,  $l_t/b = 0.2$ ), and of root chord to beam,  $l_r/b$  (typically,  $l_r/b = 0.8$ ).
5. Calculate aspect ratio,  $AR = \frac{2}{l_r/b + l_t/b}$
6. Select appropriate value for trim angle,  $\tau$ , from Figure 4-2.
7. Determine value of angle,  $\gamma$ . ( $\gamma$  is the angle between the spray-root line and the centerline, in plan view. The spray-root line is the forward boundary of the region of the bottom that is wetted by solid water, and therefore the forward boundary of the region that is to be cambered.) First, determine the value of  $\gamma$  for the case of a prismatic surface (without camber), from either the equation or the graph of Figure 4-3. Then add a correction factor of five degrees to that value to obtain the value for the case of a planing surface with camber.)
8. The planing surface in plan view is now fully determined. Accordingly, the following two angles can either be determined by drawing the planing surface and measuring them, or they can be determined from the figures, as indicated.
9. Determine value of  $\phi$  from either the equation or the graph of Figure 4-4 ( $\phi$  is angle of sweep of 50% chord line).
10. Determine value of  $\theta$  from either the equation or the graph of Figure 4-5 ( $\theta$  is sweepback angle of the step).
11. Determine  $(C_{Lb\beta} / C_{Lb0})_{DL}$  from Figure 4-6. "DL" indicates Davidson Laboratory.
12. Determine  $\frac{(C_{Lb\beta} / C_{Lb0})_{Exp.}}{(C_{Lb\beta} / C_{Lb0})_{DL}}$  from Figure 4-7.  
The subscript "Exp." indicates a value corresponding to the experimental value that would be obtained from a test of a cambered planing surface having the configuration of the present design.
13. Multiply value from step 11 by value from step 12 to get  $(C_{Lb\beta} / C_{Lb0})_{Exp.}$

14. Divide  $C_{Lb_{\beta}}$  by value from step 13 to get  $C_{Lb_0}$ .
15. Enter the graphs of the performance characteristics of cambered planing surfaces having rectangular planform and zero deadrise (NSRDC Report 3147) with the value of  $C_{Lb_0}$  to determine  $(L/D)_J$ ,  $C_{L,d}$ , and  $\rho_{CP}/\rho_m$ . The subscript "J" indicates Virgil Johnson, who developed the theory for cambered planing surfaces. (Selected examples of the graphs given in Report 3147 are included here as Figures 4-9 - 4-11. These are the particular graphs needed for the Example of the design procedure, which is given in succeeding pages.)
16. Determine  $(L/D)_{Exp.} / (L/D)_J$ , from Figure 4-7.
17. Multiply value from step 15 by value from step 16 to get  $(L/D)_{Exp.}$ .
18. Multiply value from step 17 by 0.925 to get the value of L/D for a hull with a stabilizer (including air drag).
19. Knowing the values of the beam,  $b$ , and of the ratios,  $\rho_t/b$  and  $\rho_r/b$  (from step 4), calculate  $\rho_t$  and  $\rho_r$ . These are the chord lengths,  $c$ , of the camber curves at the chine, and at the centerline, respectively.
20. A plan view of one side of the cambered planing region should be drawn. An example is given in Figure 4-8a. This figure shows the construction lines needed for defining the position and the dimension of the mean hydrodynamic chord (M.H.C.). The length of the M.H.C. should then be scaled from the drawing. Multiplying that length by the ratio  $\rho_{CP}/\rho_m$  (determined in step 15) gives the distance of the center of pressure (which is on the centerline of the cambered planing surface) forward of the aft end of the M.H.C.
21. Figure 8b shows an example of the type of "balance diagram" used to determine where along the length of the hull the c.p. of the cambered planing surface should be located. The appropriate longitudinal position for the step can then also readily be determined.
22. Knowing  $\rho_r$  (this is the chord length of the camber curve at the centerline), and the value of  $C_{L,d}$  (from step 15), the offsets for the camber curve at the centerline of the cambered region can be determined by utilizing either the tabulated values or the equation given in figure 4-12. Taking  $\rho_t$  as the chord length,  $c$ , of the camber curve at the chine, the camber curve for that location can be determined in a similar manner.
23. The cambered region between the camber lines at the centerline and at the chine is defined by an array of straight lines connecting points on those lines which are located at equal percentage points of their chord-line lengths. For example, a

straight line connecting the point on the centerline camber curve located at 35% of its chord-line length with the point on the chine camber curve located at 35% of its chord-line length will coincide with the cambered surface, and accordingly will assist in defining it. Another way of explaining the case is to say that the configuration of the cambered region is such that the shapes of the camber curves in all of the buttock planes are geometrically similar.

Example - cambered planing surface for the case of a 20-ft boat running in salt water.

$$L_p = 20 \text{ ft}, b = 5.25 \text{ ft}, W = 2500 \text{ lbs}, V = 35 \text{ mph} (v = 51.3 \text{ fps}), \rho/2 = 1.0$$

1.  $C_{Lb\beta} = 0.9W / (\frac{1}{2}\rho v^2 b^2) = 0.031$
2. Assume Johnson three-term camber curve
3. Take  $\beta = 10 \text{ deg}$
4. Take  $q_t/b = 0.2$ , and  $q_r/b = 0.8$
5. From equation,  $AR = 2.0$
6. Take  $\tau = 2.5 \text{ deg}$  (from Figure 4-2)
7. Calculate  $\gamma$  for no camber from equation; add 5 deg for camber case. Then  $\gamma = 21.3 \text{ deg} + 5 \text{ deg} = 26.3 \text{ deg}$
8. See Figure 4-8 for a plan view of the planing surface, and also a "balance diagram"
9. Calculate  $\phi$  from equation.  $\phi = 55 \text{ deg}$
10. Calculate  $\theta$  from equation.  $\theta = 39.5 \text{ deg}$
11. To correct for effect of deadrise on lift, determine  $C_{Lb0}$  from Figure 4-6 (equals 0.04). Then  $(C_{Lb\beta} / C_{Lb0})_{DL} = 0.031/0.04 = 0.775$ . ("DL" indicates Davidson Laboratory.)
12. For  $\phi = 55 \text{ deg}$ , read  $\frac{(C_{Lb\beta} / C_{Lb0})_{Exp.}}{(C_{Lb\beta} / C_{Lb0})_{DL}} = 0.843$ , from Figure 4-7. (The subscript "Exp." indicates a value corresponding to the experimental value obtained from a test of a cambered planing surface.)
13. Then  $(C_{Lb\beta} / C_{Lb0})_{Exp.} = 0.775 \times 0.843 = 0.653$
14.  $C_{Lb0} = 0.031/0.653 = 0.0475$
15. From Report 3147, for  $C_{Lb0} = 0.0475$ ,  $AR = 2.0$ , and  $\tau = 2.5 \text{ deg}$ , read  $(L/D)_J = 12.9$ ,  $C_{L,d} = 0.045$ , and  $q_{cp}/q_m = 0.62$ . (Alternatively, use Figures 4-9 - 4-11, which are taken from Report 3147.)
16. From Figure 4-7,  $(L/D)_{Exp.} / (L/D)_J = 0.895$
17. Then  $(L/D)_{Exp.} = 0.895 \times 12.9 = 11.5$
18. Multiply value from step 17 by 0.925 to get the value for a hull with a stabilizer (including air drag)
19. The chord lengths of the camber curves of the cambered region are calculated to be 1.05 ft (12.6 in) at the chine, and 4.2 ft (50.4 in) at the centerline
20. A plan view of one side of the cambered planing region can now be drawn, as shown in Figure 4-8a. By drawing the indicated construction lines on the figure the position and dimension of the M.A.C. can be defined. Its length is found to equal 2.95 ft. Multiplying that dimension by the value of 0.62 for the ratio  $q_{cp}/q_m$  gives a value of 1.83 ft for the distance of the center of pressure on the cambered planing surface fwd of the aft end of the M.H.C.



21. When the position of the CG for the planned design has been determined a balance diagram like Figure 4-8b should be drawn. Assume for the present case that, on average, the C.G. of the boat will be located at 50% of the length,  $L_P$  forward of the stern. The “balance diagram” shown in Figure 4-8b then indicates the procedure for determining the appropriate longitudinal location on the hull of the c.p. of the cambered planing surface. At the high-speed design point the cambered planing surface is intended to carry 90% of the weight of the boat. This result will be attained if the cambered planing surface is located such that its center of pressure is 11.11 ft forward of the stern of the boat. The “point” of the step (i.e., the intersection point of the step with the keel ) is found, by scaling from the drawing, to be 0.93 ft aft of the c.p. Accordingly, on the plan-view drawing of the boat the point of the step should be positioned at  $(11.11 \text{ ft} - 0.93 \text{ ft}) = 10.18 \text{ ft}$  forward of the aft end of  $L_P$ .
22. Knowing the chord length of the camber curve at the keel (50.4 in), and the value of  $C_{L,d}$  (0.045) the offsets of that camber curve can be determined by utilizing the tabulated values given in Figure 4-12. For example, the offset for the camber curve at 55% of the chord-line length from the leading edge (i.e., at  $x/c = 0.55$ ) equals  $50.4 \times 0.045 \times 0.0715 = +0.16 \text{ in}$ . The offset at the aft end of the cambered region (which corresponds to the step position) equals  $50.4 \times 0.045 \times (-0.1698) = -0.38 \text{ in}$ . This offset dimension will probably not be adequate to be taken as the dimension for the depth of the step. Instead the depth of the step should be equal to about 1% of the chine beam, or equal to about 0.6 in.
- 23 A typical complete cambered planing region for a Vee-bottom boat is illustrated in the “PLAN” view of Figure 1-3. This complete region consists of two similar curved surfaces (mirror images of each other) which are joined at the centerline plane. Each curved surface is defined by an array of straight lines connecting points on the centerline camber curve with points on the chine-position camber curve which are located at equal percentage points of their chord-line lengths. For example, a straight line connecting the point on the centerline camber curve located at 35% of its chord-line length with the point on the chine camber curve located at 35% of its chord-line length will coincide with the cambered surface, and accordingly will assist in defining it. Another way of explaining the case is to say that the configuration of each of the two similar cambered regions is such that the shapes of the camber curves in all of the buttock planes are geometrically similar.

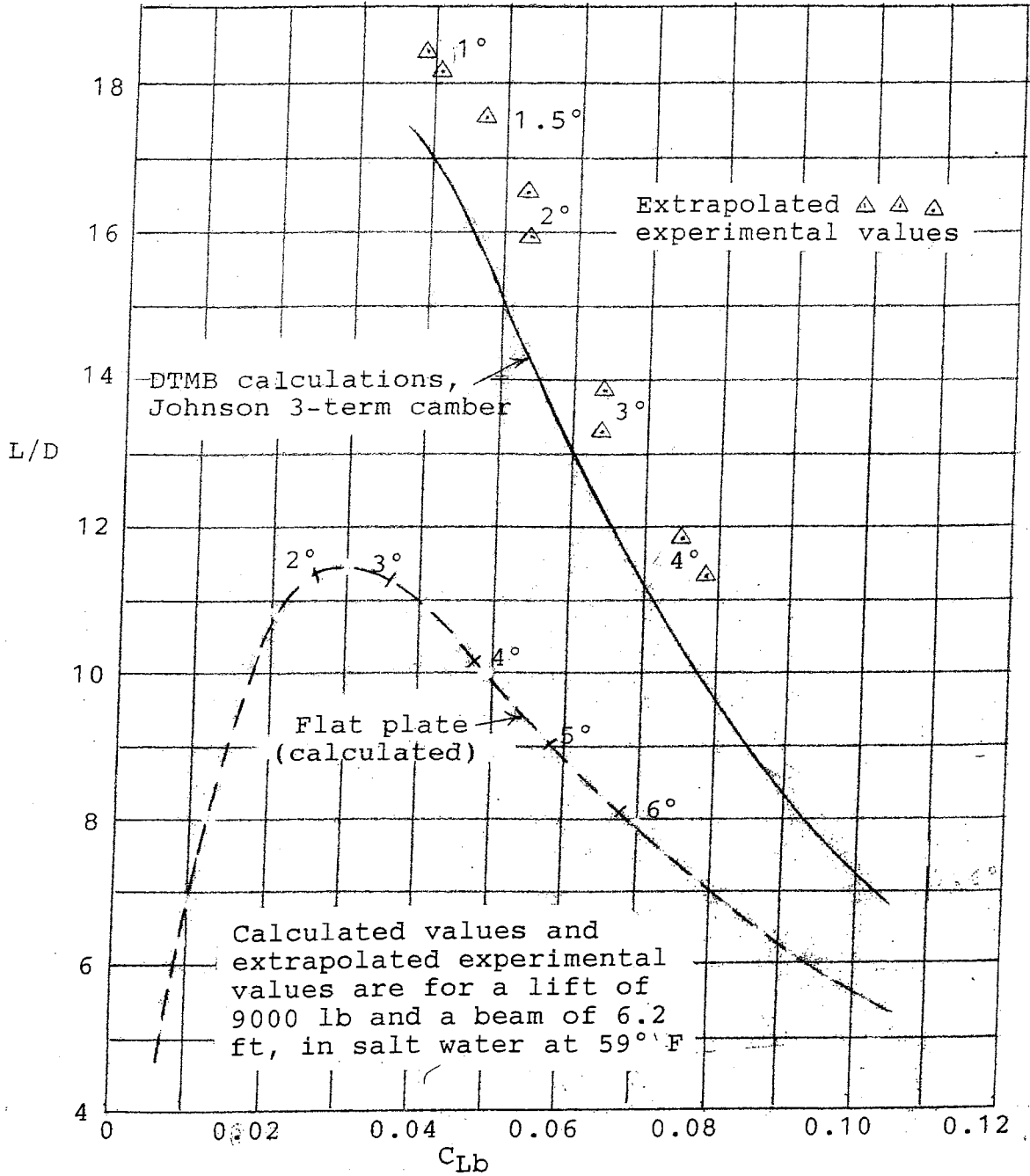


Figure 4-1 - Comparison of Calculated and Experimental Values of Lift/Drag Ratio for a Cambered Planing Surface Having the Johnson 3-Term Section. Comparison also with a Flat Plate. Aspect Ratio = 2.0

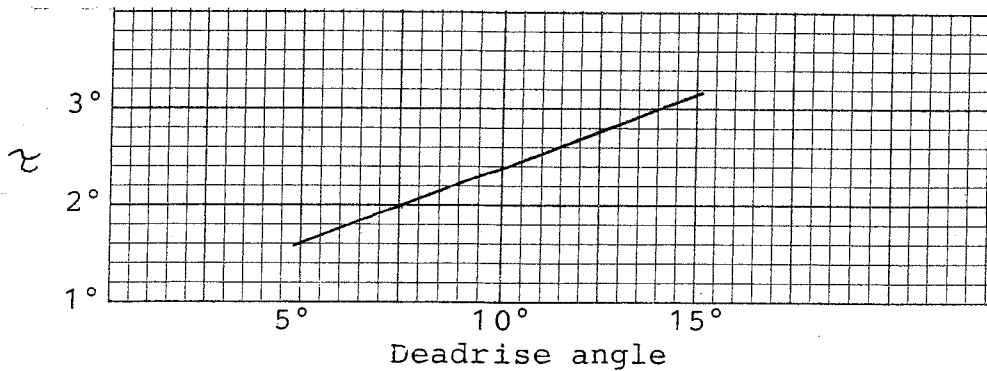


Figure 4-2 - Approximate Relationship Between Deadrise Angle and Design Angle of Attack for a Cambered Planing Surface.

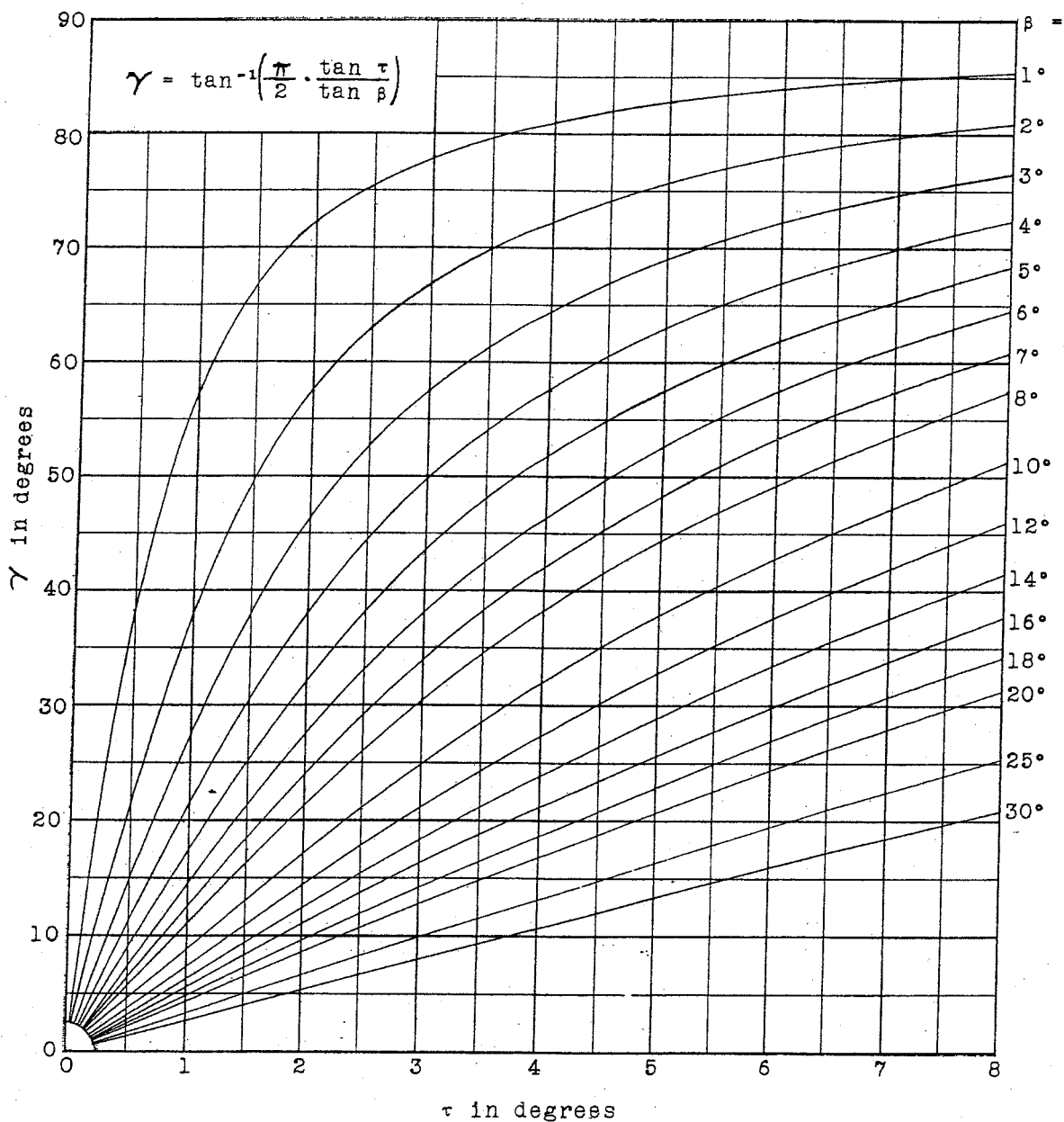


Figure 4-3 - Angle Gamma ( $\gamma$ ) Between Spray-Root Line and Centerline, in Plan View, For Prismatic Planing Surfaces.

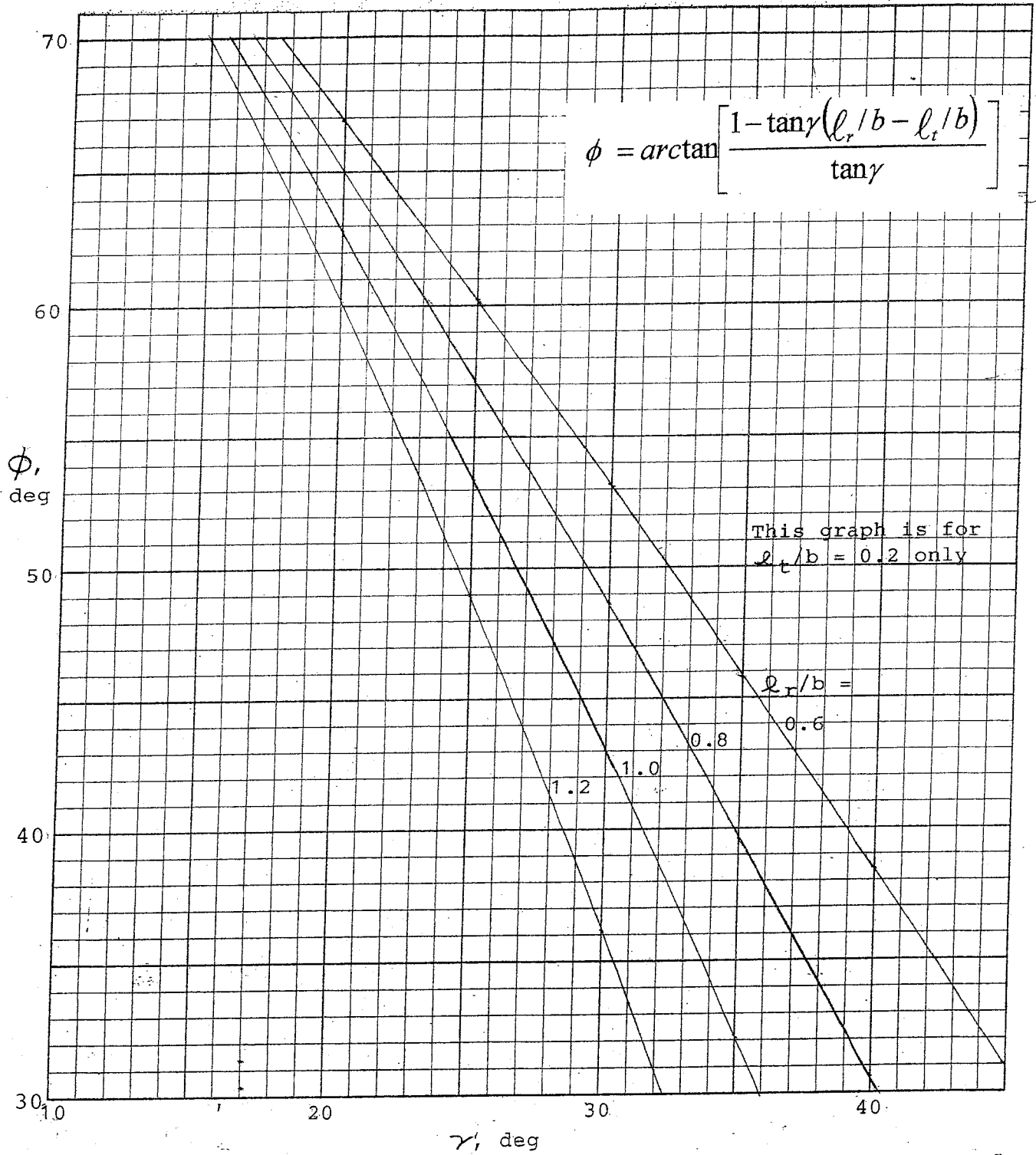


Figure 4-4 - Angle of Sweep of 50% Chord Line (Angle  $\phi$ ), Versus Angle Between Spray-Root Line and Centerline in Plan View (Angle  $\gamma$ ), for  $l_t/b = 0.2$ .

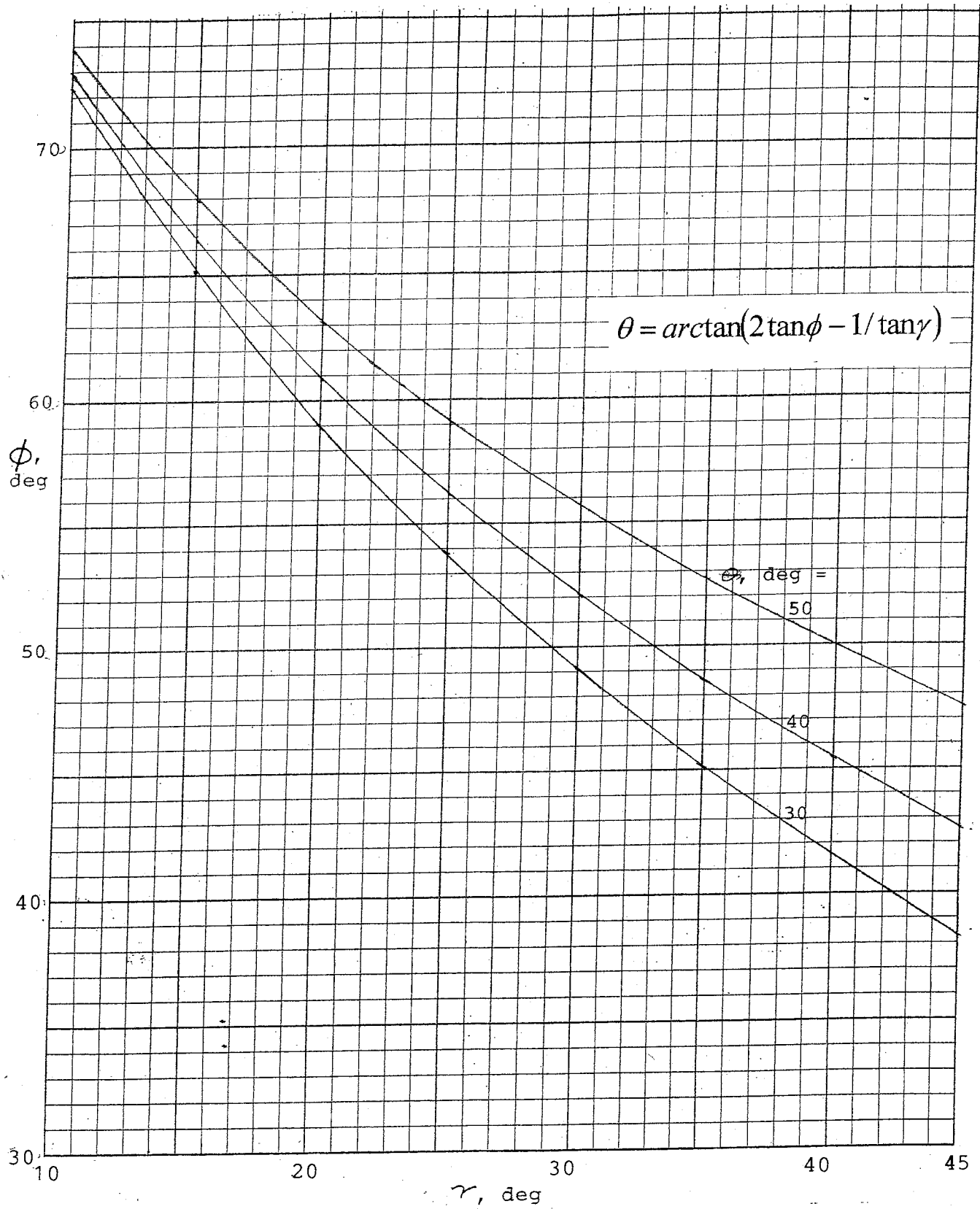


Figure 4-5 - Curves of Step Sweepback Angle as a Function of Angles  $\gamma$  and  $\phi$ .

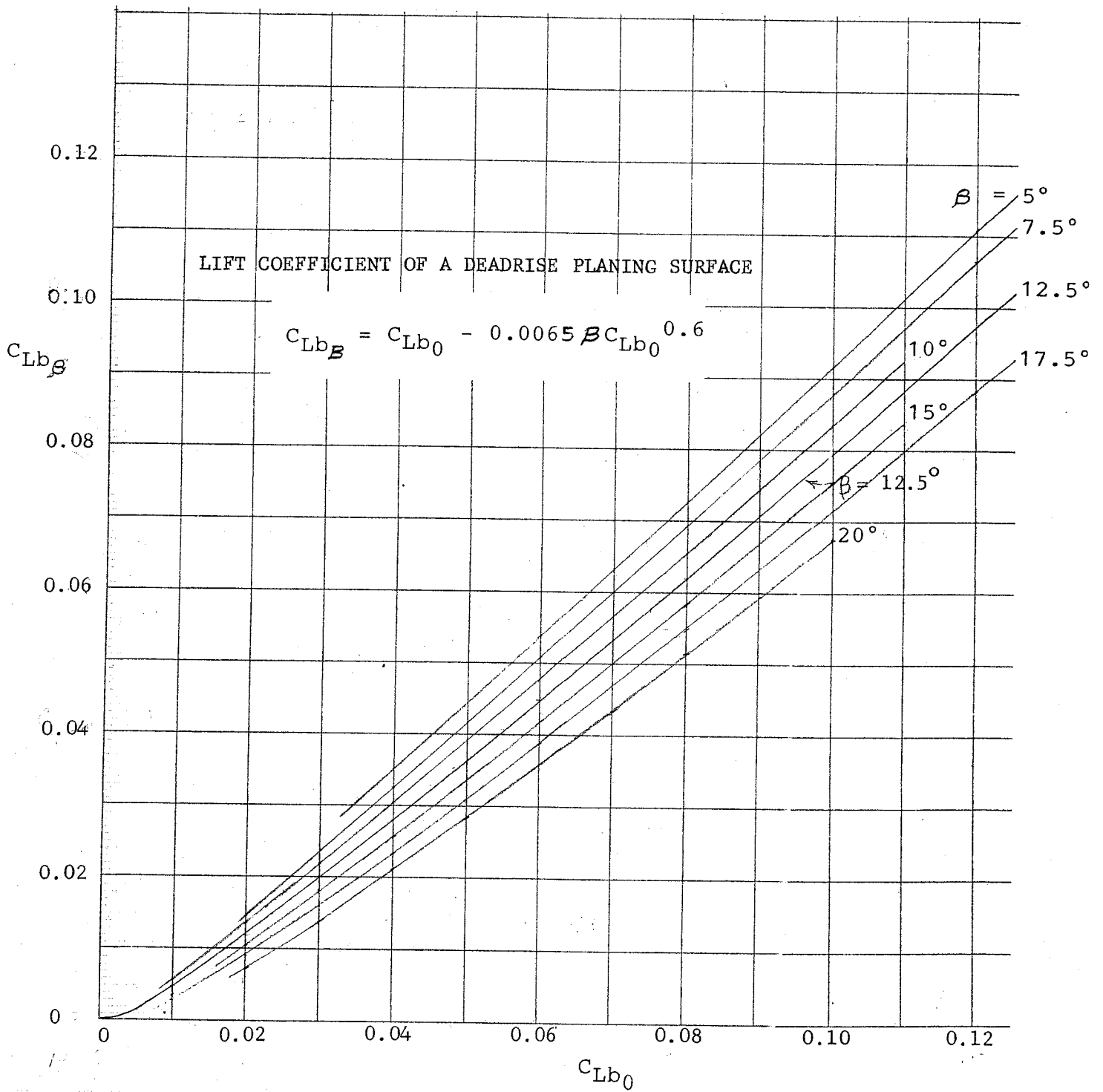


Figure 4-6 - Lift Coefficient with Deadrise versus Lift Coefficient without Deadrise for Prismatic (Uncambered) Planing Surfaces -- from the Davidson Laboratory.

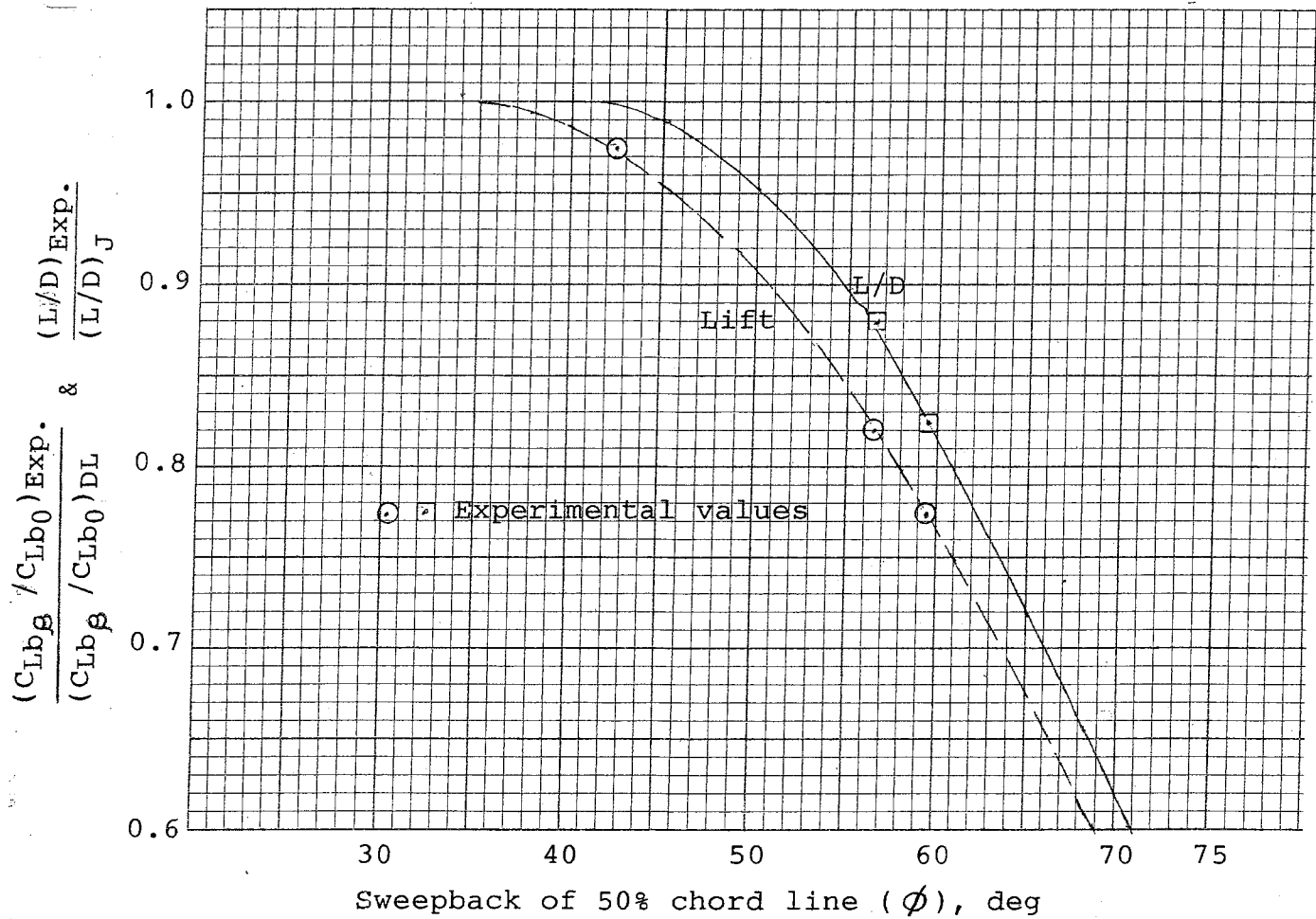
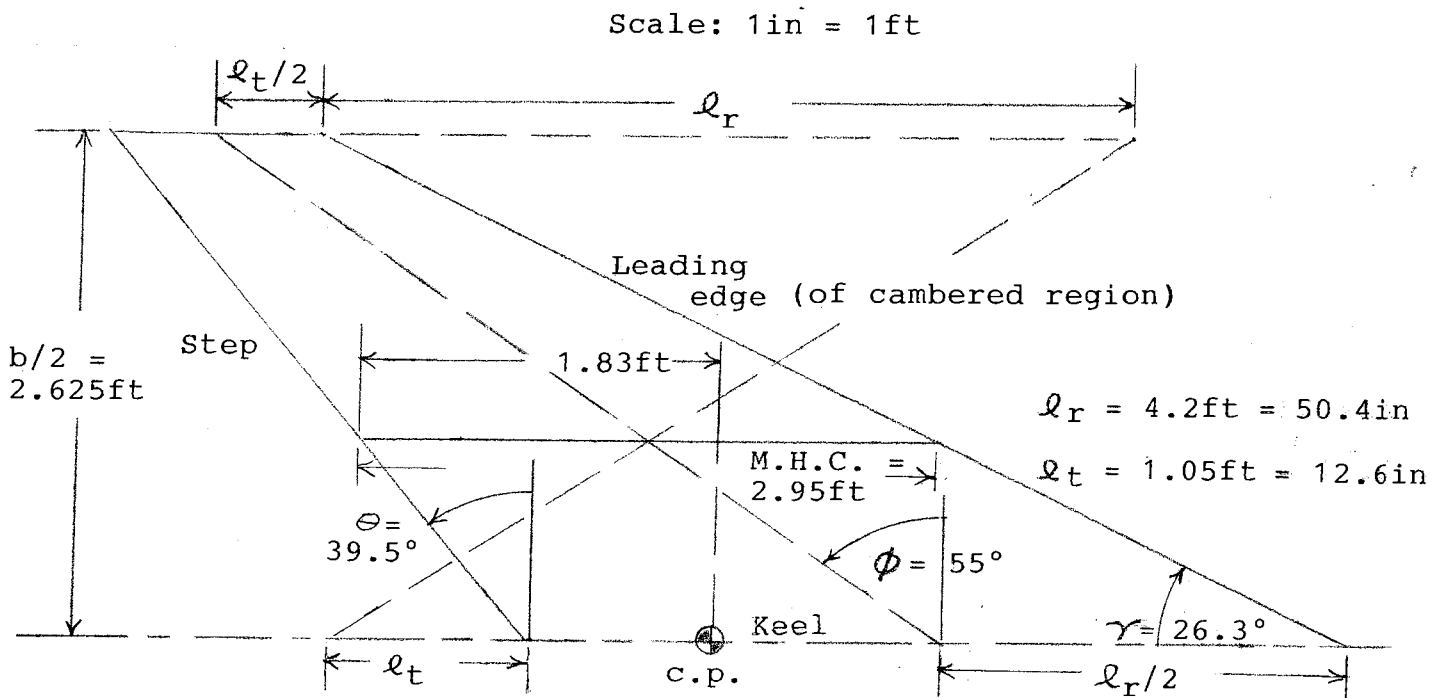
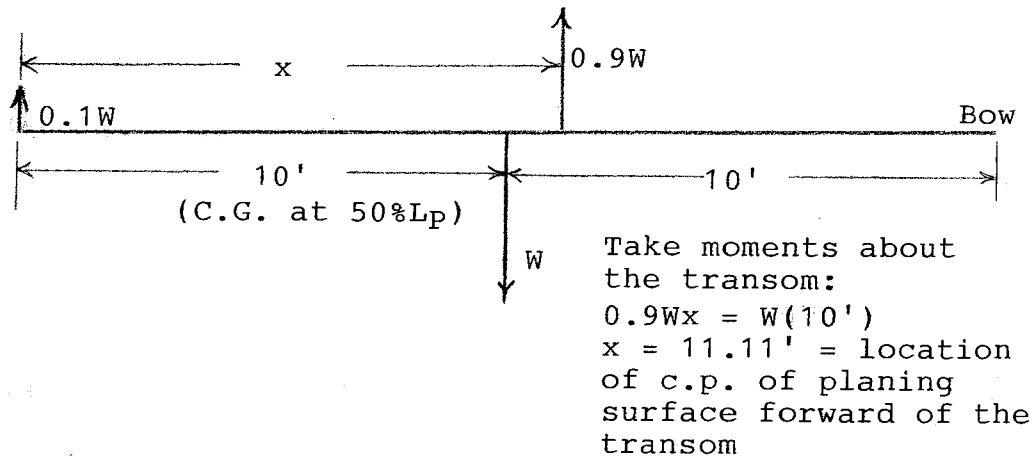


Figure 4-7 - Cambered Planing Surfaces - Corrections for Sweepback Angle ( $\phi$ ) to Lift and L/D.



8a - Plan View of the Planing Surface, with Construction Lines for Determining the Location and Length of the Mean Hydrodynamic Chord (M.H.C.).



8b - Balance Diagram for the Case of a 20' Boat with an Adjustable Hydrofoil at the Transom Which Provides 10% of the Lift.

Figure 4-8 - Plan View and Balance Diagram for Example Calculation.



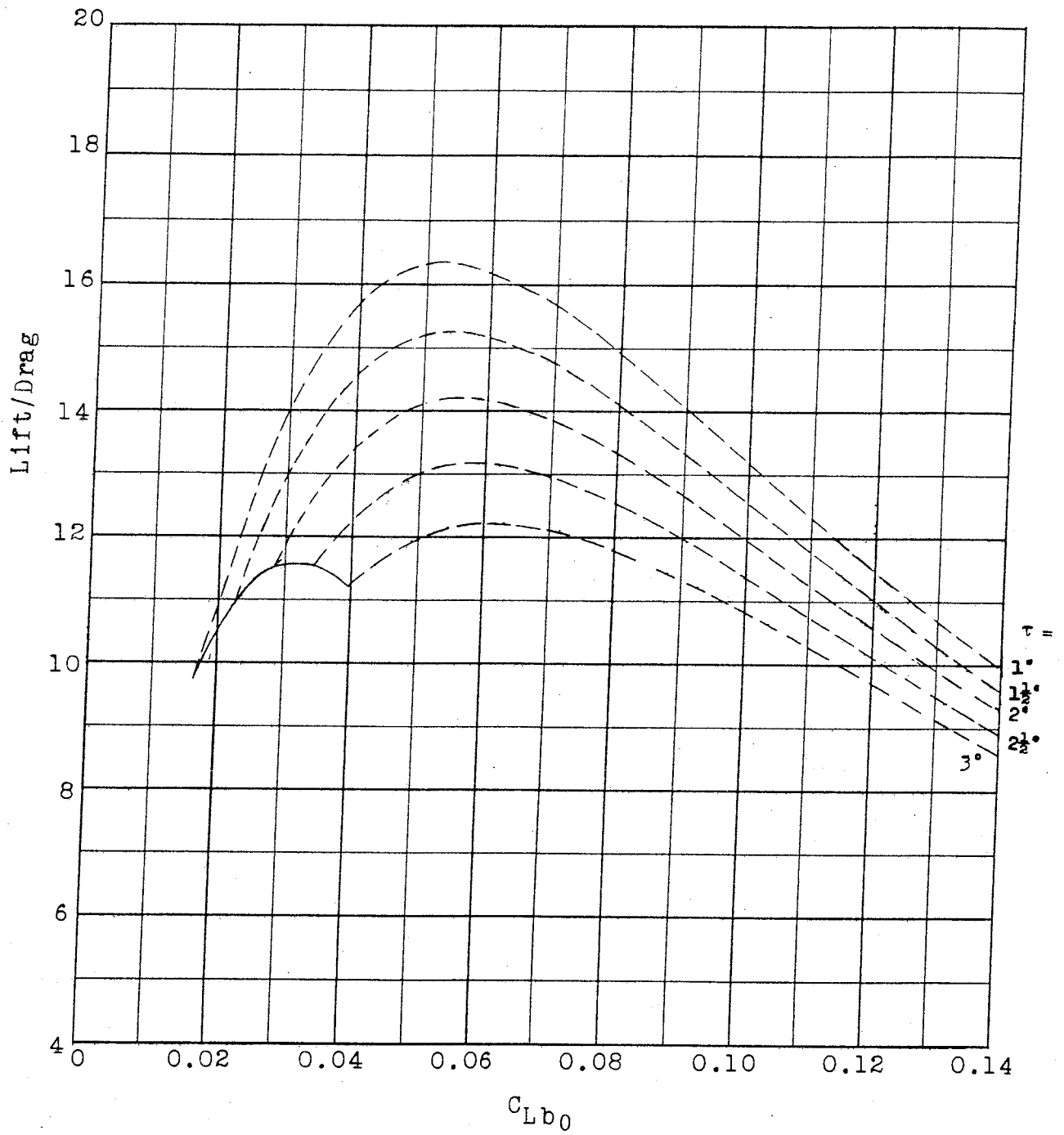


Figure 4-9 - Lift/Drag versus  $C_{Lb_0}$  for Rectangular Planing Surfaces Having the Johnson Three-Term Section and Zero Deadrise,  $Re = 10^7$ , Aspect Ratio = 2.0.

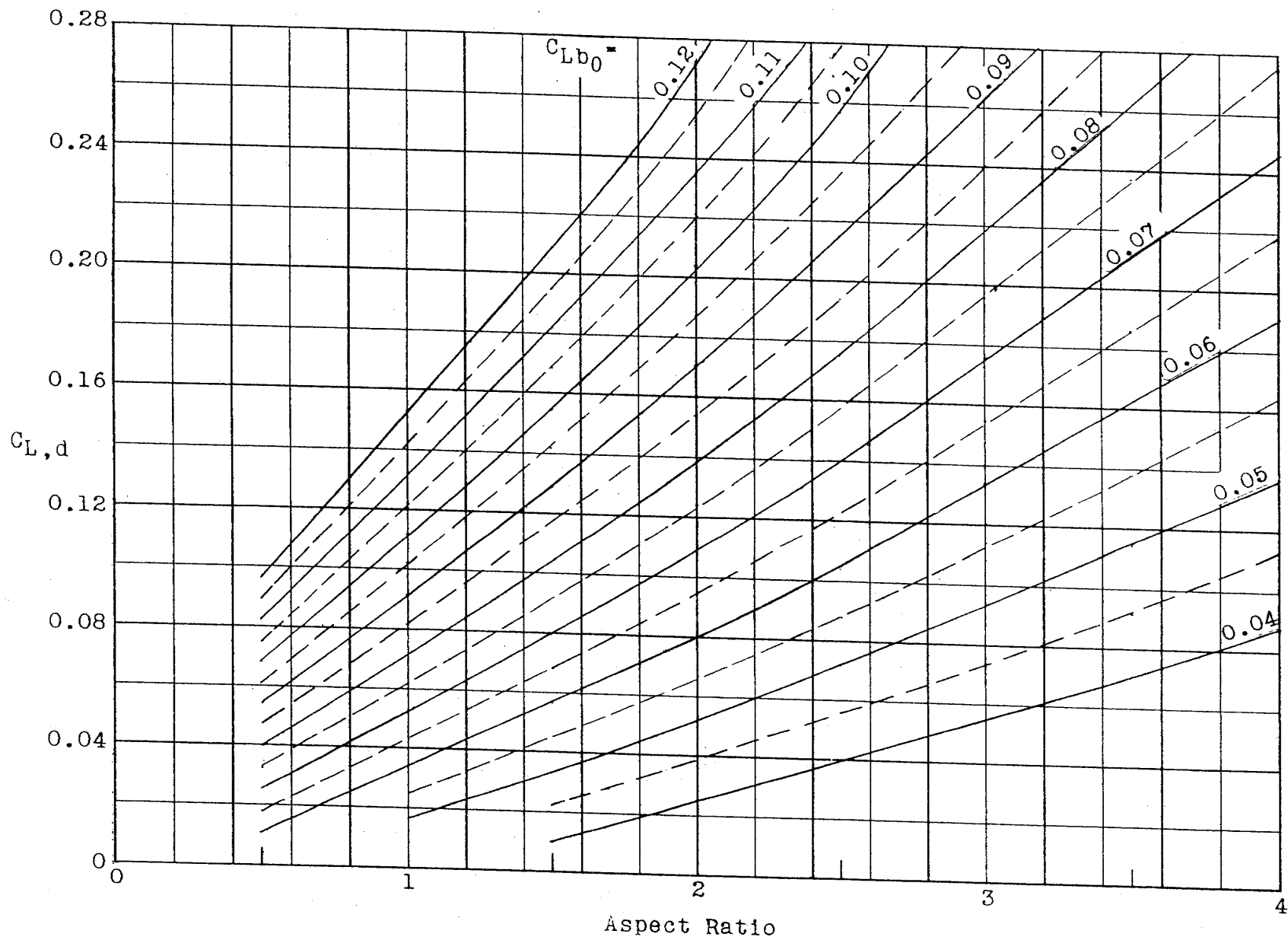


Figure 4-10 -  $C_{L,d}$  versus Aspect Ratio for Rectangular Planing Surfaces Having the Johnson Three-Term Section and Zero Deadrise,  $\tau = 2\frac{1}{2}^\circ$ .

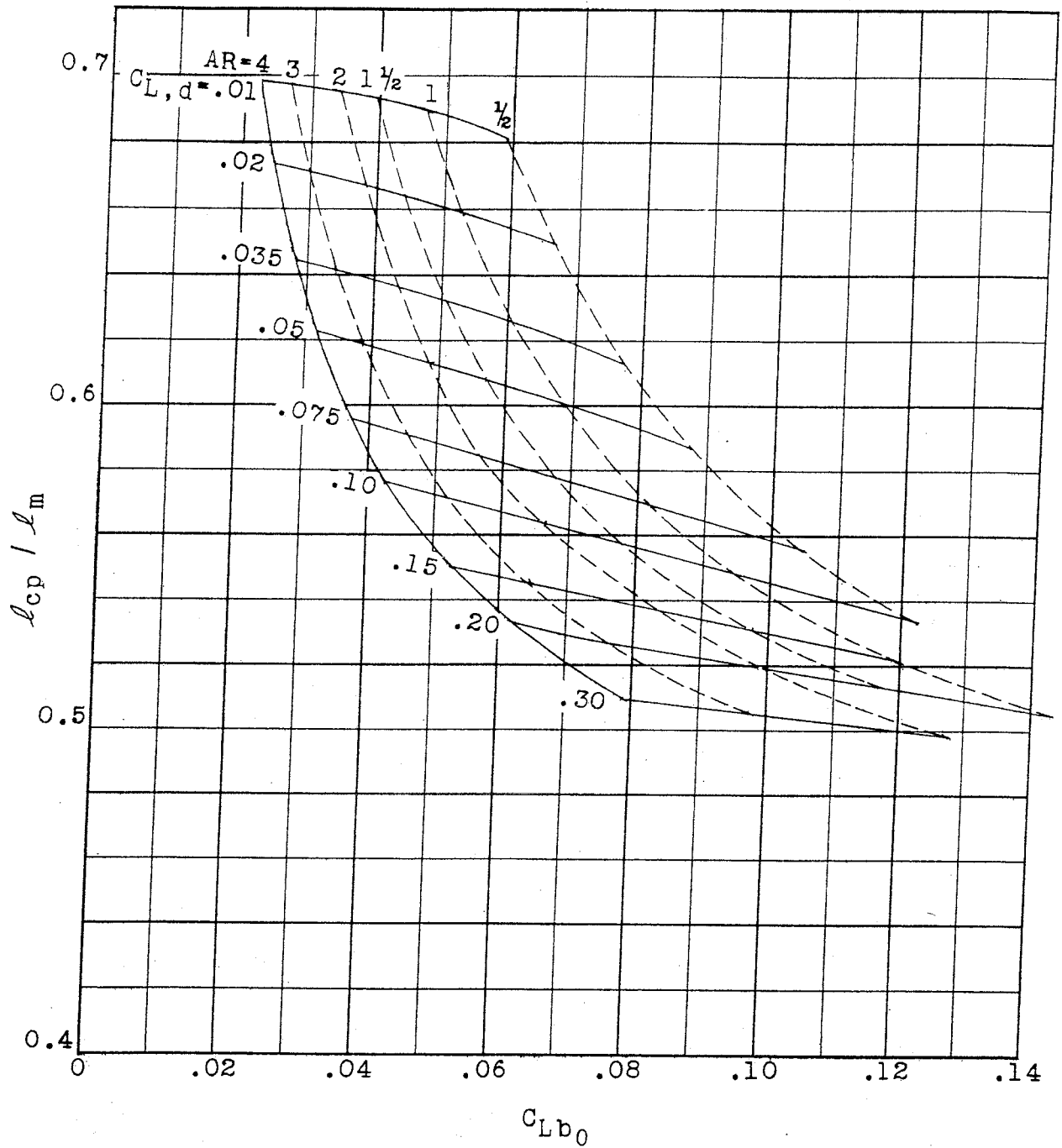


Figure 4-11 - Location of Center of Pressure versus  $C_{Lb_0}$  for Rectangular

Planing Surfaces Having the Johnson Three-Term Section  
and Zero Deadrise,  $\tau = 2\frac{1}{2}^\circ$ .

Equation of the Johnson  
three-term camber curve:

$$\frac{Y}{C_{L,d}} = (-20X^{3/2} + 80X^2 - 64X^{5/2}) \times \frac{1}{7.5\pi}$$

$$X = \frac{x}{c} \quad Y = \frac{y}{c}$$

$\frac{x}{c}$	$\frac{y}{c \cdot C_{L,d}}$
0.0	0.0
0.02	-0.0012
0.04	-0.0022
0.06	-0.0026
0.08	-0.0024
0.10	-0.0015
0.15	0.0034
0.20	0.0113
0.25	0.0212
0.30	0.0322
0.35	0.0433
0.40	0.0536

$\frac{x}{c}$	$\frac{y}{c \cdot C_{L,d}}$
0.45	0.0623
0.50	0.0686
0.55	0.0715
0.60	0.0704
0.65	0.0645
0.70	0.0530
0.75	0.0353
0.80	0.0108
0.85	-0.0214
0.90	-0.0618
0.95	-0.1110
1.00	-0.1698

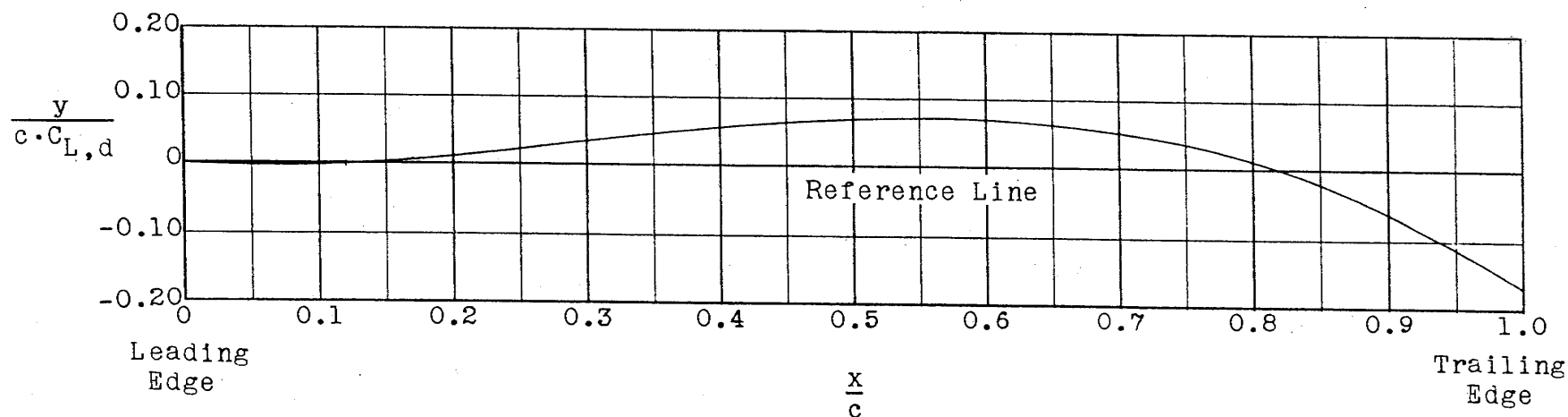


Figure 4-12 - Dimensionless Offsets of Johnson Three-Term Camber Curve

## **Chapter 5**

### **Design of the Step and Afterbody, and Drag at the Hump**

#### **Stepped boats have humps in their curves of resistance**

The chief merit of an appropriately designed stepped boat is that at high speed it will have much less resistance than a corresponding unstepped boat. In the lower part of the speed range, however, a stepped boat tends to have more resistance than a conventional unstepped boat. The combined effect of these two factors is that for a stepped boat there is usually a "hump" in the curve of resistance versus speed. An example of this was shown in Figure 1-3. It is obviously desirable that the hump resistance not be unduly high. It is essential that it be less than the available propulsion thrust, and by a sizeable margin (20% would be adequate), so that the boat can be accelerated to the desired planing speed. It is also important that a boat have a satisfactory range at a low "cruising speed." Suitable details of design for the step and the afterbody are required in order to achieve those important ends.

#### **Design requirements for the afterbody**

There are two main requirements governing the design of the afterbody for an efficient stepped planing boat. At high speed the afterbody of the hull should run clear and dry above the surface of the water. The needed lift aft should then be provided by an efficient, adjustable, trim-control device. In the lower part of the speed range, however, and particularly at the hump, lifting support aft is needed from the afterbody of the hull as well as from the trim-control device. (The dynamic lift of the latter derives from the forward speed of the boat, and is therefore very much reduced at low speed.) The afterbody should accordingly be in contact with the wake from the forebody in the lower part of the speed range so that it can contribute both buoyant and planing lift. This lifting support is essential to minimize the magnitude of the drag at the "hump." Both of the afterbody requirements will be met if the angle between the forebody and afterbody keels is such that the afterbody keel is close to being horizontal when the hull is running at its design angle of attack. The form of the bottom of the afterbody should consist simply of two flat surfaces meeting at a suitable deadrise angle. The deadrise angle of the afterbody should be less than that of the forebody in order to give an approximately constant depth of the step across the bottom. (In the case of the hullform shown in Figure 1-1 the deadrise just forward of the step (before addition of the camber) was 12.5 degrees and the deadrise of the afterbody was constant at 10.7 degrees.) When the design of the forebody (including the cambered region) has been completed, and the afterbody keel angle has been selected, a value for the afterbody deadrise angle that will give an approximately constant depth of the step can readily be arrived at during the succeeding steps of the drafting process.

#### **Location and depth of the step**

The mean step position should be at approximately 45% of the chine length from

the stern, and the depth of the step equal to about 1% of the beam of the main planing surface. (The step edge must be sharp.) A depth of step at the keel equal to the trailing edge camber line offset for the centerline section of a Johnson 3-term camber curve will often be adequate. The average step depth for the 8-foot long Model No. 5115A (shown in Figures 1-5 - 1-7) was 0.28 in., which is approximately 1.3% of the chine beam at the step. It is suitable to maintain an approximately constant depth of the step across the bottom of the hull. If the step sweep-back angle is large (more than about 20 degrees) vent pipes should be provided, as indicated in Figure 1-1, to assist the separation of the flow from the afterbody.

### **Drag at the hump**

A value for drag at the hump can be estimated by means of Figure 5-1. This figure presents experimental values of resistance at the hump from the tests of Model 5115 (at different weights and LCG positions). It was learned from previous testing of models of stepped seaplane hulls that experimental values of resistance at the hump tend to collapse along a single line when plotted against the dimensionless ratio,  $\frac{\nabla}{(LCG)^2 b}$ , where  $\nabla$

is the volume of water displaced at rest, LCG is the distance of the center of gravity forward of the stern, and b is the width over the spray strips at the location of the center of gravity. Accordingly the hump-drag data for Model 5115 have been plotted against that coefficient. In the case of a new design the value of the coefficient can be calculated, in the early stages of a design, from the values of W, LCG, and b, and a value for the resistance/weight ratio at the hump can then be determined from Figure 5-1. The available model-test data indicate that the speed at the hump for a Dynaplane-type boat will correspond to a value of  $F_{\nabla}$  of approximately 2.25. A complete resistance curve for one particular Dynaplane design (represented by Model 5115) is given in Figure 5-2. This resistance curve can be utilized to construct a resistance curve for the hump-speed region for other similar designs. The procedure recommended is to multiply the values of R/W from Figure 5-2 (at a number of values of  $F_{\nabla}$ ) by the ratio of the hump R/W for the new design (determined from Figure 5-1) to the hump R/W from Figure 5-2 (equals 0.12). The resistance at high speed will be derived as a part of the design procedure for the (cambered) forebody planing surface of the new design, and the curve of hump-speed resistance can then be faired to connect with the new value of the resistance at high speed to give a relatively complete curve of resistance versus speed.

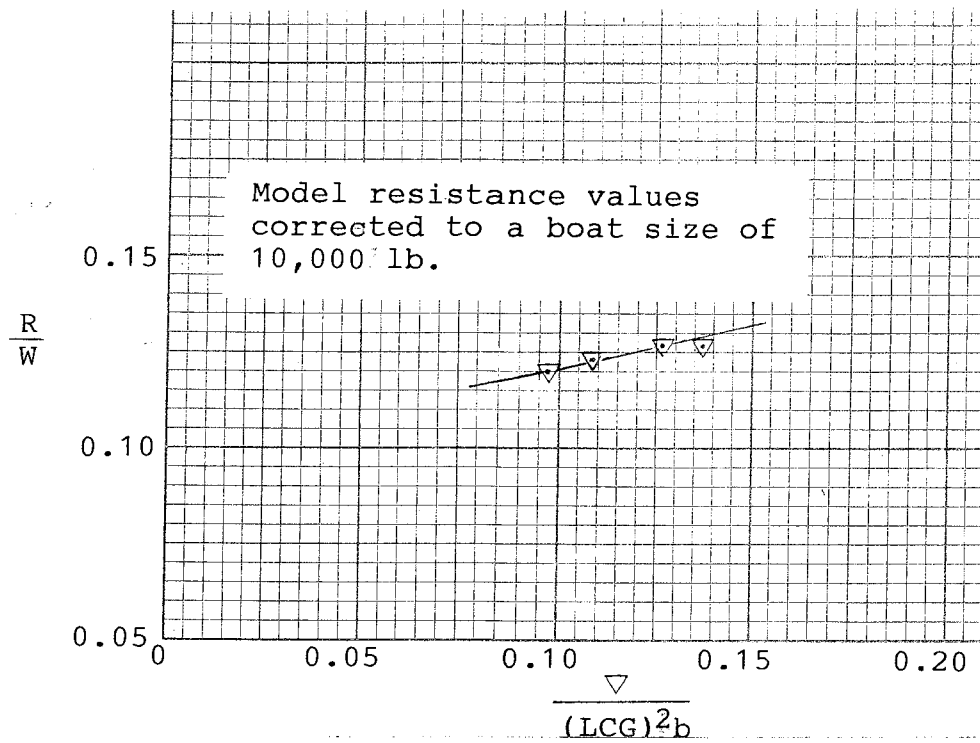
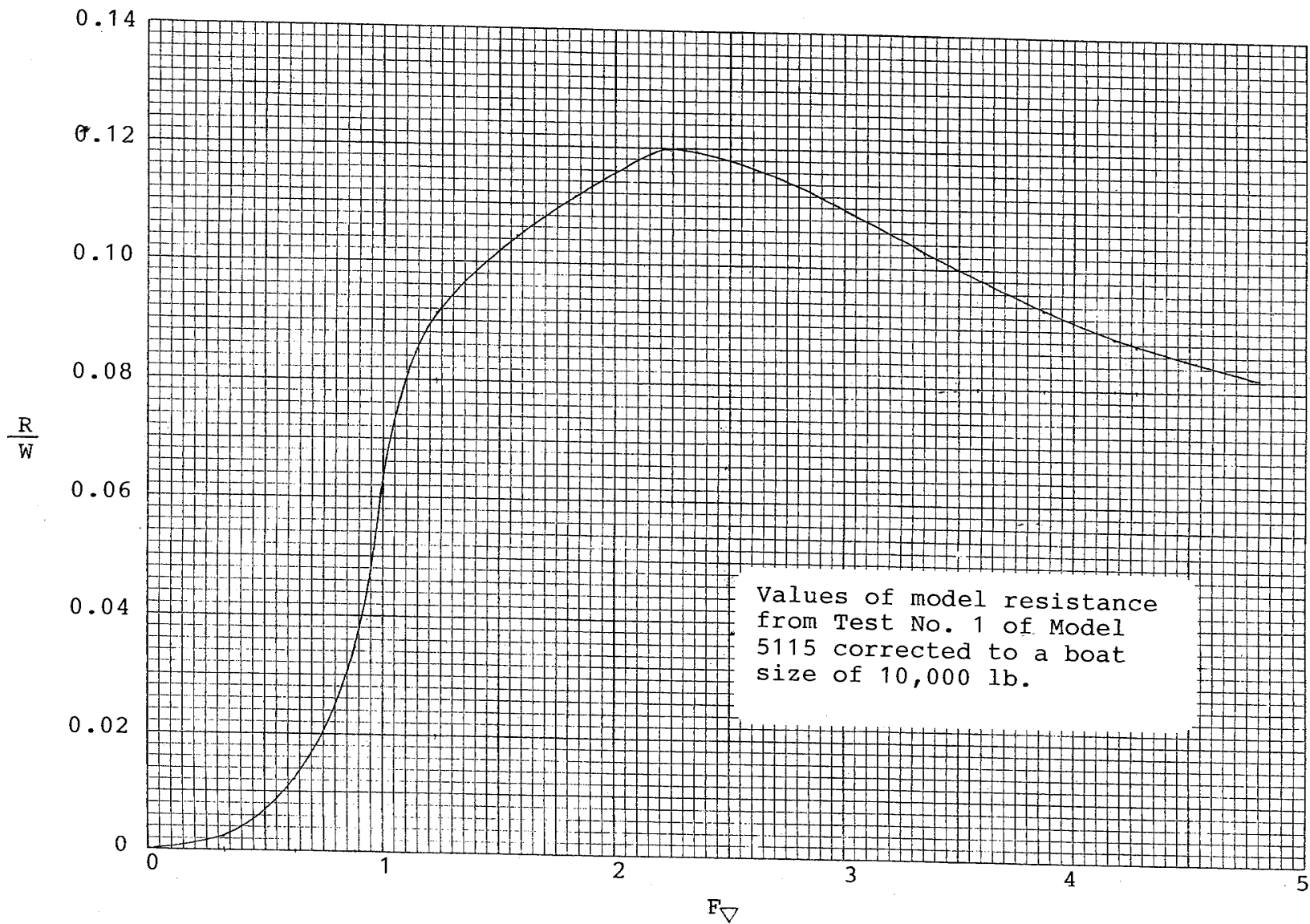


Figure 5-1 - Values of Resistance at the Hump from Tests of Model 5115 at Different Weights and LCG Positions.

51



51

Figure 5-2 - Curve of Resistance versus Speed for an Airplane-Configuration Stepped Boat Represented by Model 5115.



## Chapter 6

### A Surface-Piercing Vee Hydrofoil as the Trim-Control Device for A Stepped Planing Boat

Superior planing boat performance can be achieved with a stepped configuration in which a cambered main planing surface located near amidships carries approximately 90% of the weight, and an adjustable lifting surface at the stern carries the remainder of the weight (and in addition provides a means of controlling the boat's trim angle). The resistance of such a configuration (at planing speeds) is chiefly determined by the resistance of the cambered main planing surface. An important factor for keeping this major drag component to a minimum, at different boat weights and speeds, is having the ability to trim the main planing surface to the angle giving the least drag, by means of the stern trim-control device.

The type of stern trim-control device that particularly recommends itself is a surface piercing Vee hydrofoil. The foil should be adjustable vertically in order to be able to vary the amount of its submersed area, and therefore the amount of its lift. Towing tank tests of some surface-piercing Vee hydrofoils, and also their successful utilization for several hydrofoil boats, provide background information on which suitable foil designs can be based. Data from some of the towing-tank tests of surface-piercing Vee hydrofoils that have been made are given in Reference 4. Those tests were made in the old NACA seaplane towing tank. The purpose of the testing was to determine the effects of angle of dihedral and depth of submersion on the performance of hydrofoils. The foils tested had the NACA 16-509 section shape. That shape had been previously developed as one of a series of airfoil section shapes which would have a pressure distribution as nearly constant as possible. (The series has been widely referred to as the "16-Series.") When used as a hydrofoil this section shape can be run at a particularly high speed before it will cavitate. The 16-509 designation indicates that the section is designed to have optimum characteristics at a lift coefficient of 0.5, and that it is 9% thick.

The hydrofoils for which the data are given in Reference 4 each had a chord length of 5 inches and a span of 30 inches. They were rectangular in planform, with square tips. The dihedral angles tested were 10, 20, and 30 deg. The foils were tested at different depths, and over ranges of speeds and angles of attack. Tests of the hydrofoil having 30-deg dihedral, in the half-submerged condition, and when submerged to the foil tips, produced some particularly promising results. Those favorable results were obtained at angles of attack close to zero deg. (This was to be expected since the design angle of attack for the 16-509 airfoil section was zero deg.) The hydrofoil with 30-deg dihedral is shown (with the two test water levels also shown) in Figure 6-1. The test results are given in Figures 6-2 and 6-3. It can be seen that in the half-submerged condition (aspect ratio then equaled 3.0), values of lift/drag ratio in the range of 14 to 16 were obtained, for speeds up to 60 fps. When the foil was submerged to its tips (aspect ratio then equaled 6.0), L/D values in the range of 18 to 25 were obtained, for speeds in the range of 40 to 60 fps. (The strut tares were subtracted from the drag values in the case of the latter configuration.) Values of L/D for the foils having the three different dihedral angles, at a

speed of 40 fps, when half-submerged, were compared in Reference 4. The maximum values of  $L/D$  for that case were 6 for the foil with 10 deg dihedral, 12.5 for the foil with 20 deg dihedral, and 16 for the foil with 30 deg dihedral. A clear implication from this comparison is that the optimum dihedral angle (giving the highest values of  $L/D$ ) would probably be greater than 30 deg.

Cavitation was observed to occur on the foils reported on in Reference 4, during the test runs at the higher angles of attack. The speeds and angles of attack at which cavitation occurred are indicated in the report. No cavitation was observed on the 30-deg dihedral foil at the low angles of attack which are of interest for design purposes, and for which the lift and drag data are given in Figures 6-2 and 6-3. The marked decreases in the lift coefficients, and the increases in the drag coefficients, with increase in speed, which are shown in those figures are therefore surprising. There is, of course, a corresponding marked decrease in the values of  $L/D$  with increase in speed. This deterioration in performance is presumably to be attributed to flexing of the strut-foil assembly from the hydrodynamic forces, resulting in an unfavorable distortion of the foil configuration. Details of the strut-foil assembly are accordingly of interest. Both struts and foils were machined from "hard brass." The struts were biconvex in section, approximately 28 inches long, and tapered toward the hydrofoil. At the point of attachment to the upper surface of the hydrofoil, the struts had a chord of 2.9 inches and a thickness of  $3/8$  inch; at the top, the chord of each strut was 4 inches and the thickness was  $3/4$  inch. The center line of each strut intersected the upper surface of the foil at the half-chord point. The method of attaching the struts to the hydrofoil is not explained in the report. It is probably also of significance, with regard to the likelihood of flexing, that when the struts were vertical the angle of attack of the hydrofoil was 6 deg. Accordingly, when the foil was running at the angle of attack of zero degree (the design angle for the foil section, and the angle giving the maximum values of  $L/D$ ) the struts were raked back at an angle of 6 deg. It can be concluded that measures that would reduce the amount of flexing of surface-piercing Vee-foils mounted on actual motorboats would markedly improve the values of  $L/D$  attainable at high speeds.

The promising test results reported in Reference 4, for the foil having 30 deg dihedral, suggested the likelihood that there would be practical applications for surface-piercing Vee-hydrofoils. Also, as noted, the results indicated that the optimum dihedral angle would be greater than the 30 deg angle that had been tested. Accordingly, several companies and individuals have experimented with higher dihedral angles, and have designed and built boats that were supported by either three or four Vee-hydrofoils having approximately 40 deg dihedral angle. Noteworthy among these were Gordon Baker and Tom Lang. Many interesting particulars about the hydrofoils of Baker and Lang can be found in References 12-14. Both Baker and Lang utilized the NACA 16-510 section for their hydrofoils. (This was essentially the same as the section that had been used for the NACA tests, but with the thickness ratio increased from 9% to 10%.) Also, both formed their aluminum Vee-hydrofoils from straight lengths that had been produced by extrusion of the material through a die. A typical Baker foil (with the 42 deg dihedral angle that he preferred) is shown in Figure 6-4. Lang concluded that, "... the maximum efficiency of

surface piercing hydrofoils should occur at a dihedral above 30 deg and probably below 45 deg.” Numerous additional helpful recommendations regarding the shape, manufacture, and mounting of surface-piercing Vee-hydrofoils can be found in References 12-14.

The excellent performance of the hydrofoil boats of Baker and Lang indicate that a suitable foil for a trim-control device would be one that closely followed their successful practice. The type of hydrofoil that recommends itself, therefore, is a V-foil of 40 deg dihedral angle, with the same NACA 16-510 section that was used by both Baker and Lang. Their practice should be followed also by starting with a straight extrusion (formed by extruding aluminum through a die of the specified section shape) and then bending the extrusion into a form such as that shown in Figure 6-4.

The patents of Baker and Lang (References 12 and 13) indicate that the design high-speed running condition for their hydrofoils was with the Vee portion half-submerged. It seems appropriate to assume the same high-speed design condition of foil submergence for the case of a hydrofoil being utilized as a stern trim-control device. This is the condition shown for the case of the Dynaplane-type boat depicted in Figure 1-1.

It is unfortunate that the program of testing reported on in Reference 4 did not include tests of a hydrofoil with 40 deg dihedral. However, straight-line extrapolation of the data for the foils with 20 deg and 30 deg dihedral should give approximate values for a foil with 40 deg dihedral. The appropriate angle of attack to adopt for design cases is zero deg. This is the design angle of attack for the 16-510 foil section; and, consistent with this, the data from the tests of the foil with 30 deg dihedral show that the maximum  $L/D$ 's were attained at, or close to, that angle (see Figures 6-2 and 6-3). Now, at zero deg angle of attack, an aspect ratio of 3, and a speed of 50 fps, the test value of  $C_L$  for the foil having 20 deg dihedral was 0.10. The test value of  $C_L$  for the foil having 30 deg dihedral, at the same conditions, was 0.19 (see Figure 6-2). Extrapolation of the foregoing two values of  $C_L$  to 40 degrees dihedral gives a value for  $C_L$  of 0.28. Also, Reference 4 reports a  $C_L$  value of 0.22 for the foil with 20 degrees dihedral, at zero degree angle of attack, an aspect ratio of 6, and a speed of 50 fps. Extrapolating as before gives a value of  $C_L$  of 0.32 for a foil with 40 degrees dihedral at an aspect ratio of 6. The foregoing numbers suggest that for the case of a foil with an aspect ratio of 4 when running at its high-speed design point it would be appropriate to assume that the applicable value of  $C_L$  would be close to 0.30. The  $C_L$  values arrived at by the foregoing extrapolations will probably tend to be high. However, there is the compensating factor that the lower corner of the foil is to be rounded, as shown in Figure 6-4, instead of having the type of sharp corner shown in Figure 6-1. Any remaining discrepancy between the  $C_L$  value assumed when designing a foil, and the value realized in practical operation can be catered for, without suffering a significant decrease in foil  $L/D$ , by adjusting the foil angle of attack.

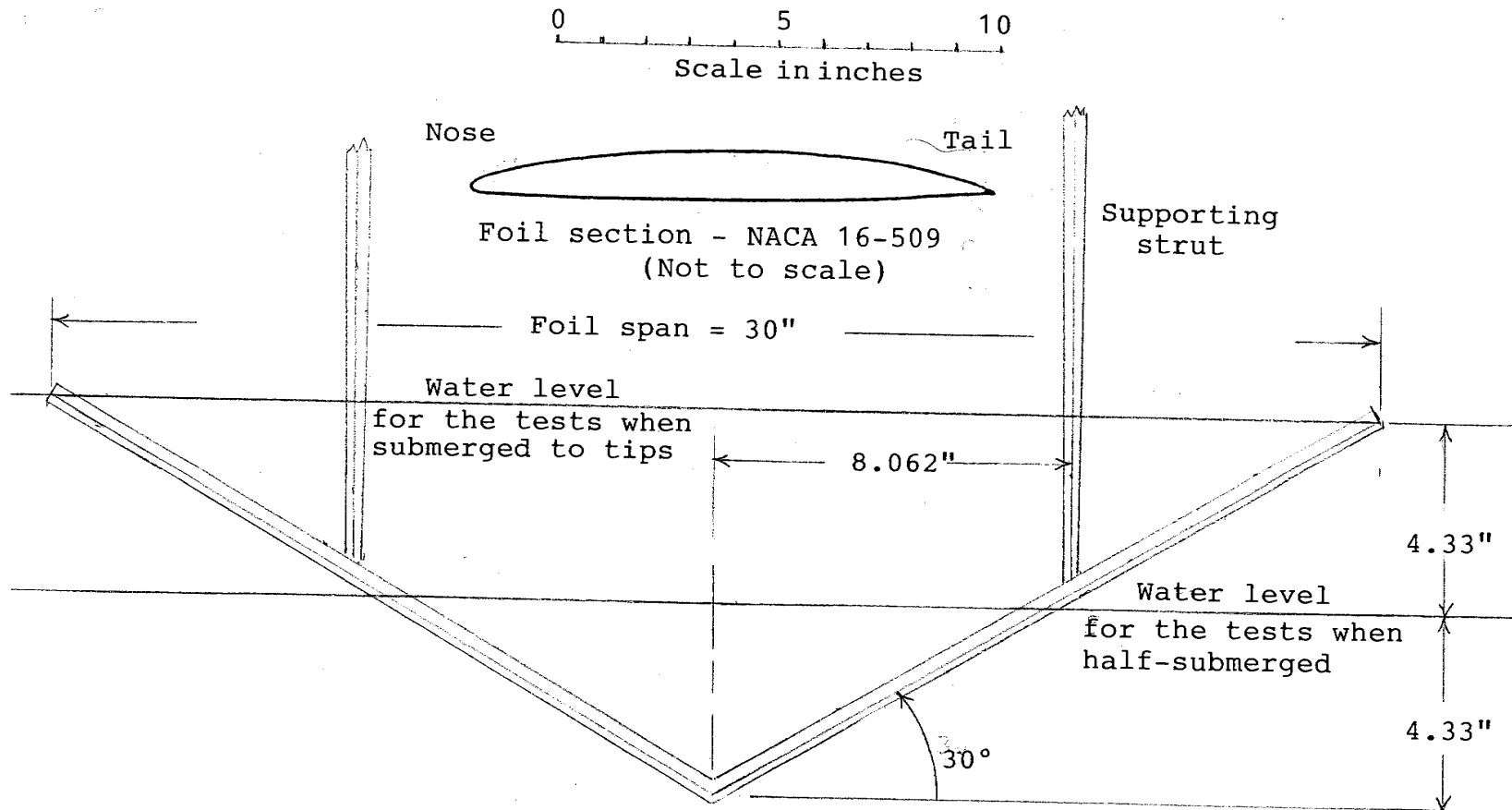


Figure 6-1 - 30-deg Dihedral Hydrofoil Showing the Water Levels for Two Test Conditions.

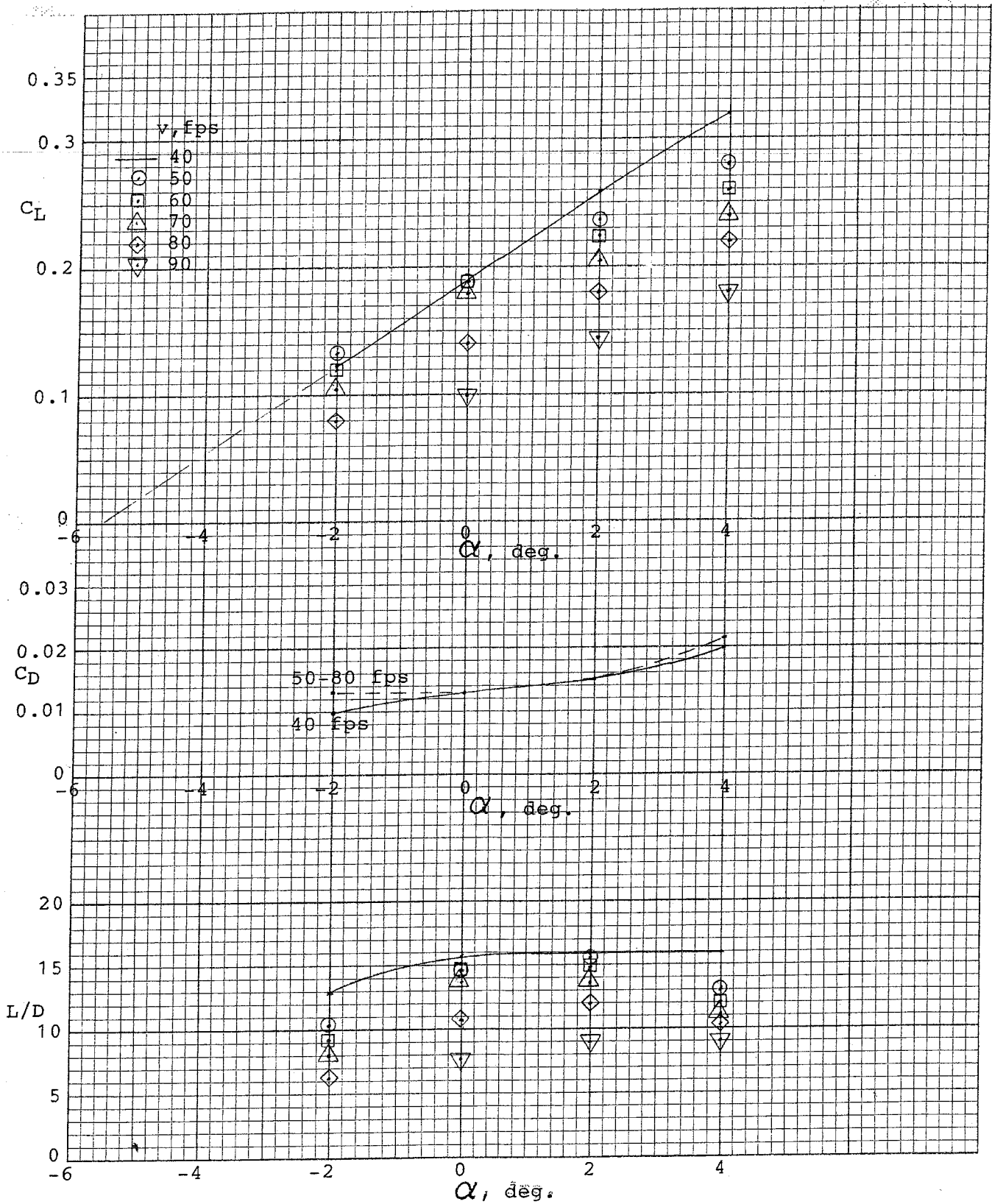


Figure 6-2 - Values of Lift Coefficient, Drag Coefficient, and Lift/ Drag, for 30-deg Dihedral Hydrofoil when Half-Submerged. Aspect Ratio = 3.0.

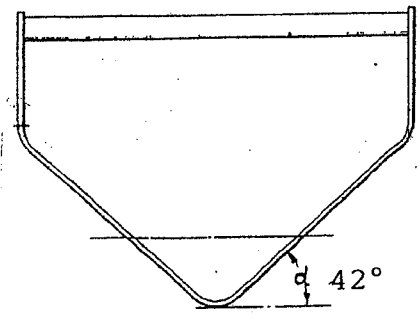
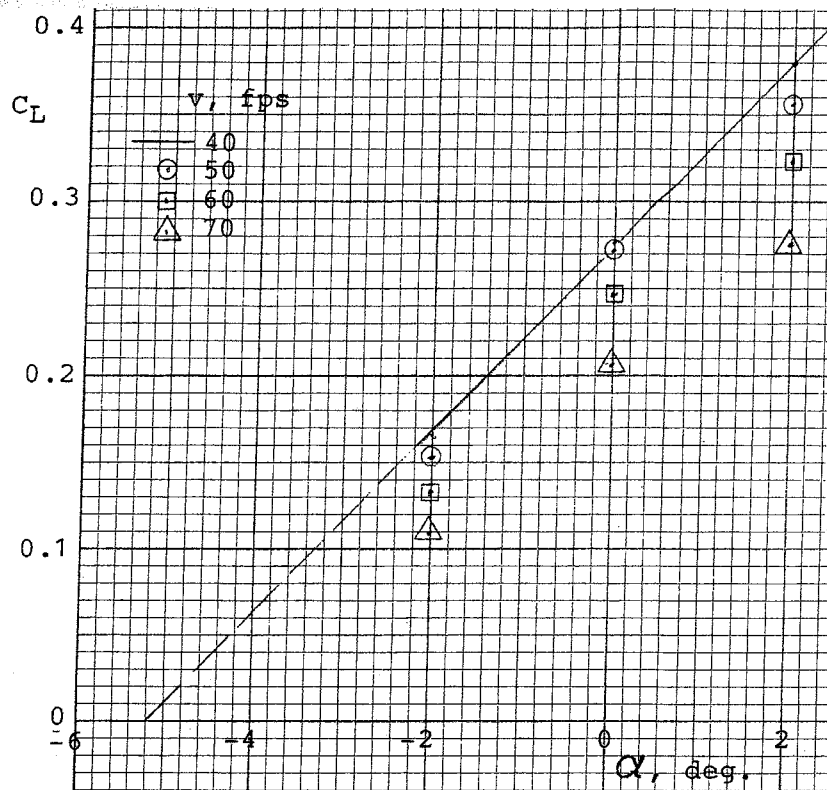


Figure 6-4 - Typical Baker Surface-piercing Hydrofoil.

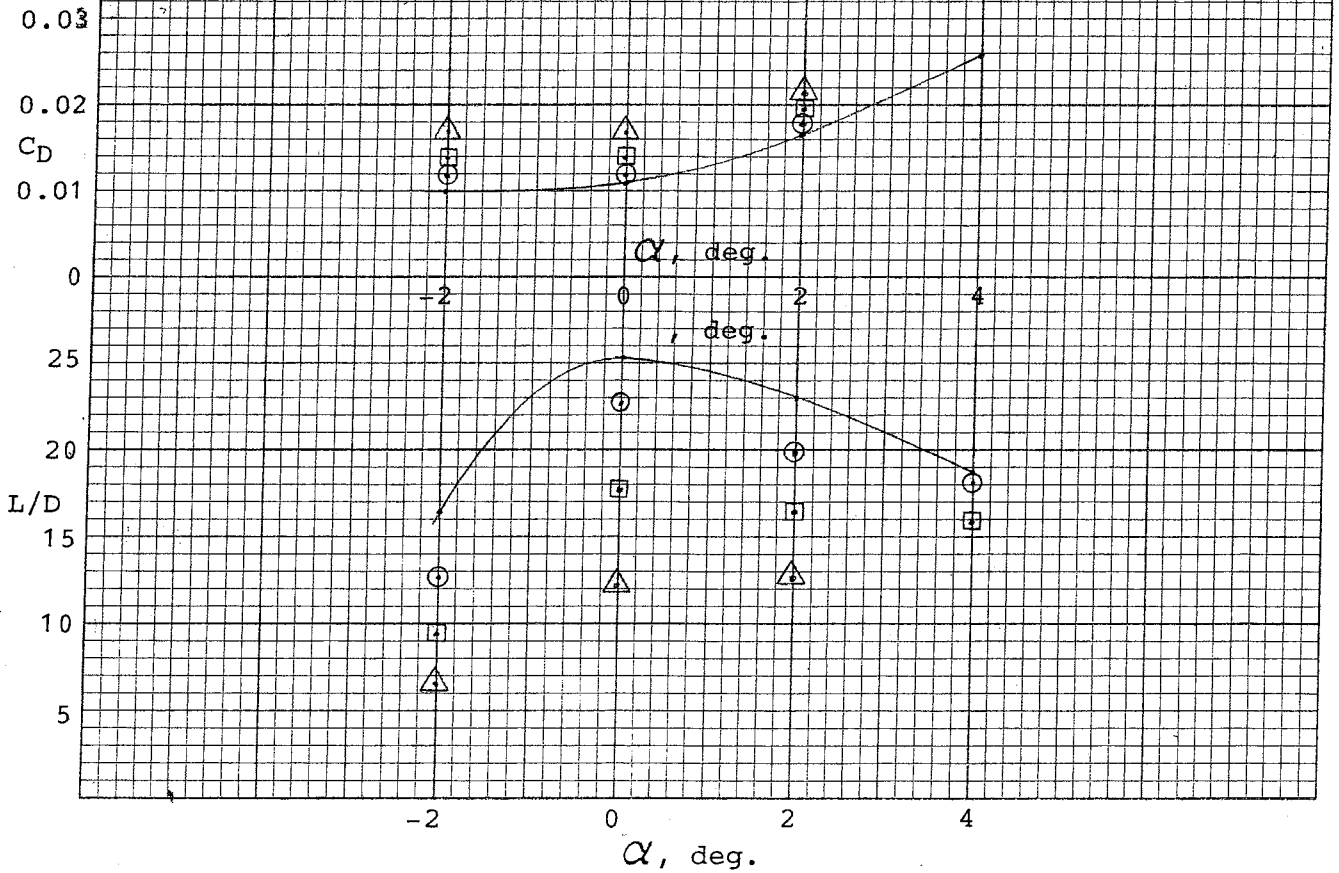


Figure 6-3 - Values of Lift Coefficient, Drag Coefficient, and Lift/Drag, for 30-deg Dihedral Hydrofoil when Submerged to the Tips. Aspect Ratio = 6.0.

## Appendix A

### Results of Tests of a Planing Surface Model with the Johnson 3-Term Camber

In Reference 9 Virgil Johnson predicted that high values of lift/drag ratio could be attained for supercavitating hydrofoils operating near the free water surface by utilizing his "3-term" type of camber curvature. It was evident that Johnson's theory should be applicable for planing surfaces as well as for submerged surfaces. Therefore a planing surface model (of rectangular planform and zero deadrise), which incorporated the 3-term camber, was built and tested, in order to substantiate the applicability of Johnson's equations for the planing case. Details of the test, and the results obtained, were reported in Reference 10. Drawings of the model are given in Figure A-1. As can be seen, the aspect ratio of the cambered region was 2.0. The value of  $C_{L, d}$  for the cambered region (this defines the amount of camber) was 0.075. The graphs derived from Johnson's equations, for the planing case, had shown that with an aspect ratio of 2, and for trim angles in the practical range of 2 deg to 3 deg, this value of  $C_{L, d}$  would result in the maximum values of lift/drag ratio (see Figure A-2.). The forward end of the cambered region of the model was tangent to the flat region ahead of it. (The "Reference Line" shown in Figure A-1 is also tangent to the camber line at its forward end.) Trim angle was taken to be the angle with the horizontal of the flat center portion of the model. The model was made of transparent Plexiglas, and longitudinal markings were provided on the bottom, so that the wetted lengths when running could be observed.

The model was tested in the high-speed basin of DTMB, on Carriage 3, using the towing gear shown in Figure A-3. Test runs were made with the model fixed in trim but free to heave. Runs were made at a number of trim angles, and at a number of speeds for each trim angle. All the runs were made with the model carrying a load of 70 lb. Each test run was started with the model out of the water, and when the carriage had attained the desired test speed the model was lowered into the water so that the 70-lb load on the model (applied by the counterbalance rig shown in the figure) was balanced by the hydrodynamic lift. The drag was then measured, and the length of the bottom of the model that was wetted by solid water was observed visually. The test runs at the various speeds and trim angles resulted in a range of conditions of wetted length. The wetted-length condition of particular interest was, of course, that at which the wetted length of the model coincided with the length of the cambered region. A particular aim of the testing, therefore, was to determine, at each trim angle, the speed that would give that specific condition, and then to record the drag at that condition. Drag and bottom wetted length were also recorded, however, for those test runs at which the wetted length was greater or less than the length of the cambered region, and those values are included here.

Air drag values were measured with the model attached to the towing gear. Those measurements were made for a range of speeds and angles of attack, with the trailing edge of the model one inch above the water surface. There was no significant variation of the air drag with change of model angle of attack. The air drag values were subtracted

from the measured total drag values to give the net values of hydrodynamic drag which are reported here

The experimental values of lift coefficient for the model, for the test points at which the wetted length coincided with the cambered length, are compared with the calculated values of lift coefficient in Figure A-4. It can be seen that there is very close agreement between the experimental and the calculated values. It is presumed therefore that dependable values for the lift of cambered planing surfaces for a range of values of aspect ratio, angle of attack, and amount of camber, are given by Johnson's equations. A comprehensive set of graphs presenting those values of lift is given in Reference 11.

The calculated values of drag coefficient are compared with the experimental values in Figure A-5. This shows that the experimental values of drag were below those calculated from Johnson's equations. In planning the testing it had been considered that the combination of moderately high Reynolds numbers, short time between runs, and painted scales on the bottom of the planing surface model would ensure turbulent flow for all of the test conditions. However, in view of the low drag values that were measured, an experiment was made to determine if they were caused by partial laminar flow. A surface piercing cylindrical strut 1/16 inch in diameter was positioned in the water ahead of the model in such a manner that the turbulence generated was approximately the width of the model at its wetted leading edge. This produced no significant change in drag. Therefore the laminar flow explanation for the drag discrepancy was rejected. Values of lift/drag ratio calculated from Johnson's equations can therefore be presumed to be conservatively low.

The resulting finding that the values of lift/drag ratio from experiment are even higher than those which were calculated by utilizing Johnson's equations is evidently valid. The two sets of values are compared in Figure A-6. (Figure A-7 is included to show how the values of L/D for the model varied with the extent of the bottom wetted-length.) Figure 4-1 compares values of L/D from calculation and from experiment when both sets of values have been extrapolated up to a size representative of a full-scale boat. This figure also includes a curve of L/D values for a flat plate (calculated), in order to show the great improvement in performance that can be achieved by the utilization of camber.



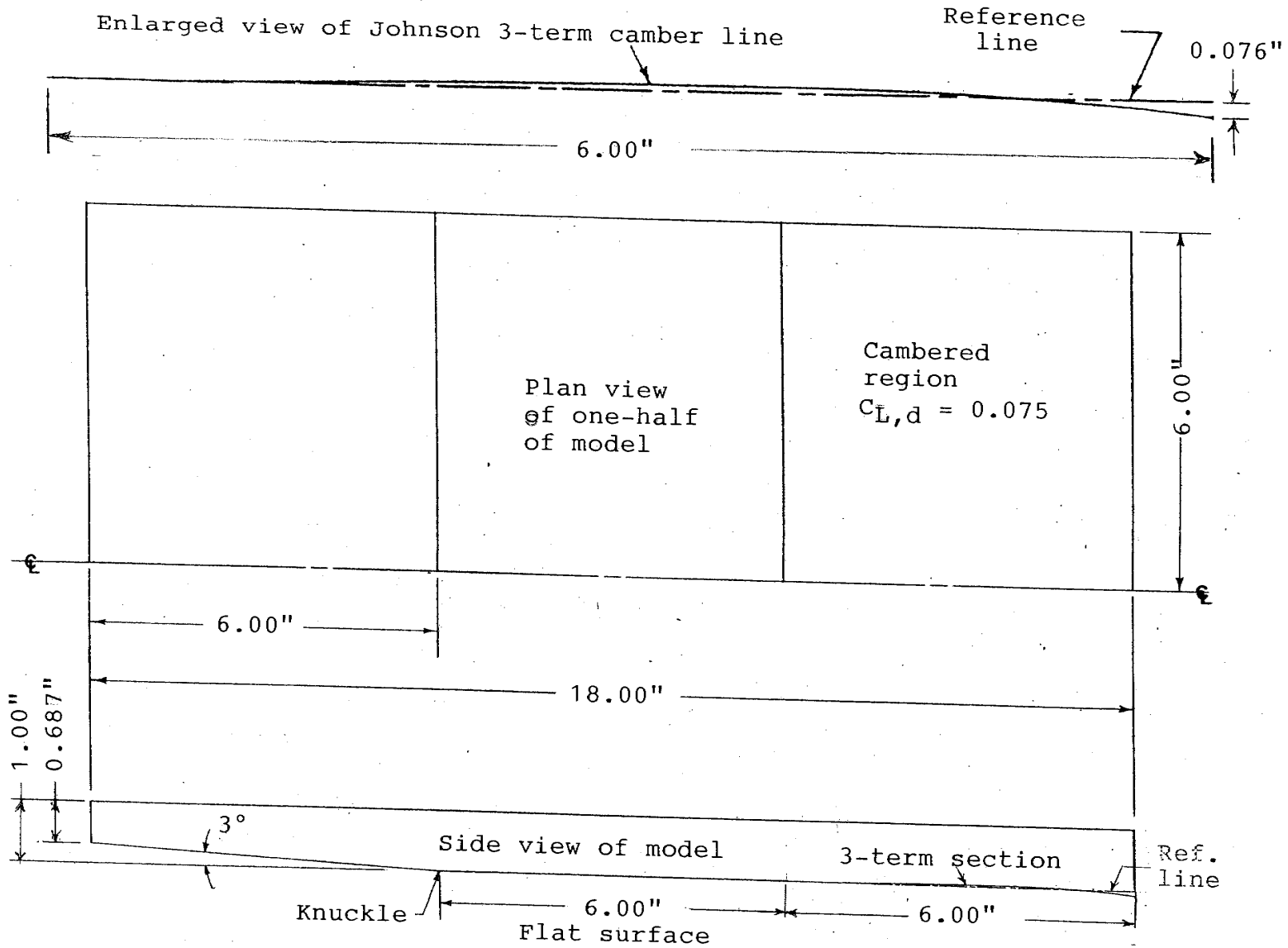


Figure A-1 - One-Foot Wide Model Incorporating Johnson 3-Term Camber in its After Six Inches

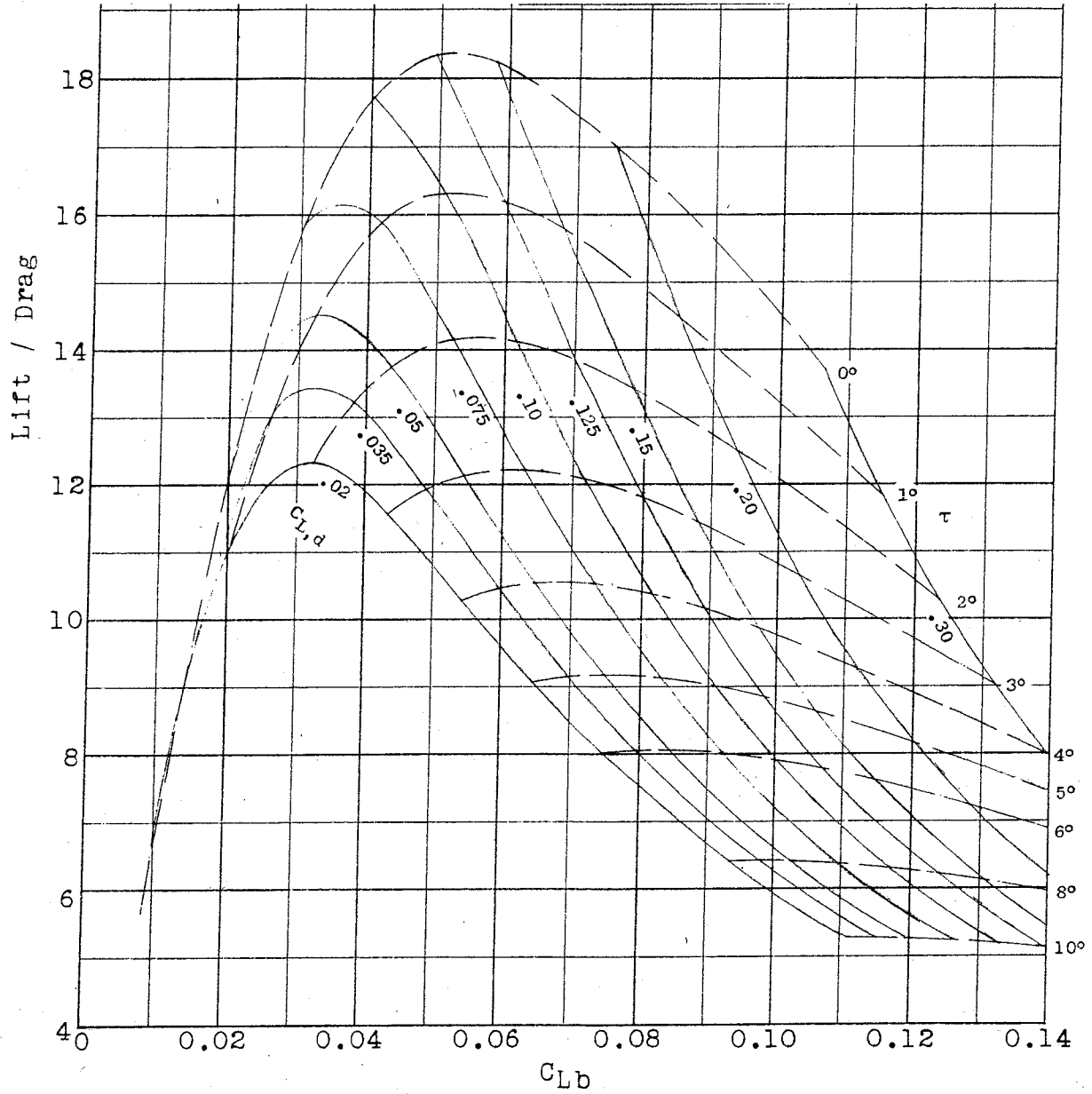


Figure A-2 - Calculated Values of Lift/ Drag Ratio Versus  $C_{Lb}$  for Ranges of Values of Trim Angle and  $C_{L,d}$ . Johnson 3-term Section, Aspect Ratio = 2.0,  $C_f = 0.00293$ .

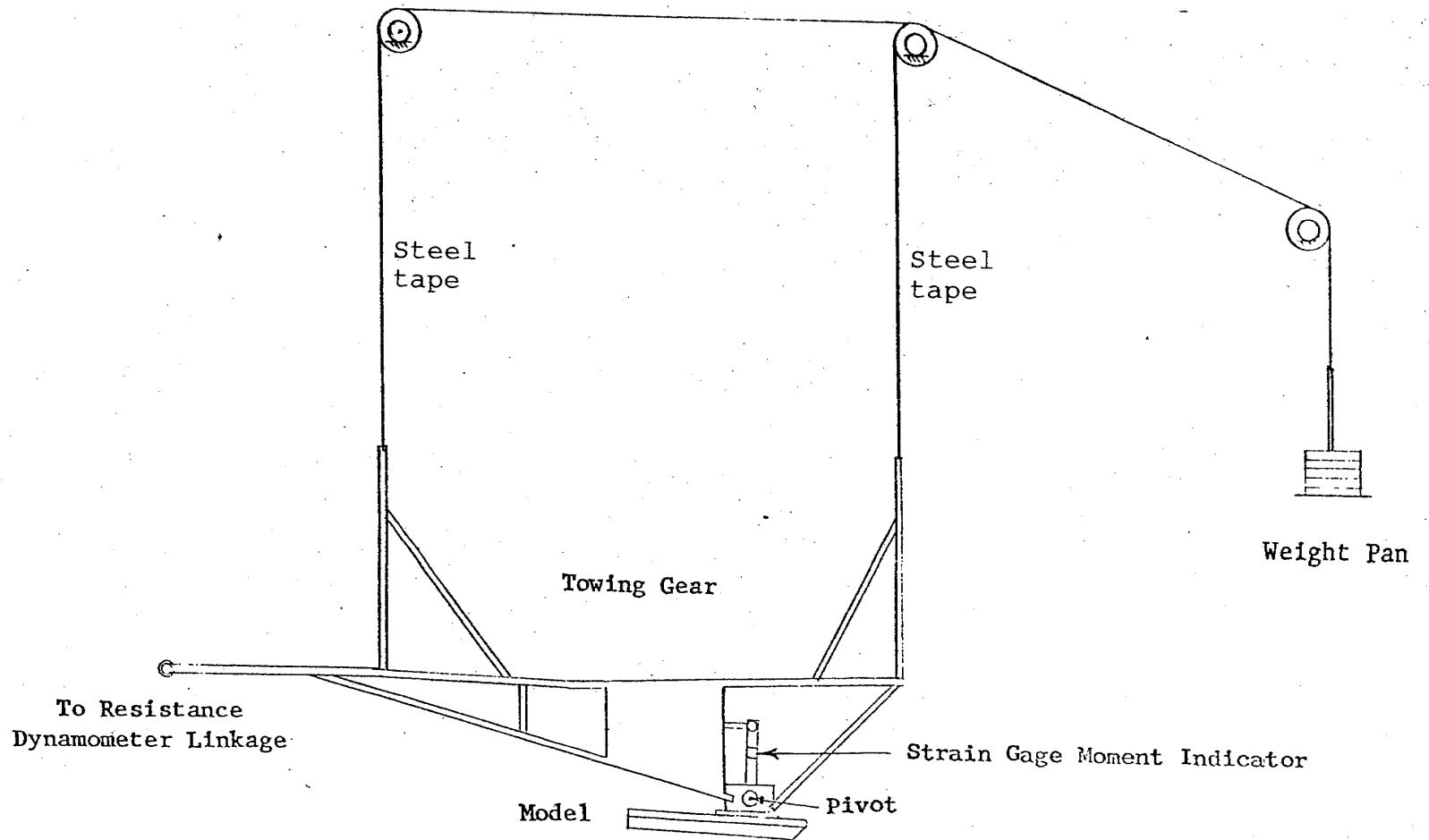


Figure A-3 - Towing Gear Used for Testing Planing Surface Model.

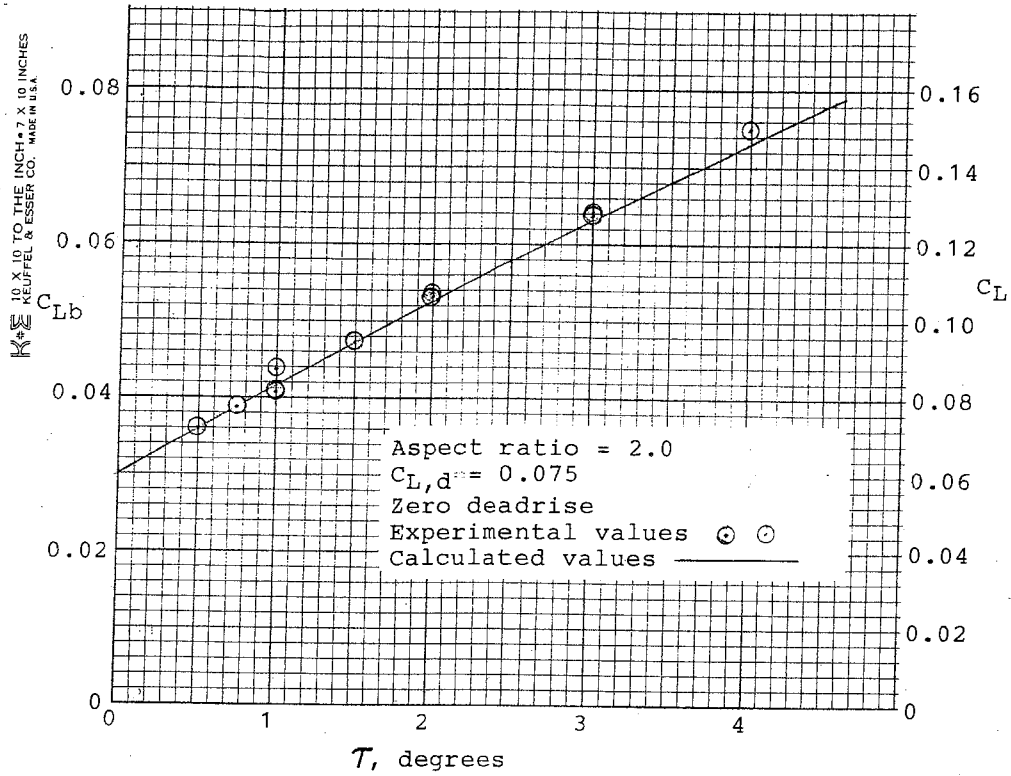


Figure A-4 - Comparison of Calculated and Experimental Values of Lift Coefficient for a Cambered Planing Surface Having the Johnson 3-Term Section. Beam = 1.0 ft, lift = 70 lb.

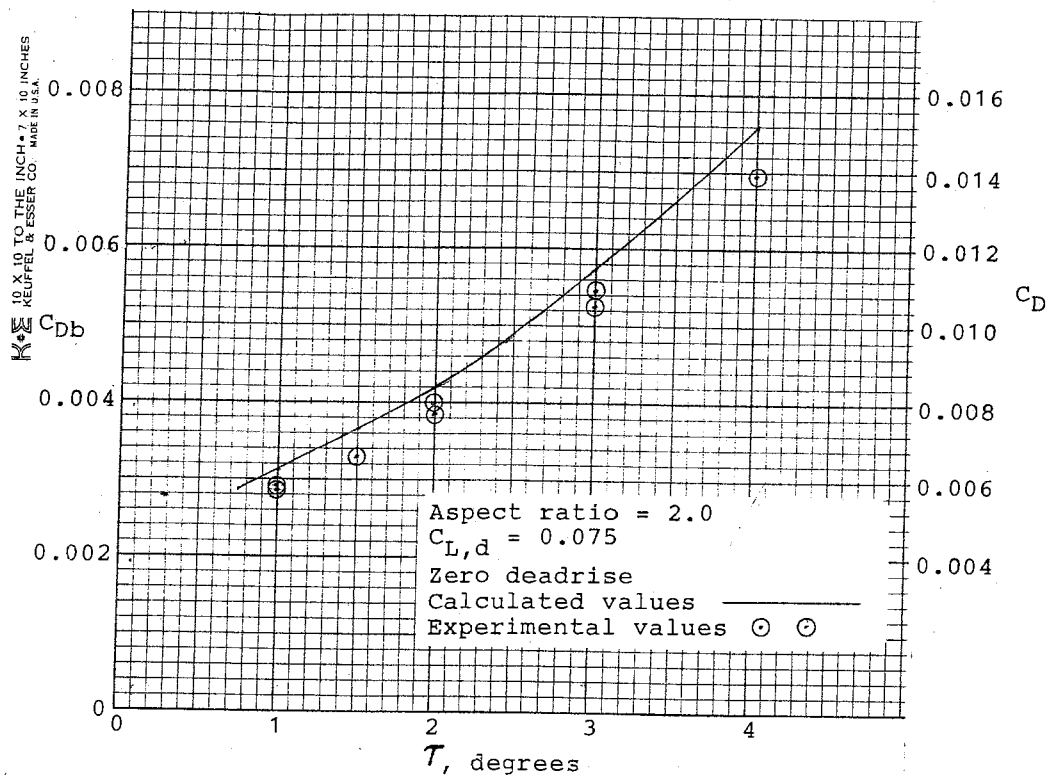


Figure A-5 - Comparison of Calculated and Experimental Values of Drag Coefficient for a Cambered Planing Surface of Rectangular Plan Form Having the Johnson 3-Term Section. Beam = 1.0 ft, lift = 70 lb.

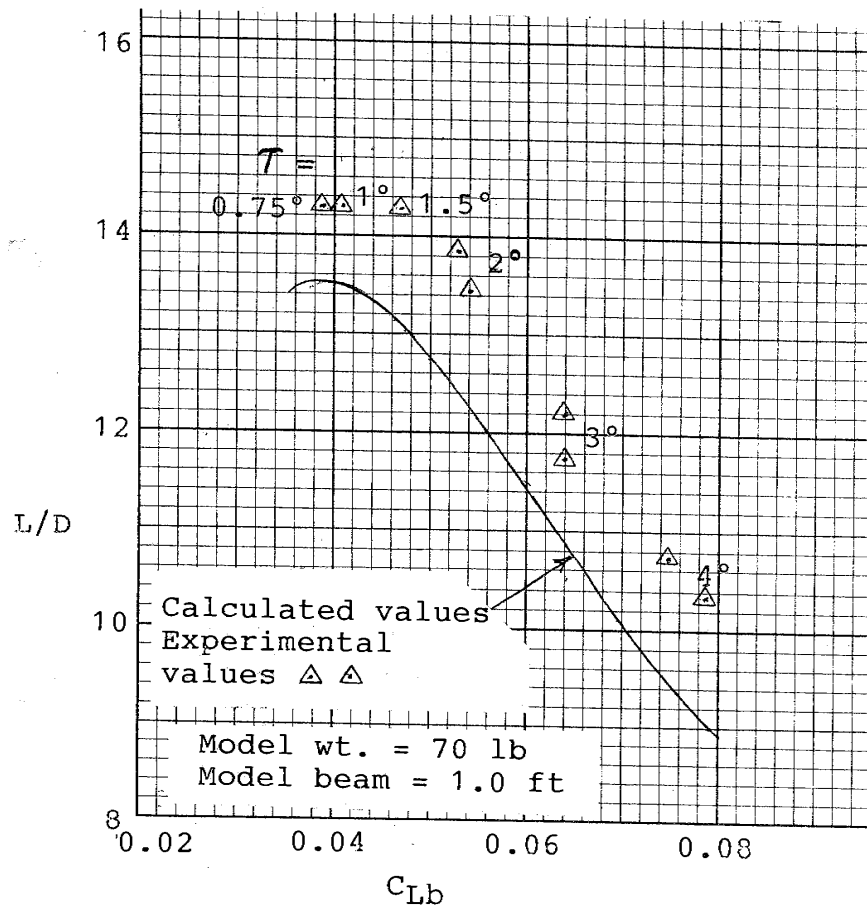


Figure A-6 - Comparison of Calculated and Experimental Values of Lift/Drag for a Model of a Cambered Planing Surface Having the Johnson 3-term Section.  $AR = 2.0$ ,  $C_{L,d} = 0.075$ .

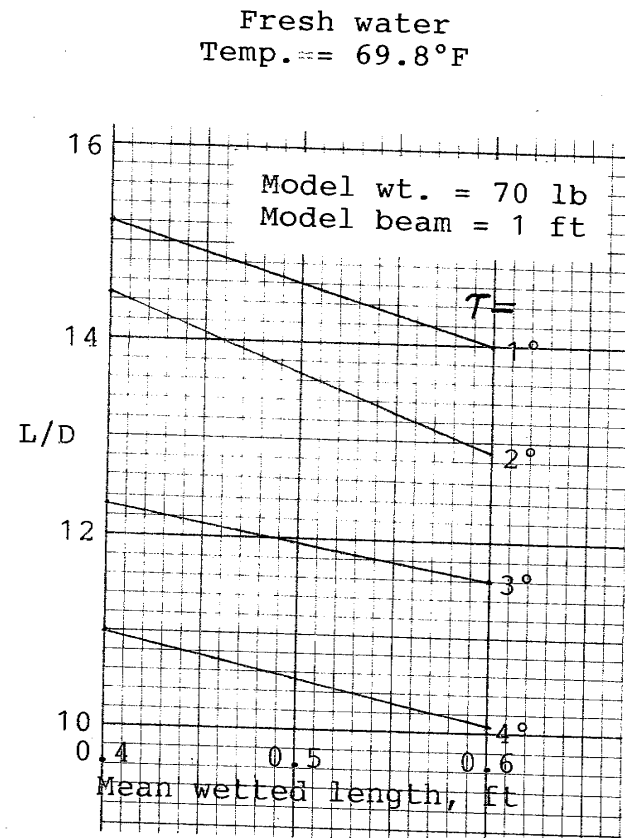


Figure A-7 - L/D Versus Wetted Length for Model That is Cambered for 0.5 ft of its Length.

## References

1. Clement, E.P., "A Configuration for a Stepped Planing Boat Having Minimum Drag (Dynaplane Boat)," published by the author ( 2005).
2. Clement, E.P., and Blount, D.L., "Resistance Tests of a Systematic Series of Planing Hull Forms," Transactions, SNAME, 1963.
3. Rodstrom, R., Edstrand, H., and Bratt, H., "The Transverse Stability and Resistance of Single-Step Boats When Planing," Swedish State Shipbuilding Experimental Tank publication Nr 25 (1953).
4. Benson, J.M., and Land, N.S., "An Investigation of Hydrofoils in the NACA Tank, I - Effect of Dihedral and Depth of Submersion," NACA W.R. L-758, Sept, 1942.
5. Akers, R., "Dancing a Fine Line," Professional BoatBuilder magazine No. 85, (April/May 2004).
6. Clement, E.P., and Koelbel, J.G., Jr., "Effects of Step Design on the Performance of Planing Motorboats," Fourth Biennial Power Boat Symposium, SE Sect., SNAME (Feb 1991).
7. Savitsky, D., and Breslin, J.P., "On the Main Spray Generated by Planing Surfaces," ETT Report No. 678 (Jan 1958).
8. Clement, E.P., "A Lifting Surface Approach to Planing Boat Design," DTMB Report 1902 (Sep 1964).
9. Johnson, V.E., Jr., "Theoretical and Experimental Investigation of Supercavitating Hydrofoils Operating Near the Free Water Surface," NASA Technical Report R-93, 1961.
10. Moore, W.L., "Cambered Planing Surfaces for Stepped Hulls - Some Theoretical and Experimental Results," DTMB Report 2387 (Feb 1967).
11. Clement, E. P., "Graphs for Designing Cambered Planing Surfaces Having the Johnson Three-Term Camber Section, Rectangular Planform, and Zero Deadrise," Naval Ship Research and Development Center Report 3147, Oct, 1969.
12. Baker, J.G., U.S. Patent No. 2,856,877, Oct. 21, 1958, "Hydrofoil System for Boats."
13. Lang, T.G., U.S. Patent No. 3,094,960, June 25, 1963, "Hydrofoil for Water Craft."
14. Lang, Tom, "The Up-Right Hydrofoil Kits," Website of The International Hydrofoil Society ([www.foils.org](http://www.foils.org)) 1 Sep 2000.